Supporting Information for

Design of two-photon absorbing fluorophores for FRET antenna-core oxygen probes

Z. Zheng, M. M. Ayhan, Y.-Y. Liao, N. Calin, C. Bucher, C. Andraud* and Y. Bretonnière*

Univ. Lyon, ENS de Lyon, CNRS UMR5182, Université Lyon 1, Laboratoire de Chimie, F-69342 Lyon (France)

* To whom correspondence should be addressed: chantal.andraud@ens-lyon.fr, yann.bretonniere@ens-lyon.fr

Contents

Crystallography

Single crystals of **A1** and **A4** were obtained by slow diffusion evaporation of a concentrated solution in chloroform. Suitable crystals were selected and mounted on a Gemini kappa-geometry diffractometer (Agilent Technologies UK Ltd) equipped with an Atlas CCD detector and using Cu radiation (λ = 1.54184 Å). Intensities were collected at 100 K or 150°K by means of the CrysalisPro software. Reflection indexing, unit-cell parameters refinement, Lorentz-polarization correction, peak integration and background determination were carried out with the CrysalisPro software. An analytical absorption correction was applied using the modelled faces of the crystal. The structures were solved by direct methods with SIR97 and the least-square refinement on *F2* was achieved with the CRYSTALS software. All non-hydrogen atoms were refined anisotropically. The hydrogen atoms were all located in a difference map, but were then repositioned geometrically. The H atoms were initially refined with soft restraints on the bond lengths and angles to regularize their geometry (C—H in the range 0.93-0.98 Å) and U_{iso}(H) (in the range 1.2-1.5 times U_{eq} of the parent atom), after which the positions were refined with riding constraints.

Table SI-1. Data collection and structure refinement parameters.

	A1	**A2**
Data Collection		
Radiation type	Cu $K\alpha$, λ = 1.54184 Å	Cu $K\alpha$, λ = 1.54184 Å
No. measured reflections	35024	27659
Independent and reflections	8884	6582
Reflections with $I > 2\sigma(I)$	6725	5821
R_{int}	0.087	0.044
θ_{max}	67.2	67.0
θ_{min}	3.9	3.2
h	−13→12	−19→22
k	−17→17	−6→8
l	−20→20	−32→33
Refinement		
$R[F^2 > 2\sigma(F^2)]$	0.088	0.040
$wR(F^2)$	0.291	0.108
S	1.07	1.02
No. of reflections	8884	6582
No. of parameters	606	428
No. of restraints	0	0
H-atom treatment	H-atom parameters constrained	H-atom parameters constrained
$(\Delta/\sigma)_{\mathrm{max}}$	<0.001	0.002
$\Delta\rho_{\mathrm{max}}$ (e Å^{-3})	0.42	0.26
$\Delta\rho_{\mathrm{min}}$ (e Å^{-3})	−0.34	−0.40

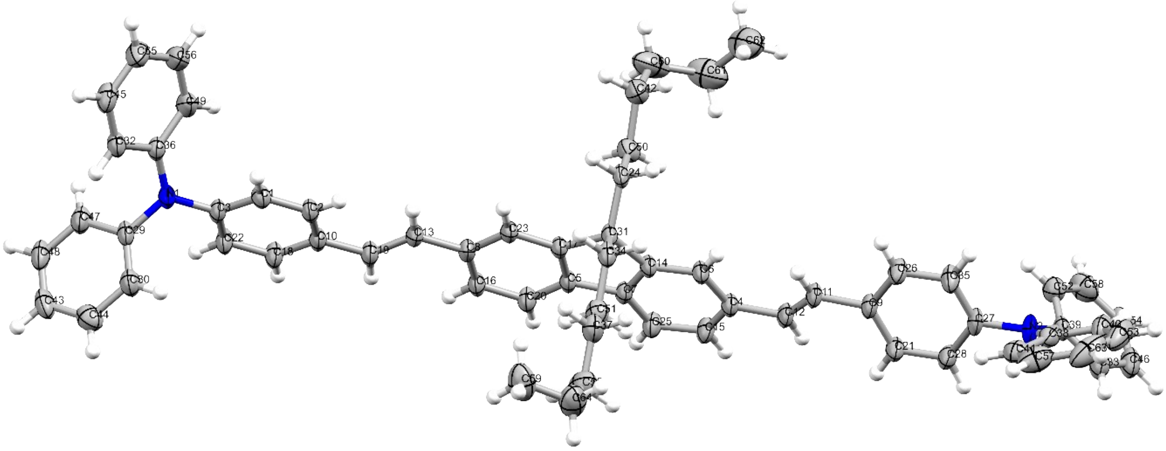

Fig. SI-1 ORTEP view of **A1** crystal structure with ellipsoid at 50% probability.

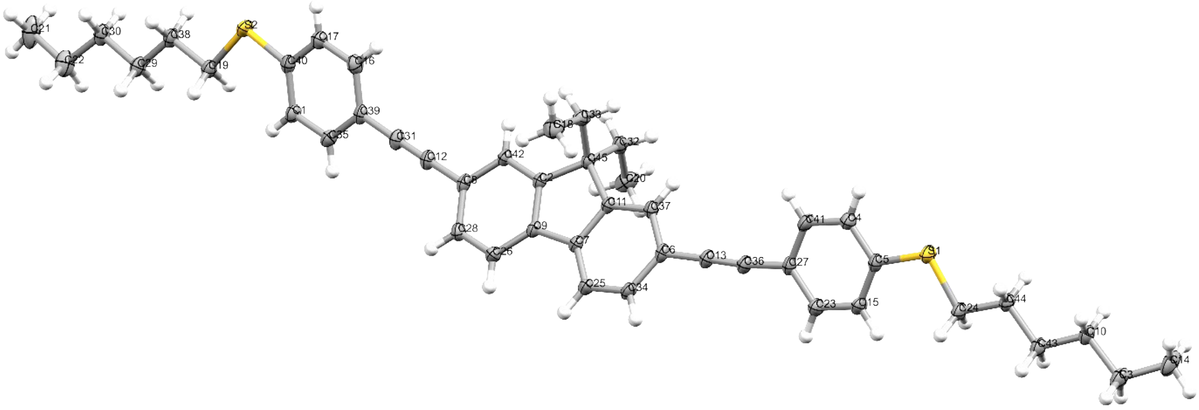

Fig. SI-2 ORTEP view of **A4** crystal structure with ellipsoid at 50% probability.

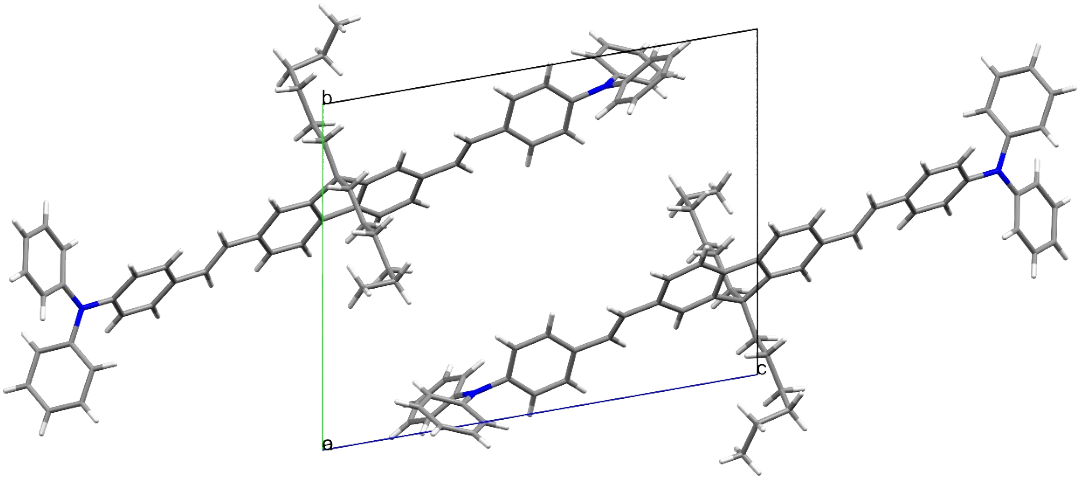

Fig. SI-3 Crystal packing of **A1** viewed down crystallographic *a* axis.

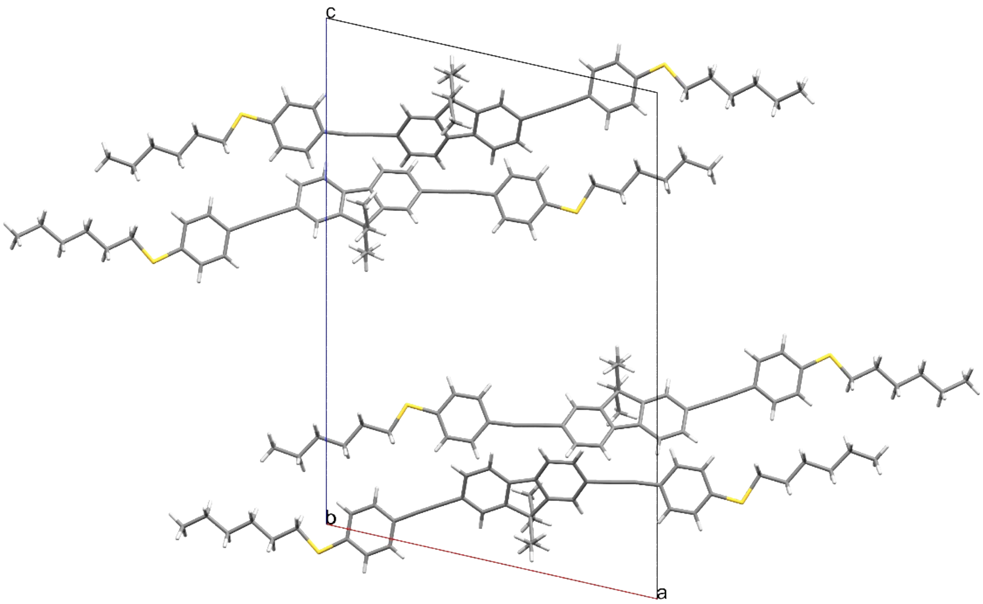

Fig. SI- 4 Crystal packing of **A4** viewed down crystallographic *b* axis.

Electrochemical studies

Solvent and Electrolyte: Dichloromethane (99.9%, Acros Organics, extra-dry/Acroseal®, stabilized with amylene) and tetra-*n*-butylammonium perchlorate (TBAP, Fluka puriss.) have been purchased and used without further purification.

Apparatus: Cyclic voltammetry (CV) and voltammetry with rotating disc electrodes (RDE) were recorded using a SP300 Bilogic potentiostat. Analytical studies have been conducted under a nitrogen atmosphere (glove box) in a standard one–compartment, three–electrodes electrochemical cell. Tetra-*n*-butylammonium in dichloromethane was used as supporting electrolytes (0.1 M). An automatic ohmic drop compensation procedure was systematically performed when using cyclic voltammetry. Vitreous carbon (Ø = 3 mm) working electrodes (CH Instruments) were polished with 1 mm diamond paste before each recording. Voltamperometry with a rotating disk electrode (RDE) was carried out with a radiometer (CTV101 radiometer analytical) equipment at a rotation rate of 500 rad min^{-1} using a glassy carbon RDE tip (Ø= 3 mm). $Ag/AgNO_3$ (CH Instruments, 10^{-2} M + TBAP(10^{-1}) M in CH_3CN) was used as a reference electrode.

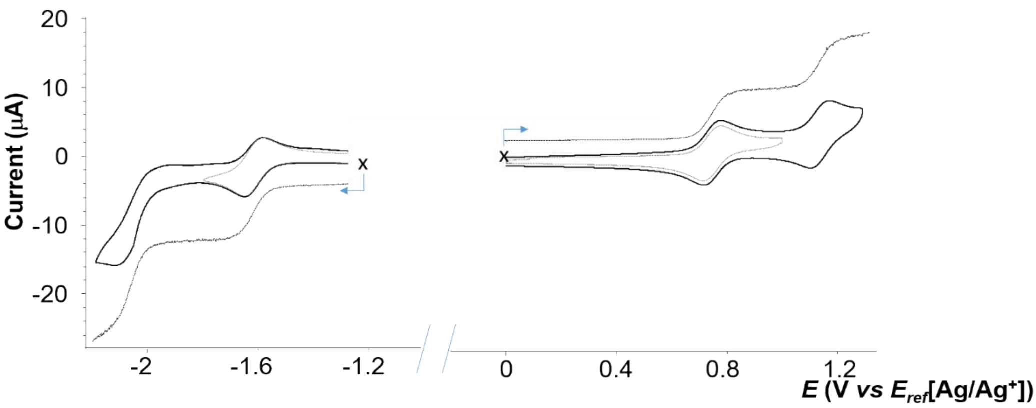

Fig. SI-5 Voltammograms for **C1**, 1 mM in CH_2Cl_2 (0.1 M TBAP) recorded under N_2 (glove box); 3 mm Ø vitreous carbon working electrode, ν = 100 mV/s, *E vs E*$_{ref}$[Ag/Ag$^+$]. RDE 10 mV/S, 500 rd/min.

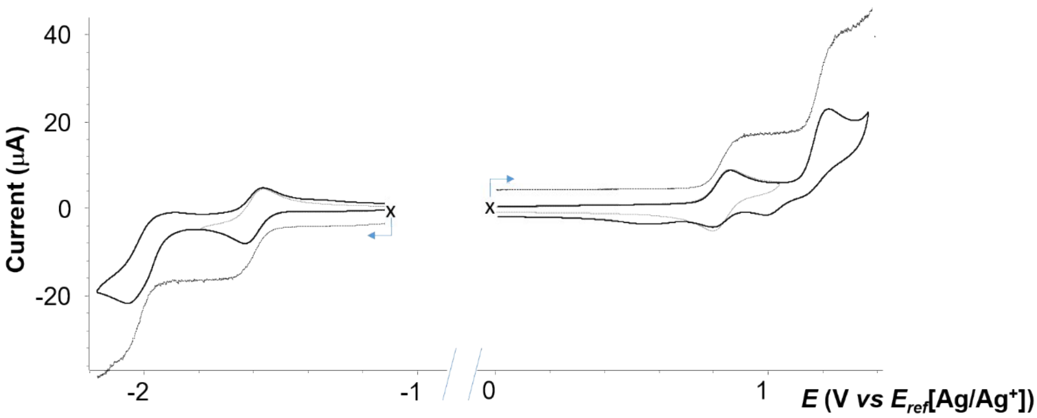

Fig. SI-6 Voltammograms for **C2**, 1 mM in CH_2Cl_2 (0.1 M TBAP) recorded under N_2 (glove box); 3 mm Ø vitreous carbon working electrode, ν = 100 mV/s, *E vs E*$_{ref}$[Ag/Ag$^+$]. RDE 10 mV/S, 500 rd/min.

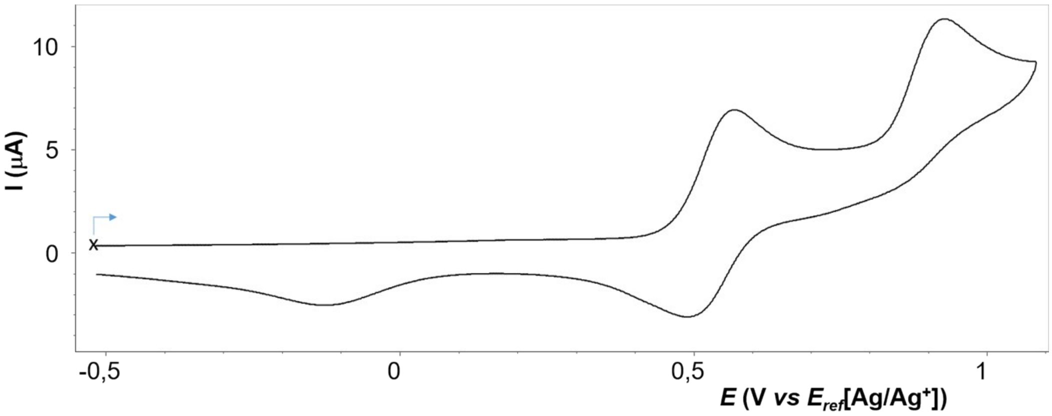

Fig. SI-7 Voltammograms for **A1**, 1 mM in CH_2Cl_2 (0.1 M TBAP) recorded under N_2 (glove box); 3 mm Ø vitreous carbon working electrode, ν = 100 mV/s, *E vs* E_{ref}[Ag/Ag$^+$].

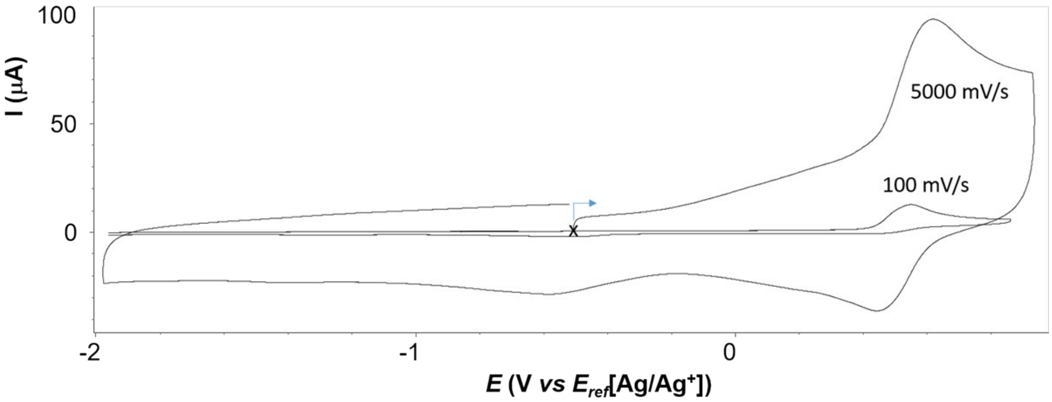

Fig. SI-8 Voltammograms for **A2**, 1 mM in CH_2Cl_2 (0.1 M TBAP) recorded under N_2 (glove box); 3 mm Ø vitreous carbon working electrode, ν = 100 mV/s, *E vs* E_{ref}[Ag/Ag$^+$].

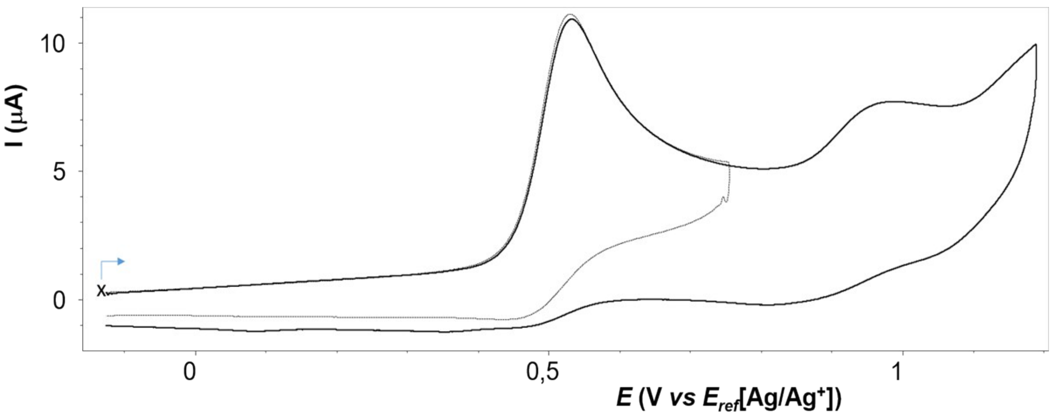

Fig. SI-9 Voltammograms for **A3**, 1 mM in CH_2Cl_2 (0.1 M TBAP) recorded under N_2 (glove box); 3 mm Ø vitreous carbon working electrode, ν = 100 mV/s, *E vs* E_{ref}[Ag/Ag$^+$].

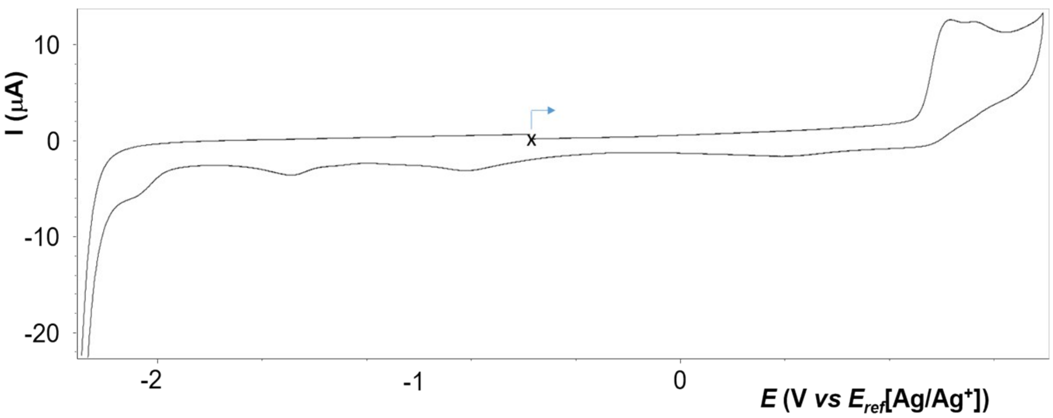

Fig. SI-10 Voltammograms for **A4**, 1 mM in CH_2Cl_2 (0.1 M TBAP) recorded under N_2 (glove box); 3 mm Ø vitreous carbon working electrode, ν = 100 mV/s, *E vs* E_{ref}[Ag/Ag^+].

Table SI-2 Half-wave (*) or peak potential (Δ) values measured a for **C1**, **C2**, **A1**, **A2**, **A3** and **A4** (1 mM) in CH_2Cl_2 + n-tetrabutylamonium perchlorate (TBAP, 0.1 M); *E vs* $E_{1/2}$[Fc/Fc^+].

	$[E_{pa}]_2$	$[E_{red}]_1$	$[E_{ox}]_1$	$[E_{ox}]_2$
C1	-2.308 Δ	-1.807 *	0.553 *	0.943 *
C2	-2.256 Δ	-1.793 *	0.632 *	1.025 *
A1			0.330 *	0.730 Δ
A2			0.354 Δ	0.955 Δ
A3			0.344 Δ	0.811 Δ
A4			0.836 Δ	0.926 Δ

a Vitreous carbon WE, Φ = 3 mm, ν = 0.1 V.s-1, E vs Ag/Ag+ (10-2 M).

Complementary spectroscopic data and figures

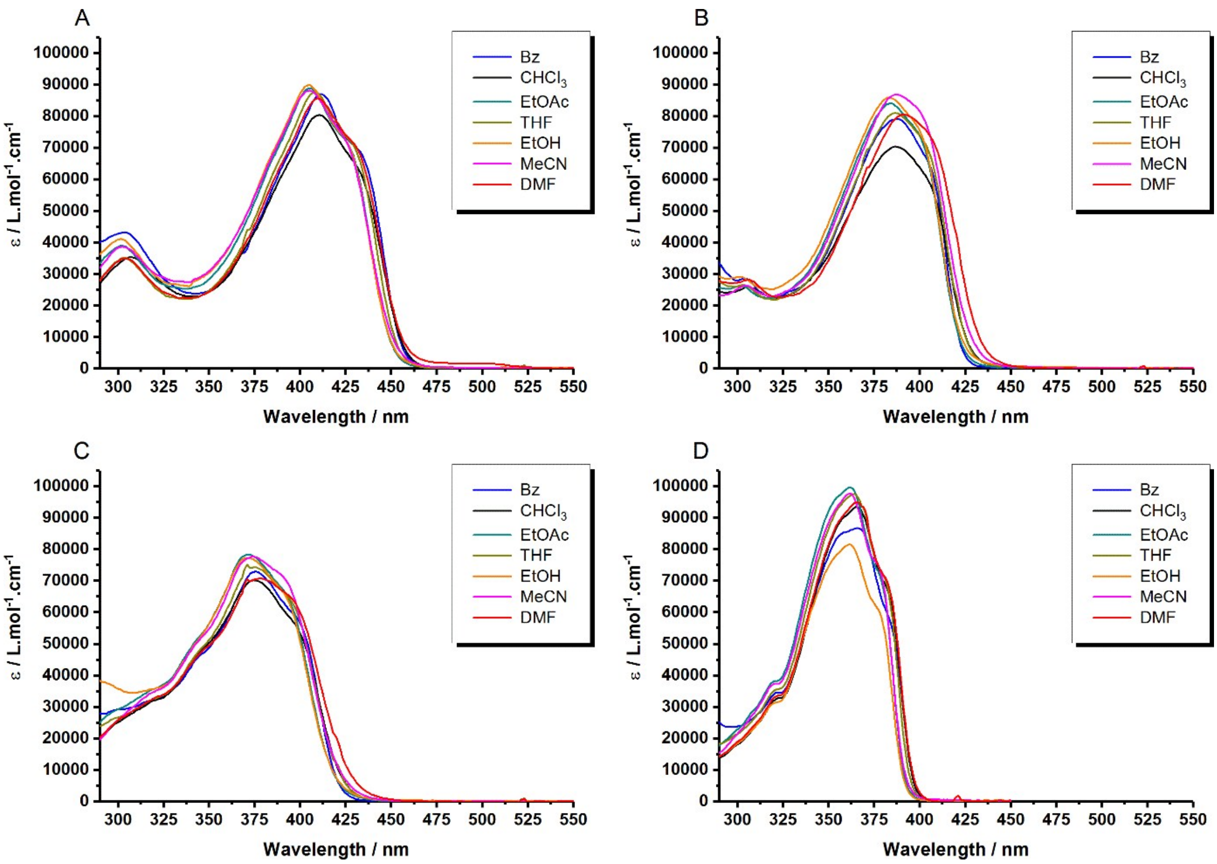

Fig. SI-11 Absorption spectra of compounds A) **A1**, B) **A2**, C) **A3**, and D) **A4** in solvents of different polarity (Bz=Benzene, $CHCl_3$=chloroform, EtOAc=Ethyl acetate, THF=Tetrahydrofuran, EtOH=Ethanol, MeCN=Acetonitrile, DMF=*N*,*N*-Dimethylformamide).

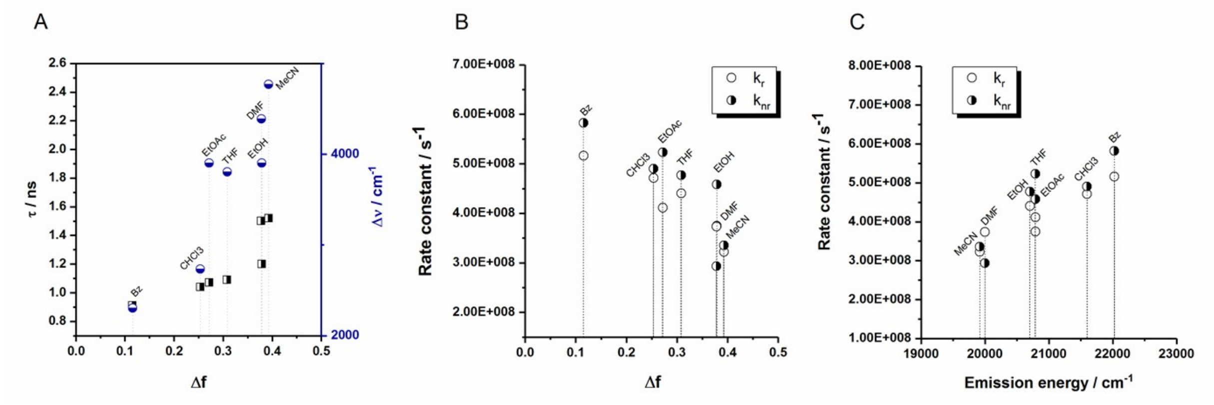

Fig. SI-12 Compound **A1**: plots of A) fluorescence lifetime (τ) *vs* the Lippert-Mataga orientation polarizability Δf; B) radiative (*kr*) and nonradiative (*knr*) constants *vs* the Lippert-Mataga orientation polarizability Δf; C) radiative (*kr*) and nonradiative (*knr*) constants *vs* Emission energy. $\Delta f=[(\varepsilon-1)/(2\varepsilon+1)]-[(n^2-1)/(2n^2+1)]$

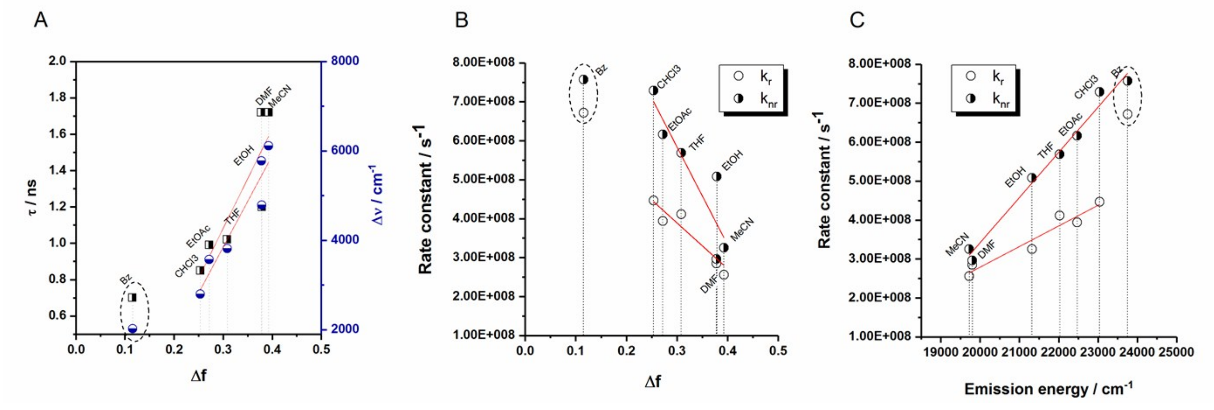

Fig. SI-13 Compound **A2**: plots of A) fluorescence lifetime (τ) vs the Lippert-Mataga orientation polarizability Δf; B) radiative (k_r) and nonradiative (k_{nr}) constants vs the Lippert-Mataga orientation polarizability Δf; C) radiative (k_r) and nonradiative (k_{nr}) constants *vs* Emission energy. Data for benzene are excluded from the linear fit. Δf=[(ε-1)/(2ε+1)]-[(n^2-1)/(2n^2+1)]

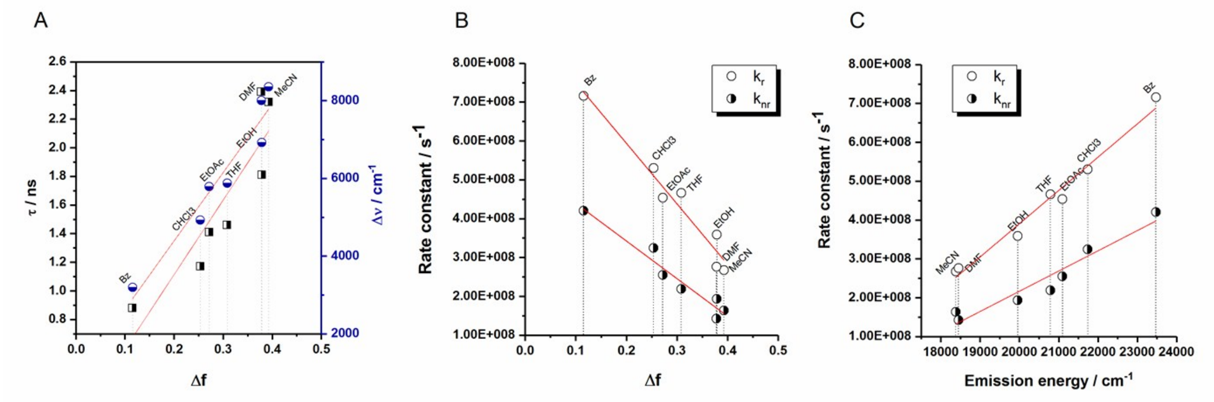

Fig. SI-14 Compound **A3**: plots of A) fluorescence lifetime (τ) *vs* the Lippert-Mataga orientation polarizability Δf; B) radiative (*kr*) and nonradiative (*knr*) constants *vs* the Lippert-Mataga orientation polarizability Δf; C) radiative (*kr*) and nonradiative (*knr*) constants *vs* Emission energy. Δf=[(ε-1)/(2ε+1)]-[(n^2-1)/(2n^2+1)]

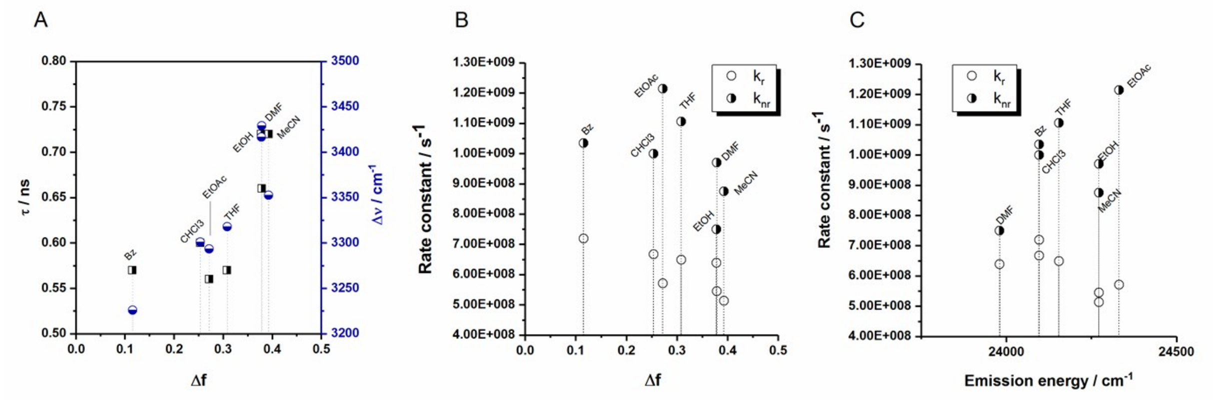

Fig. SI-15 Compound **A4**: plots of A) fluorescence lifetime (τ) *vs* the Lippert-Mataga orientation polarizability Δf; B) radiative (*kr*) and nonradiative (*knr*) constants *vs* the Lippert-Mataga orientation polarizability Δf; C) radiative (*kr*) and nonradiative (*knr*) constants *vs* Emission energy. $\Delta f=[(\varepsilon-1)/(2\varepsilon+1)]-[(n^2-1)/(2n^2+1)]$

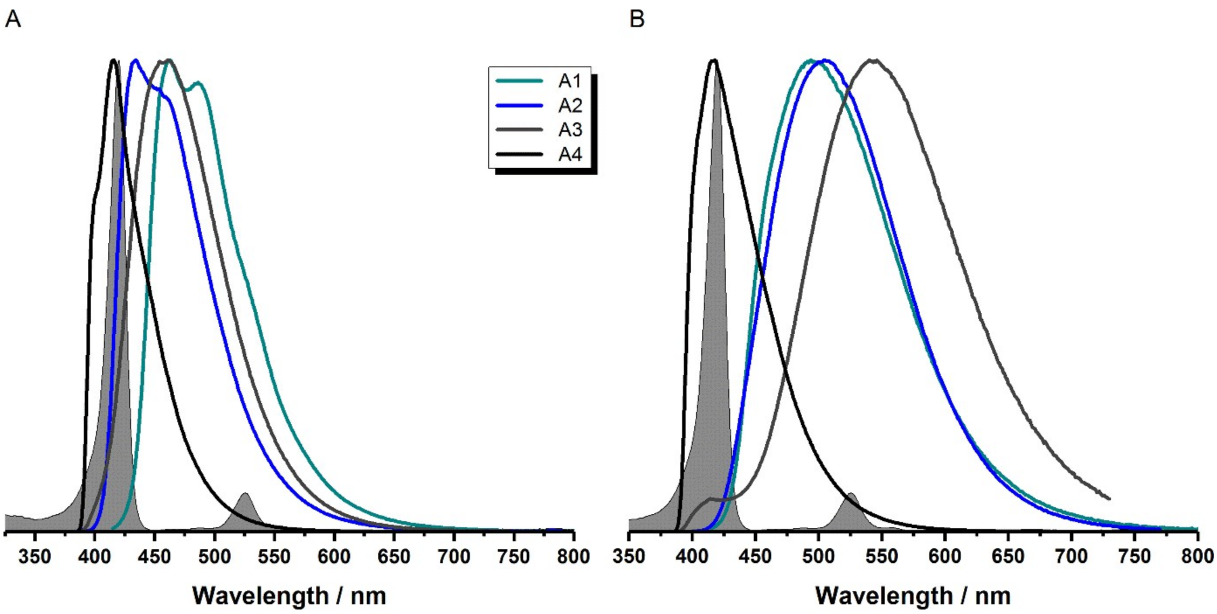

Fig. SI- 16 Absorption spectrum of **C1** and emission spectra of antennae **Ai** (i=1-4) in A) $CHCl_3$ and B) DMF, showing the spectral overlap.

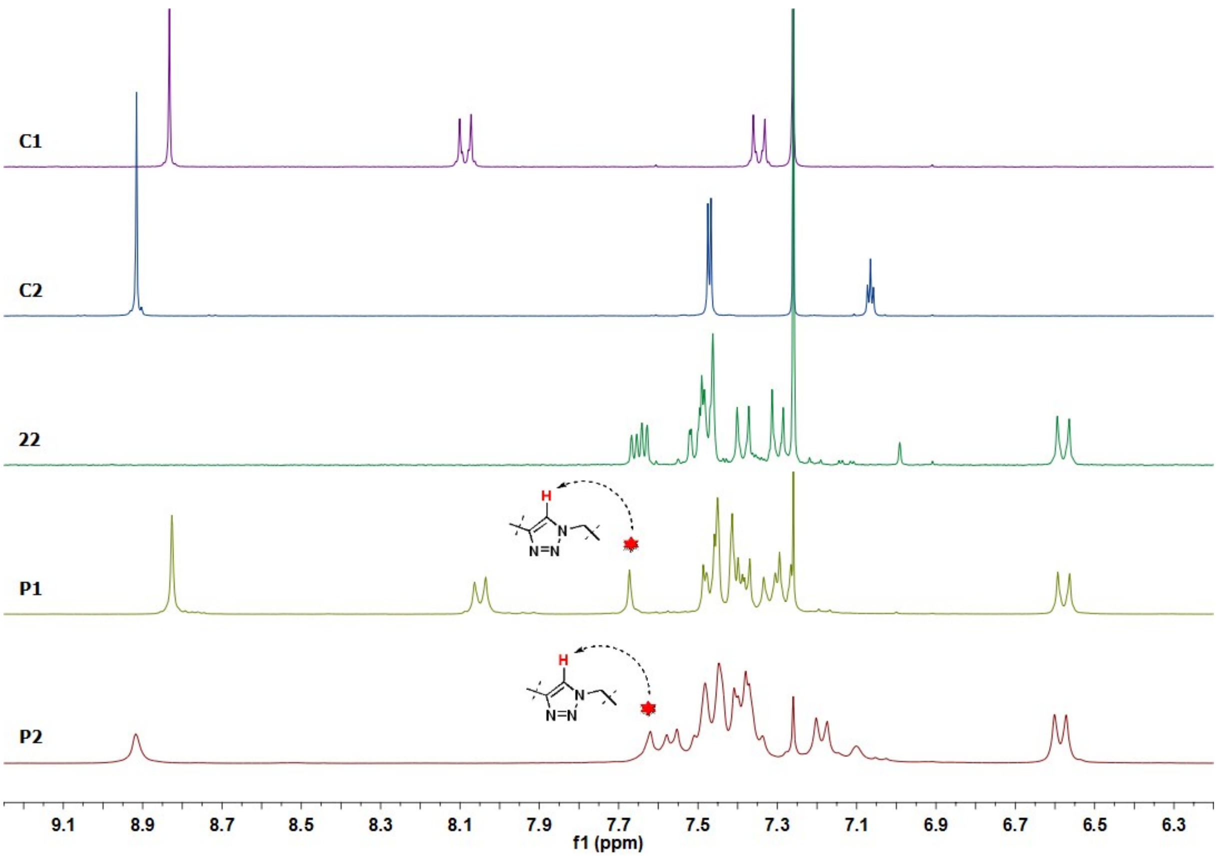

Fig. SI-17 Comparative figure of the aromatic part of the [1]H NMR spectra (300 MHz) for **C1**, **C2**, **22**, **P1** and **P2** showing the appearing of the characteristic triazole proton for compound **P1** and **P2**.

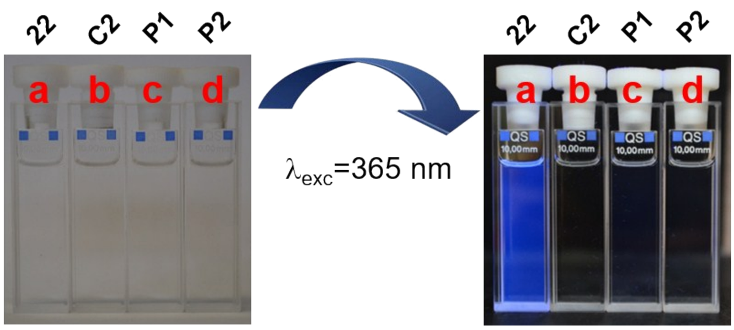

Fig. SI-18 Picture showing the quenching of fluorescence in compounds **P1** and **P2** compared to **22**. Under a handled UV-lamp (λ_{exc} = 365 nm), the intense fluorescence of compound **22** can easily be seen (cell a), whereas compounds **P1** (cell c) and **P2** (cell d) are barely emissive. **C2** is added for comparison.

A B

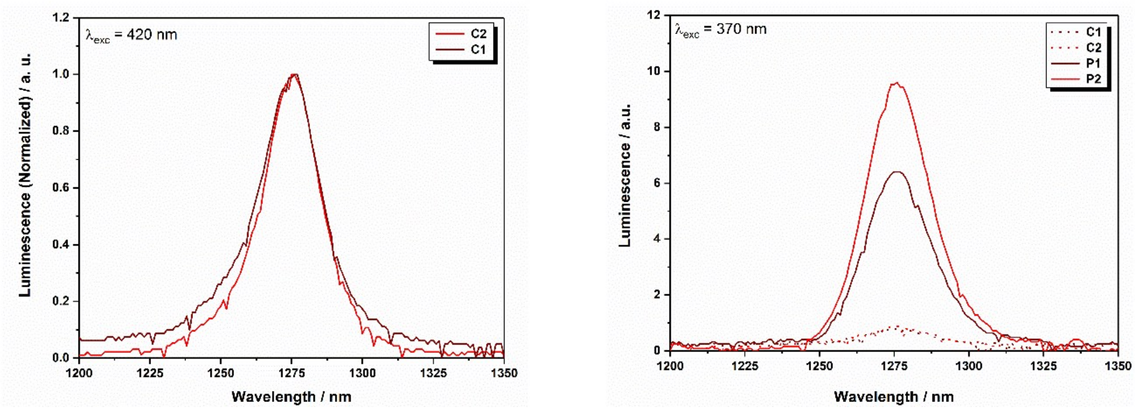

Fig. SI-19 A) Singlet oxygen luminescence observed in aerated dichloromethane solution of **C1** and **C2** following irradiation in the Soret band at $\lambda_{exc} = 420$ nm. B) Singlet oxygen luminescence observed in aerated dichloromethane solution of **P1** and **P2** following irradiation in the antenna at $\lambda_{exc} = 370$ nm. Note that for this excitation wavelength the generation of singlet oxygen by **C1** and **C2** is negligible.

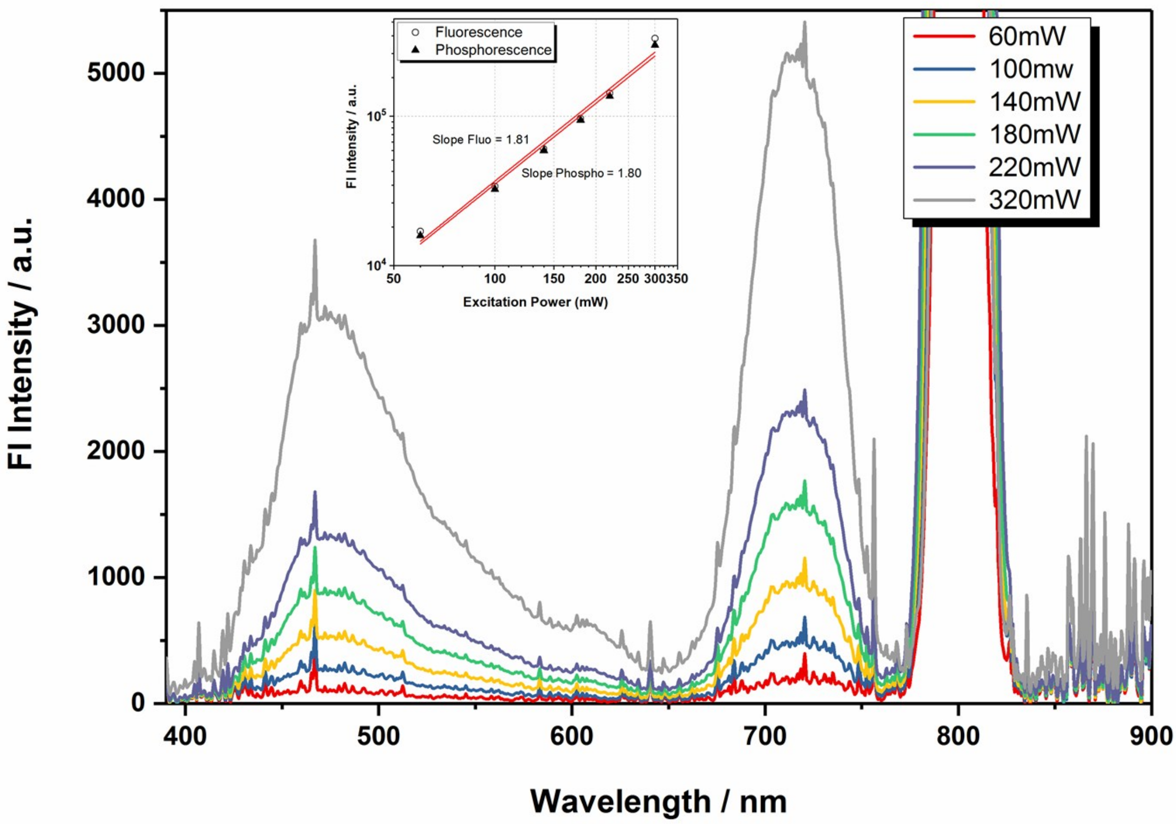

Fig. SI-20 Emission spectra of **P1** upon two-photon excitation (λ_{Laser} = 800 nm) at different laser excitation powers. Emission spectra were recorded with a cut-off filter explaining the deformation of the red part of the phosphorescence signal. Inset: power dependence emission intensity *vs* laser excitation power for the residual fluorescence (○) and the phosphorescence (▲) showing the quadratic dependence.

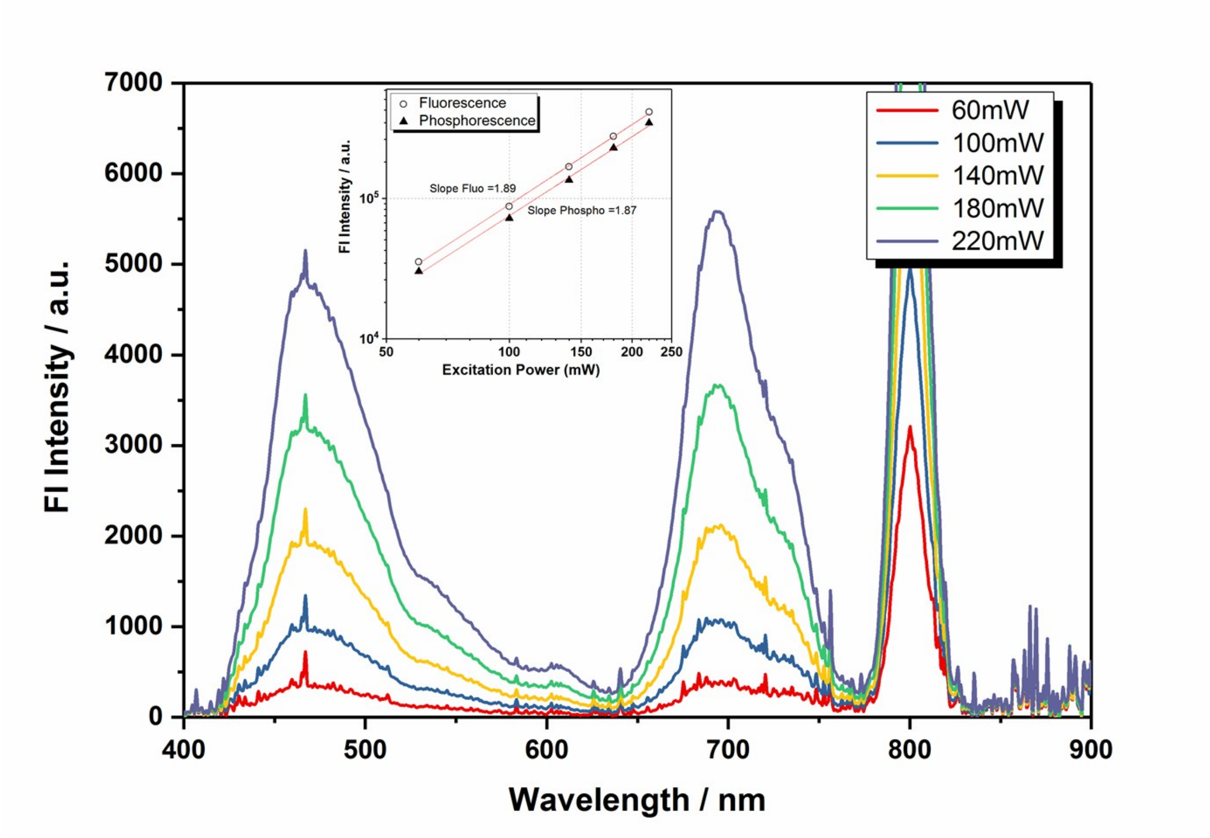

Fig. SI-21 Emission spectra of **P1** upon two-photon excitation (λ_{Laser} = 800 nm) at different laser excitation powers. Emission spectra were recorded with a cut-off filter explaining the deformation of the red part of the phosphorescence signal. Inset: power dependence emission intensity *vs* laser excitation power for the residual fluorescence (○) and the phosphorescence (▲) showing the quadratic dependence.

Compound characterization data

1-(hexylthio)-4-[2-(trimethylsilyl)ethynyl]benzene: ^{1}H NMR (300 MHz, $CDCl_3$)

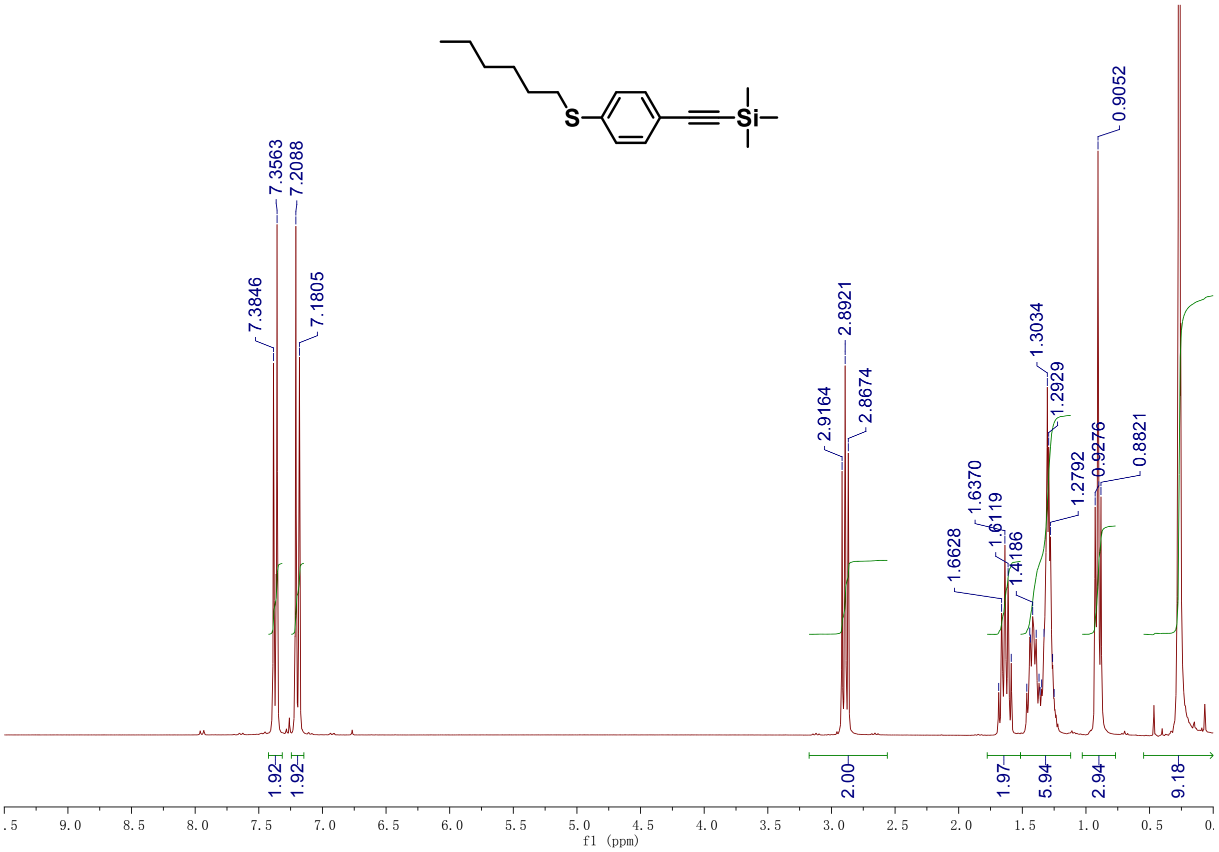

1-(hexylthio)-4-[2-(trimethylsilyl)ethynyl]benzene: ^{13}C NMR (75 MHz, $CDCl_3$)

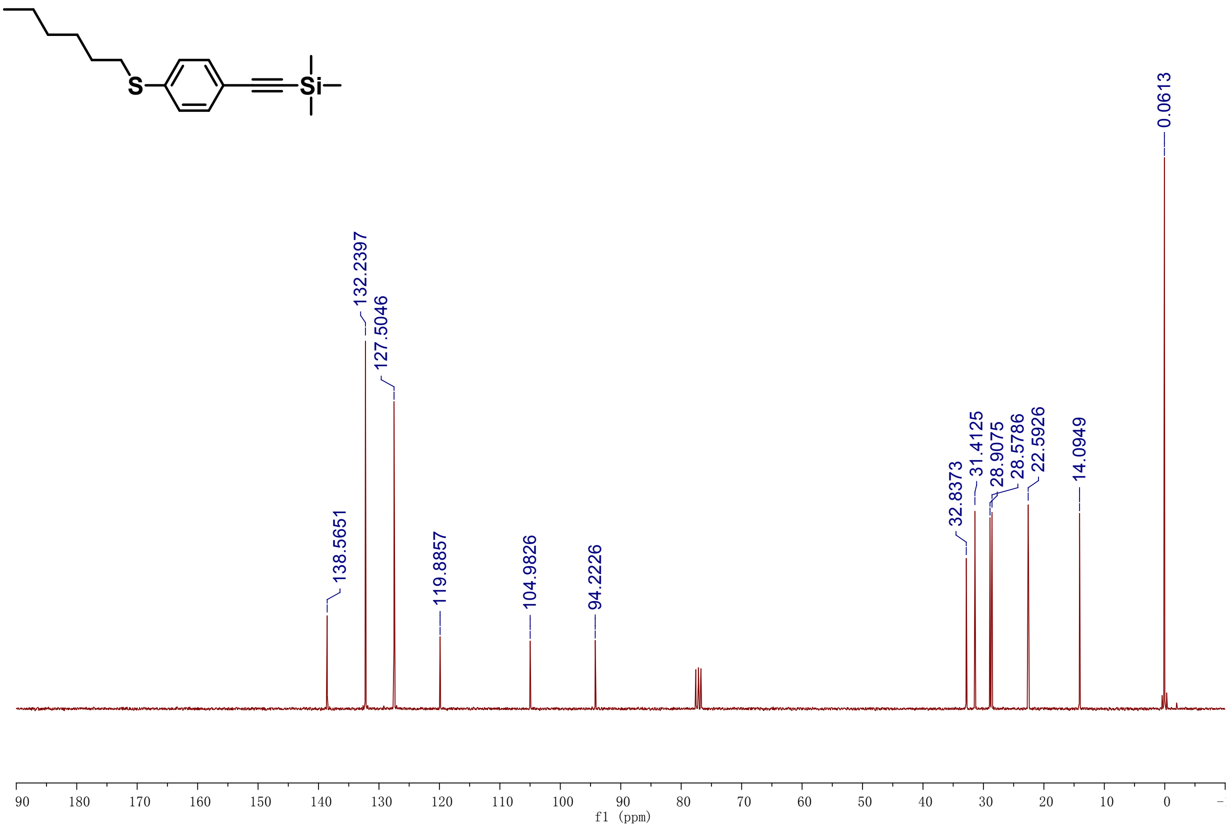

1-(hexylthio)-4-[2-(trimethylsilyl)ethynyl]benzene: HR-MS

CENTRE COMMUN DE SPECTROMETRIE DE MASSE

Analysis Info

Analysis Name	QTOF_150330_26_13.d		
Method	MS_inf_TL_50_1000_2014_woCollSweep_Pos_CCSM.m	Acquisition Date	3/30/2015 2:57:48 PM
Comment		Instrument / Ser#	micrOTOF-Q II 10231

Acquisition Parameter

Source Type	ESI	Ion Polarity	Positive	Set Nebulizer	0.4 Bar
Focus	Not active	Set Capillary	3500 V	Set Dry Heater	200 °C
Scan Begin	50 m/z	Set End Plate Offset	-500 V	Set Dry Gas	4.0 l/min
Scan End	1000 m/z	Set Collision Cell RF	600.0 Vpp	Set Divert Valve	Waste

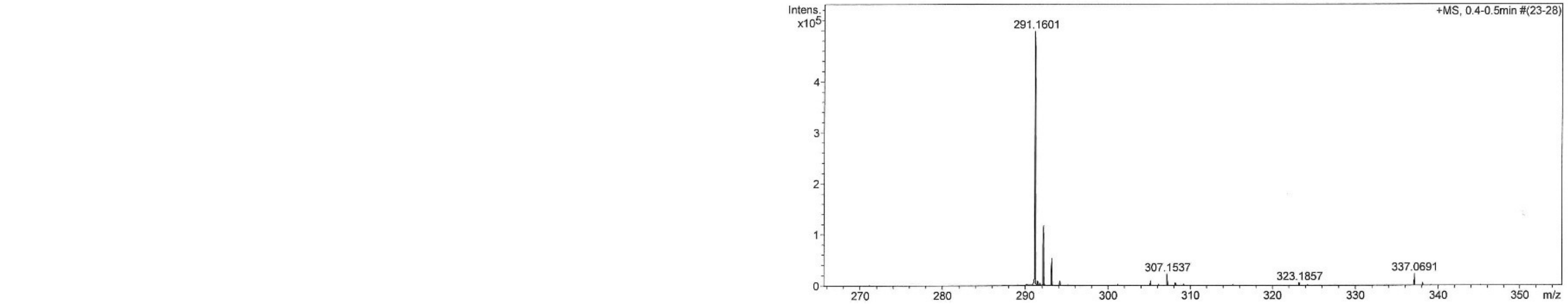

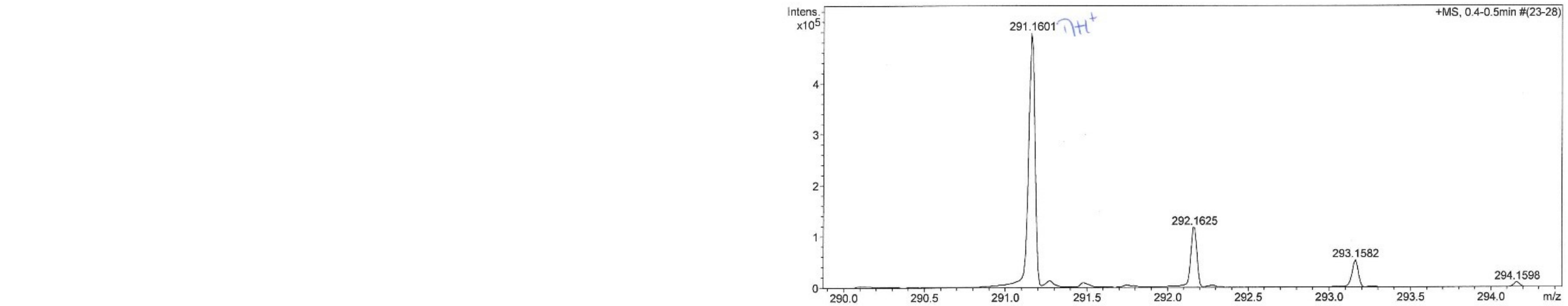

Meas. m/z	Formula	m/z	err [ppm]	mSigma
291.1601	C 17 H 27 S Si	291.1597	-1.1	3.7

Bruker Compass DataAnalysis 4.0 — Page 1 of 1

Compound **9**: ^{1}H NMR (300 MHz, $CDCl_3$)

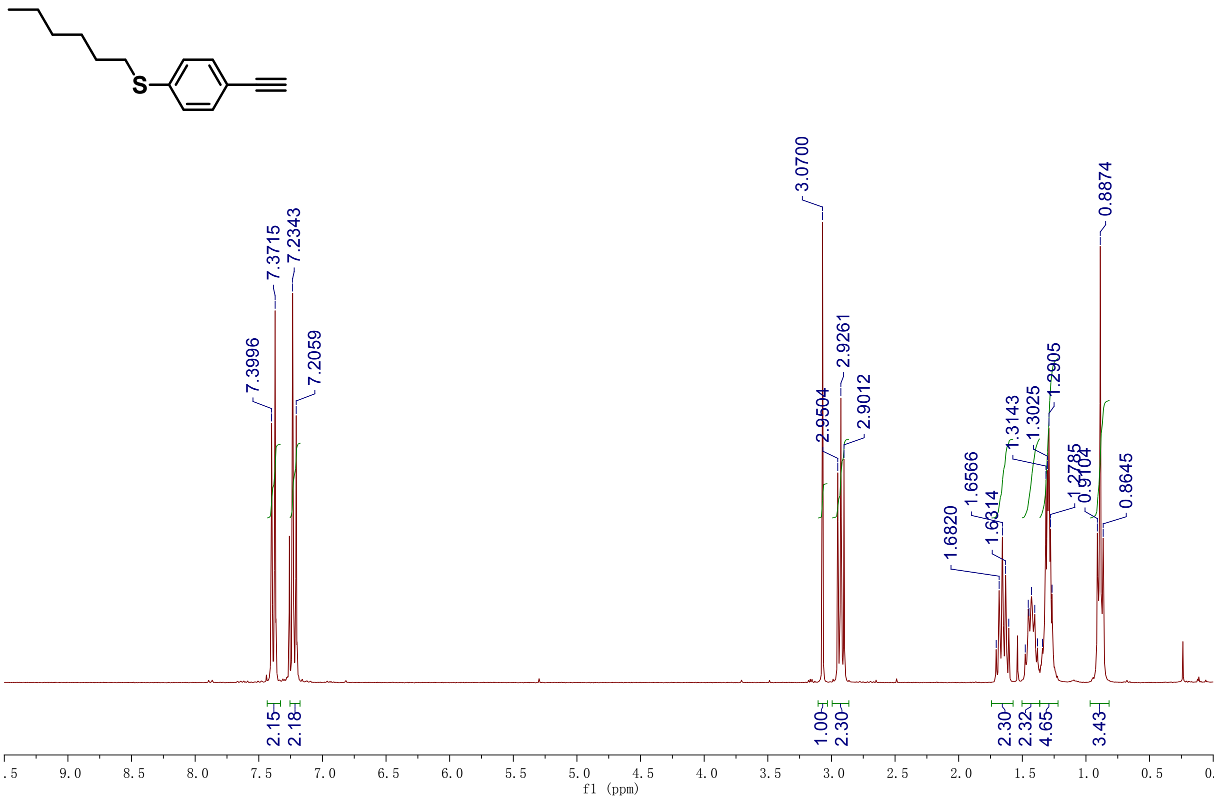

Compound **9**: ^{13}C NMR (75 MHz, $CDCl_3$)

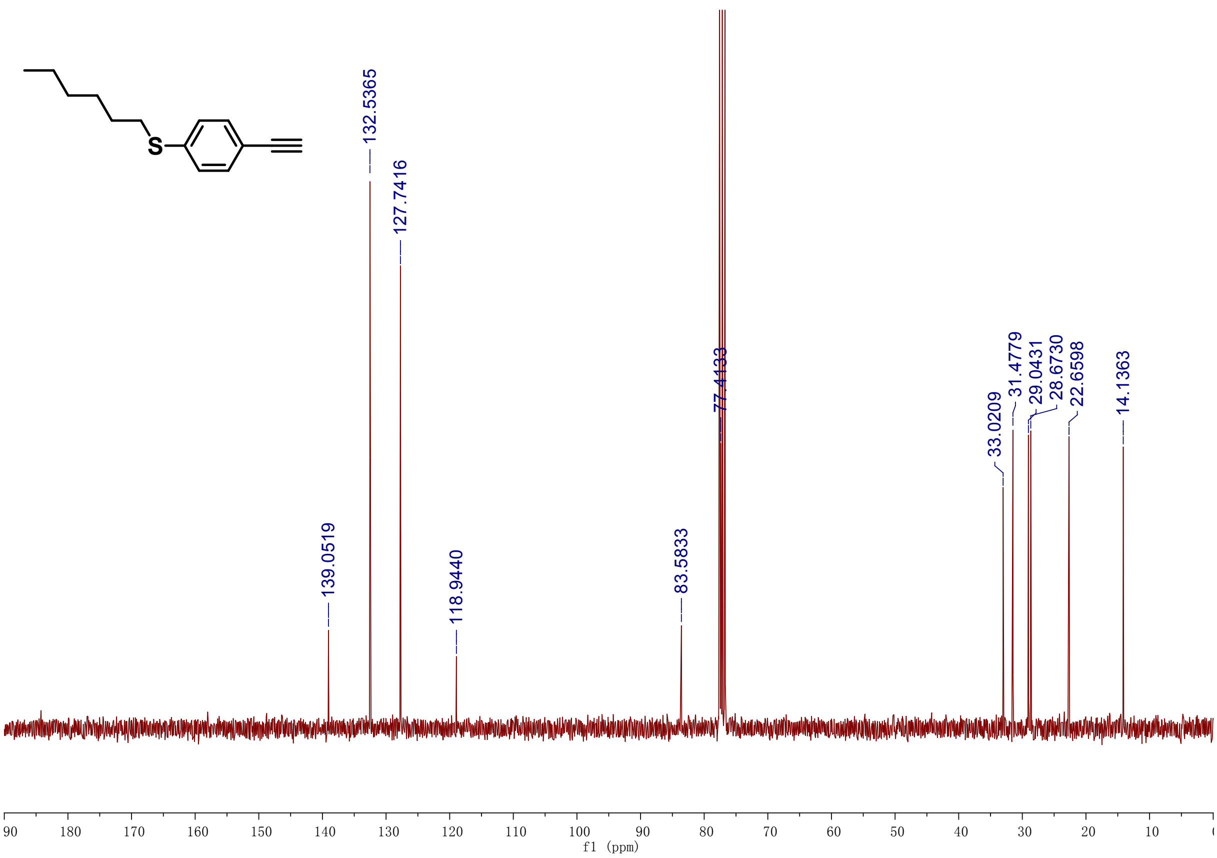

Compound **9**: HR-MS

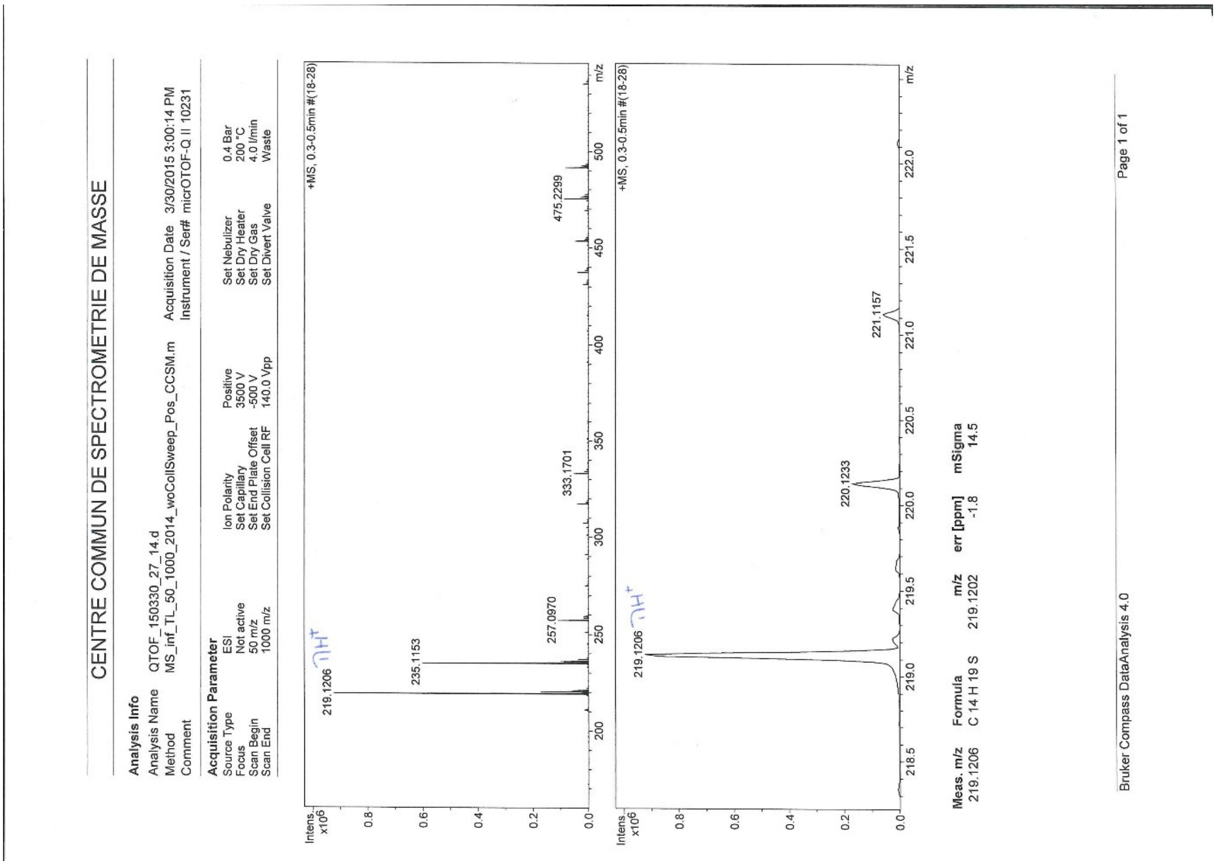

Compound **12**: ^{1}H NMR (300 MHz, $CDCl_3$) full spectrum

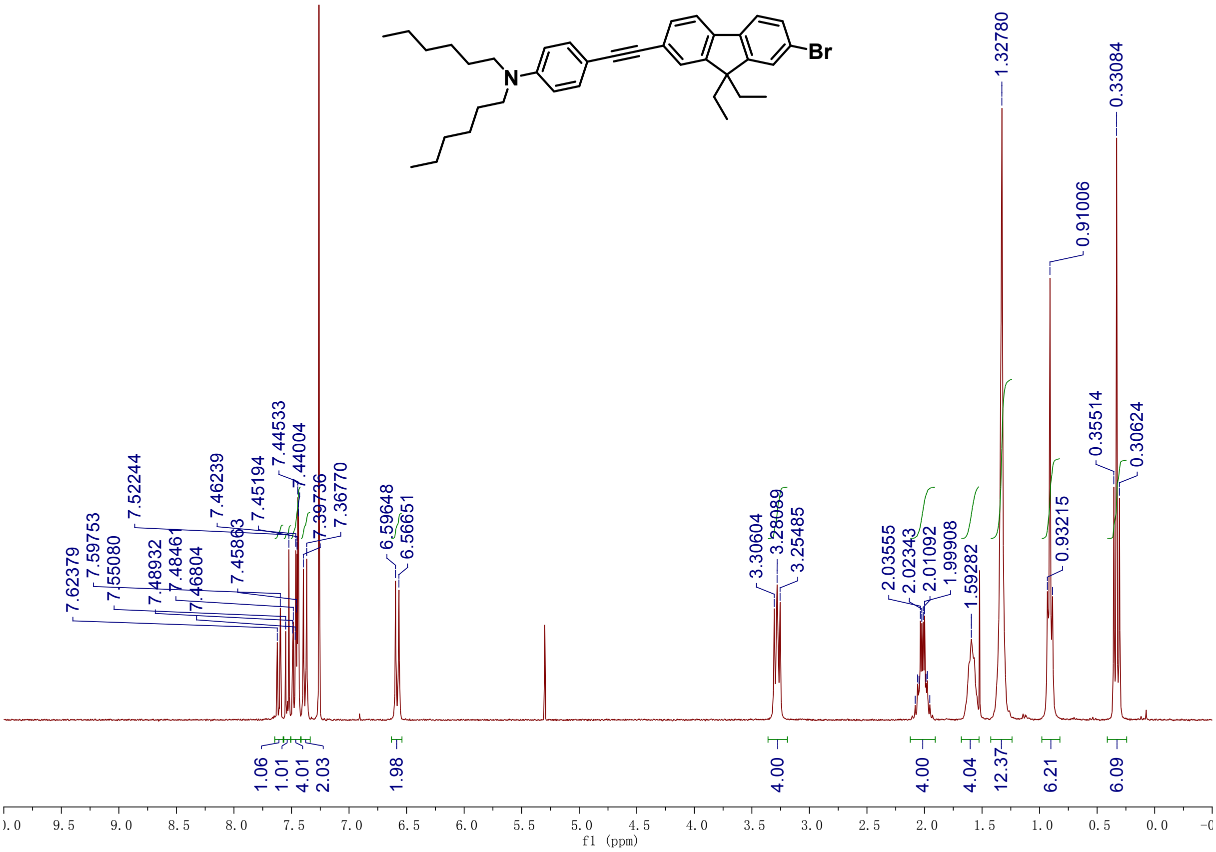

Compound **12**: ^{1}H NMR (300 MHz, $CDCl_3$) expansion aromatic protons

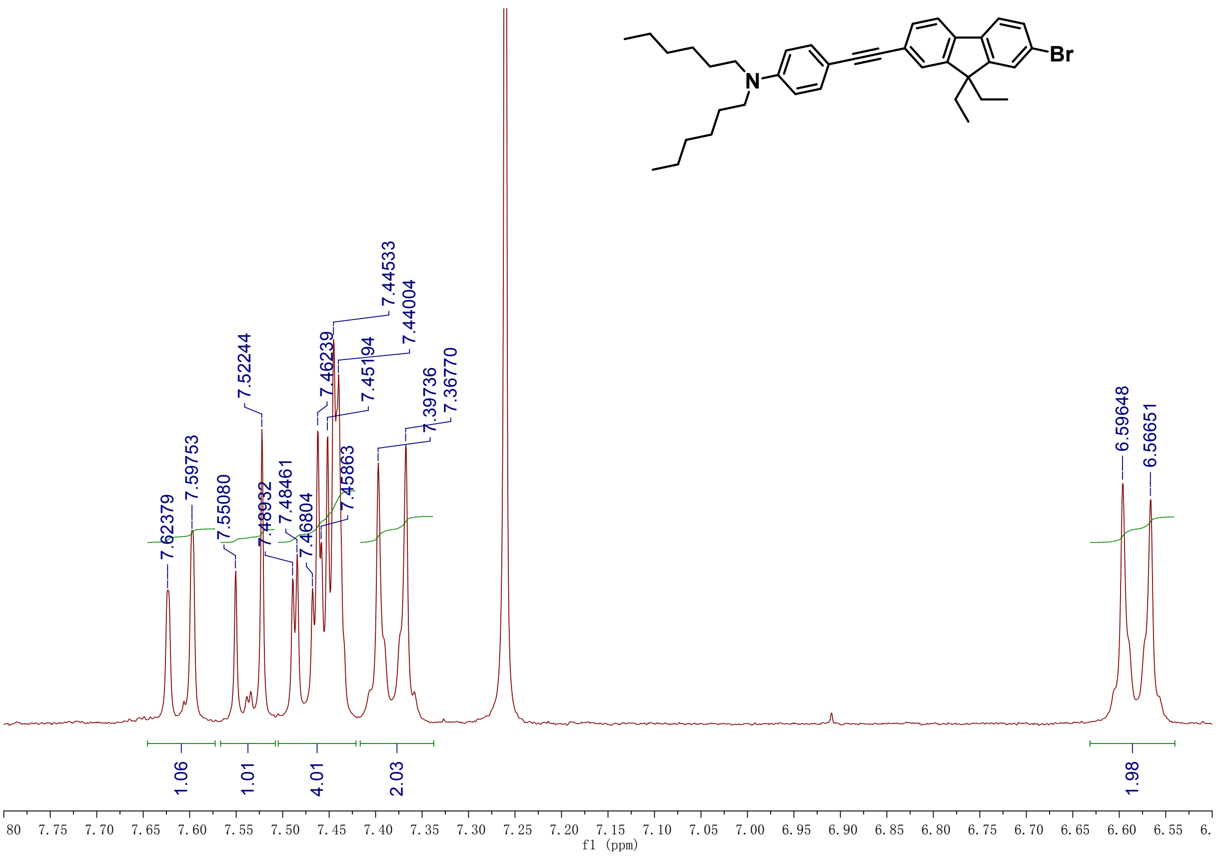

Compound **12**: ^{13}C NMR (75 MHz, $CDCl_3$)

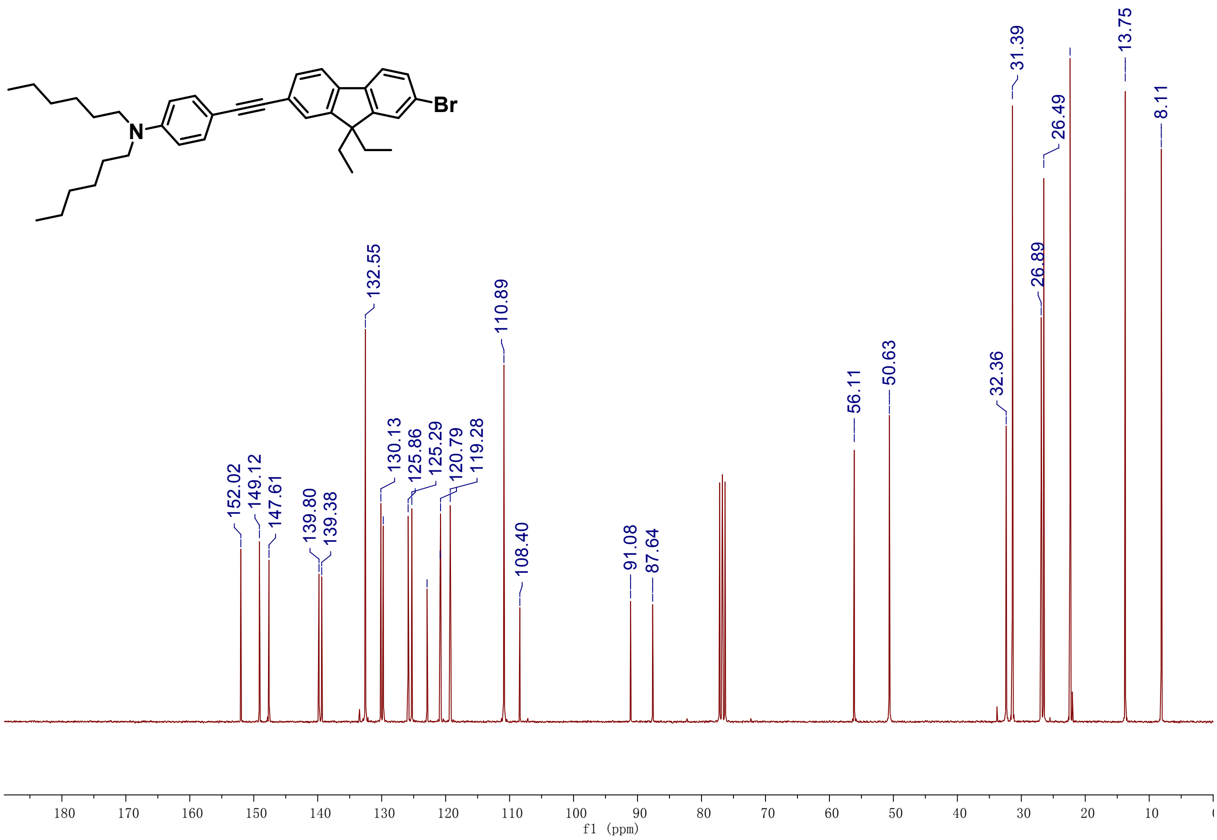

Compound **12**: HR-MS

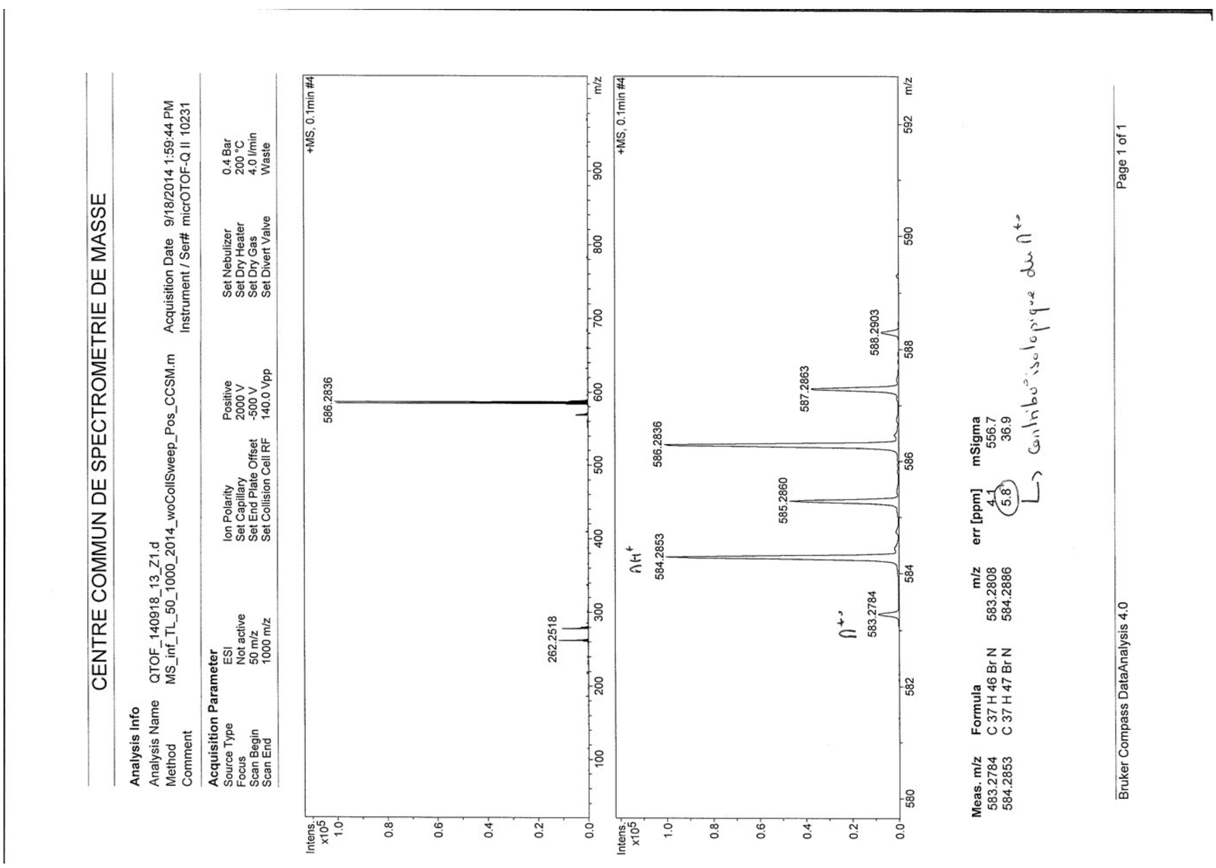

Compound **A2**: ^{1}H NMR (300 MHz, $CDCl_3$)

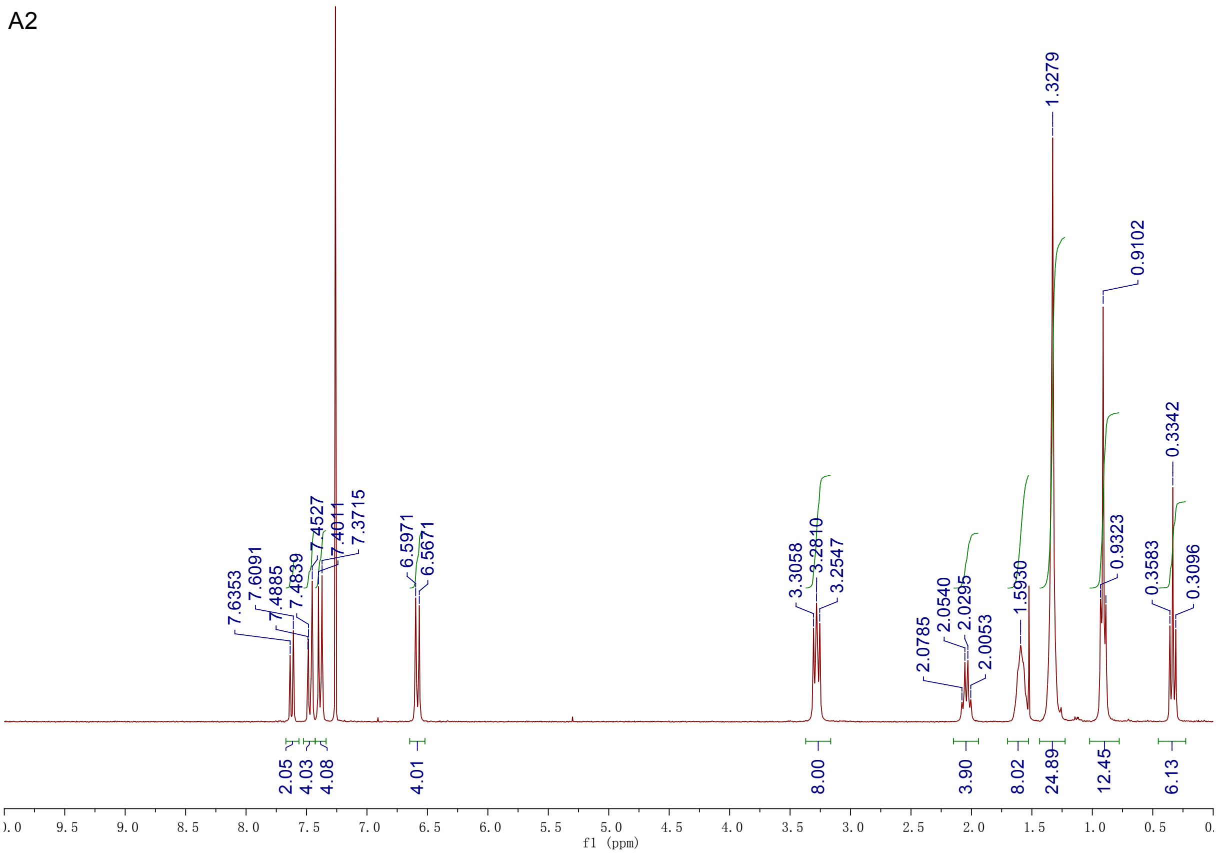

Compound **A2**: ^{13}C NMR (75 MHz, $CDCl_3$)

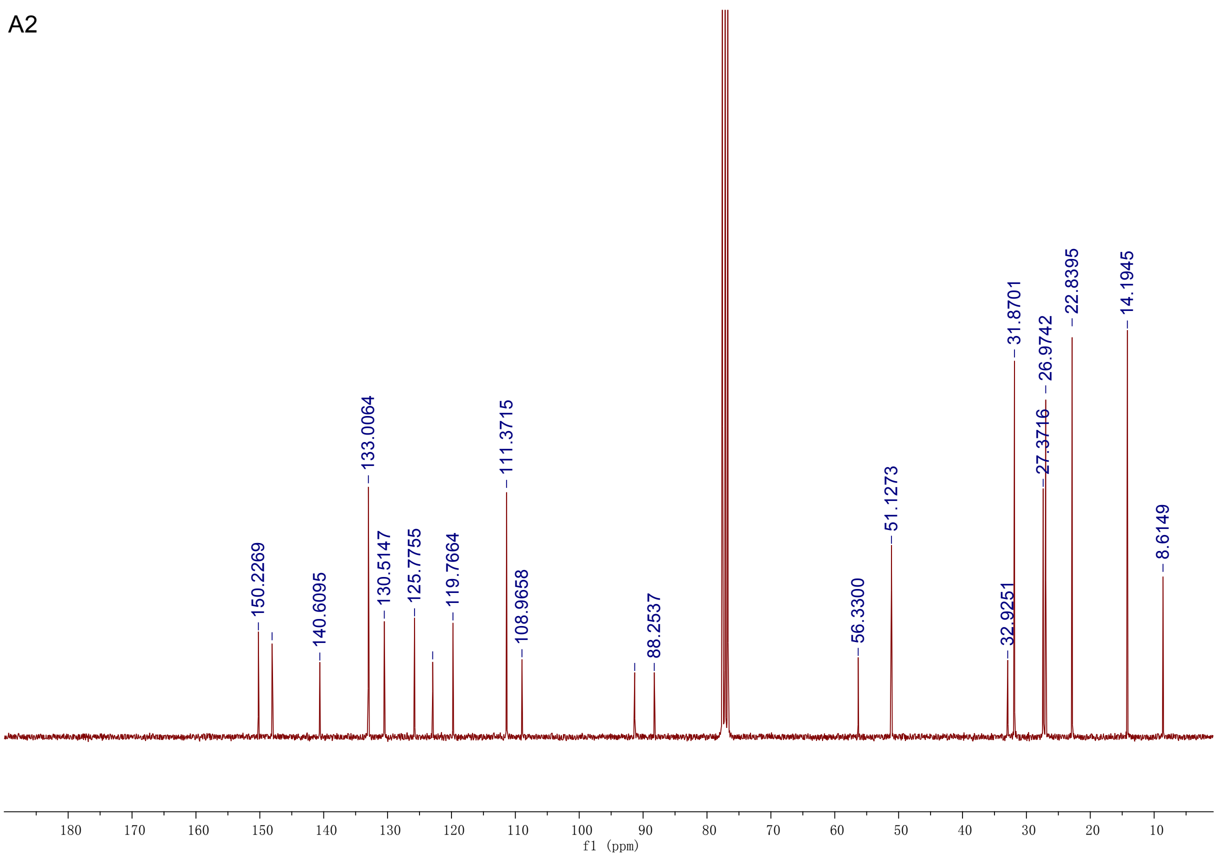

Compound **A2**: HR-MS

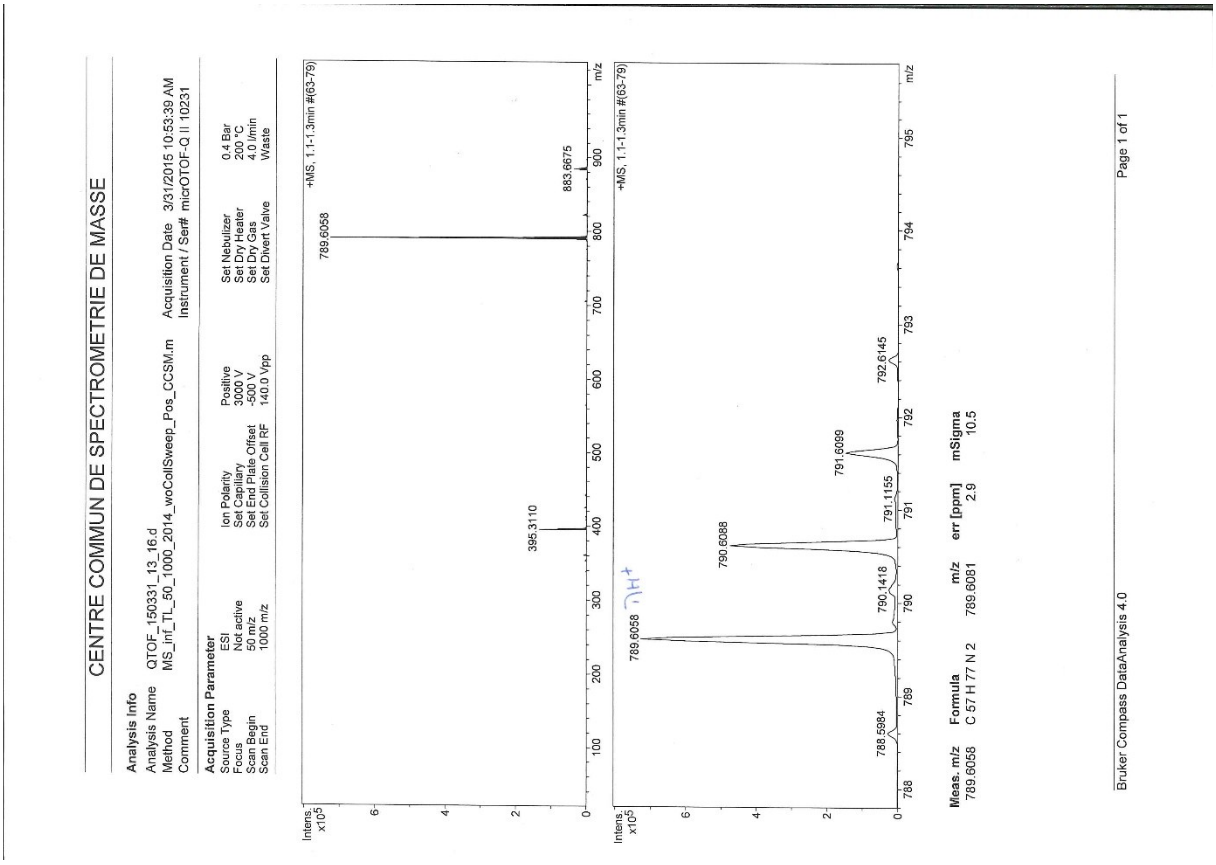

Compound **A3**: ^{1}H NMR (300 MHz, $CDCl_3$) full spectrum

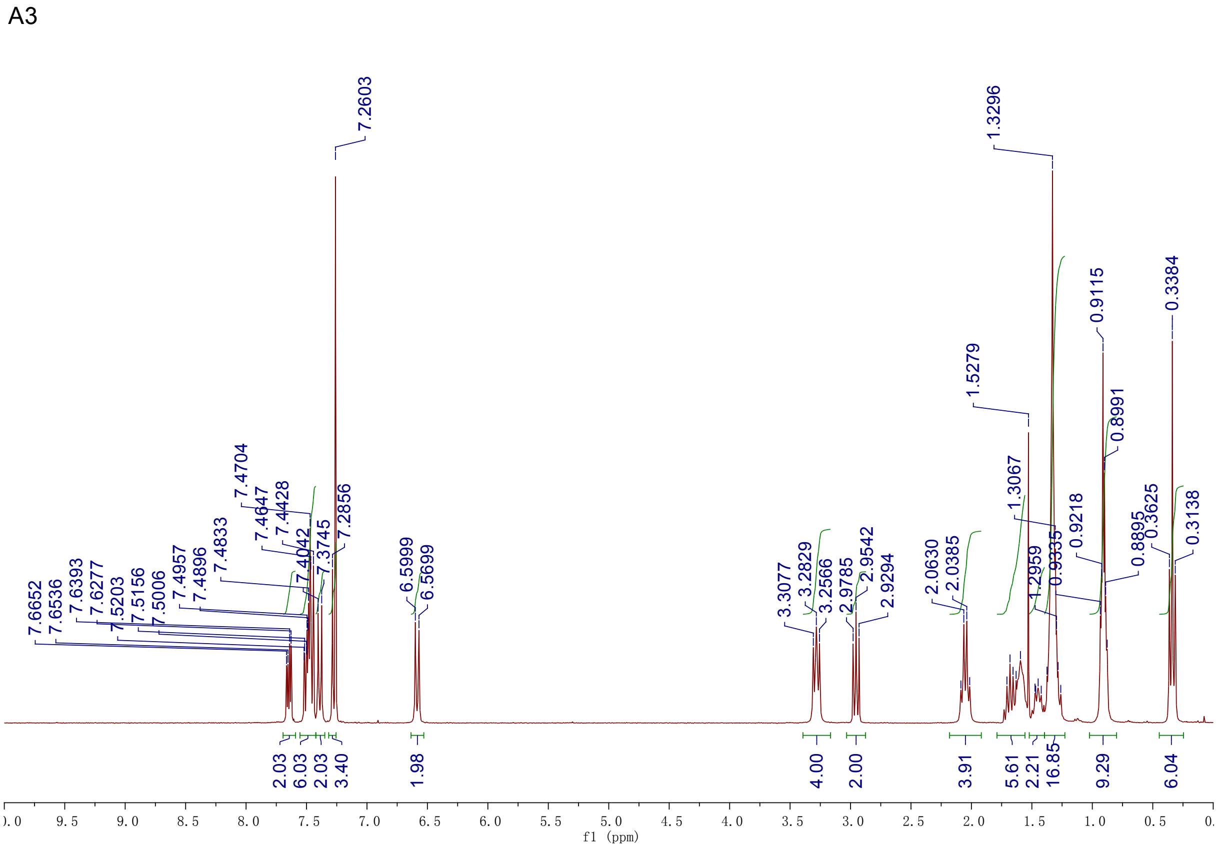

Compound **A3**: ^{1}H NMR (300 MHz, $CDCl_3$) expansion aliphatic protons

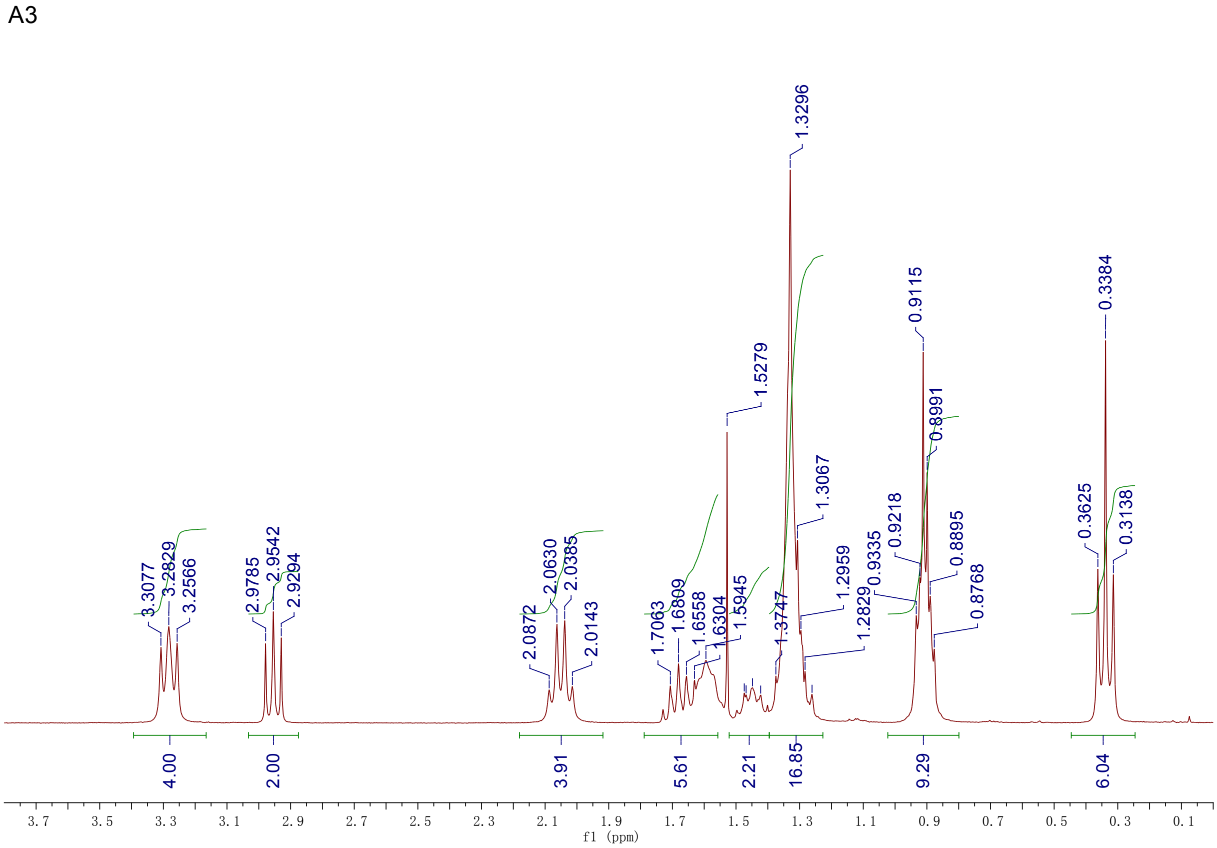

Compound **A3**: ^{1}H NMR (300 MHz, $CDCl_3$) expansion aromatic protons

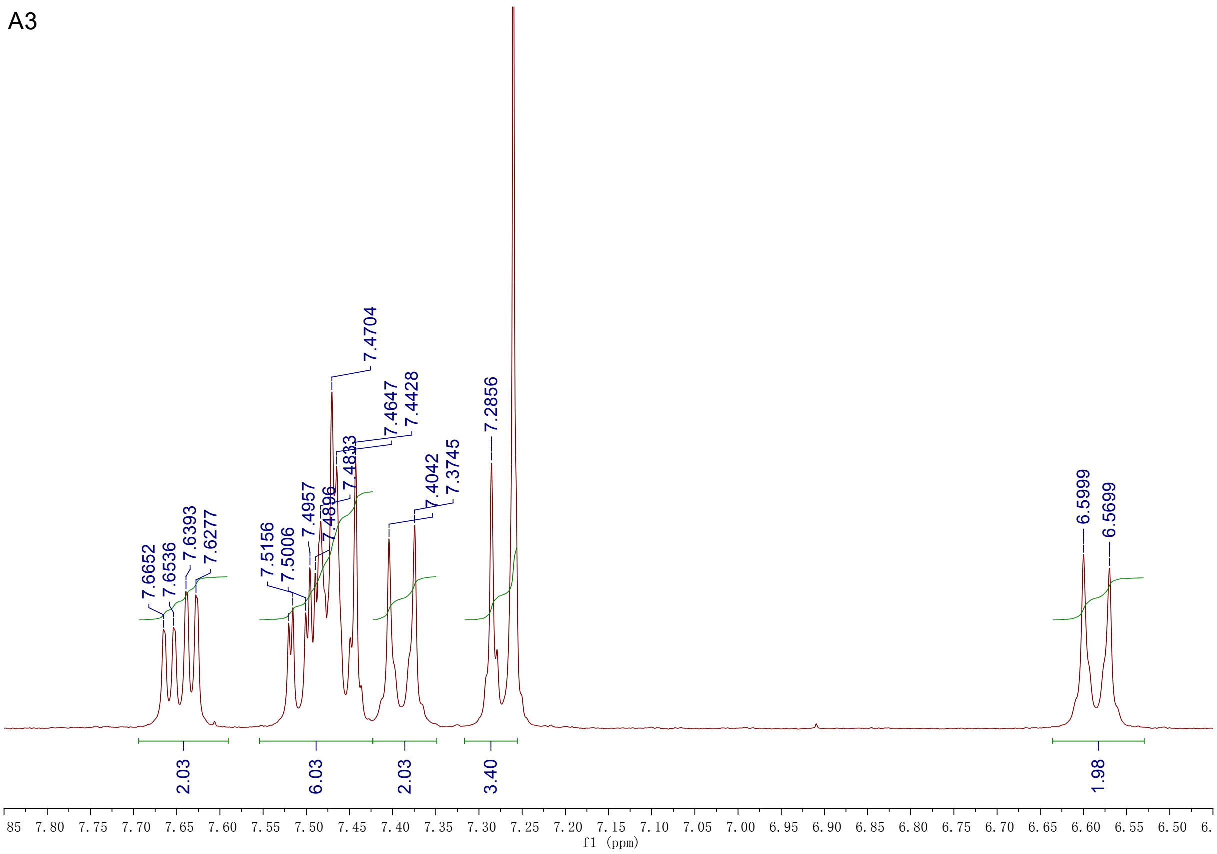

Compound **A3**: ^{13}C NMR (75 MHz, $CDCl_3$)

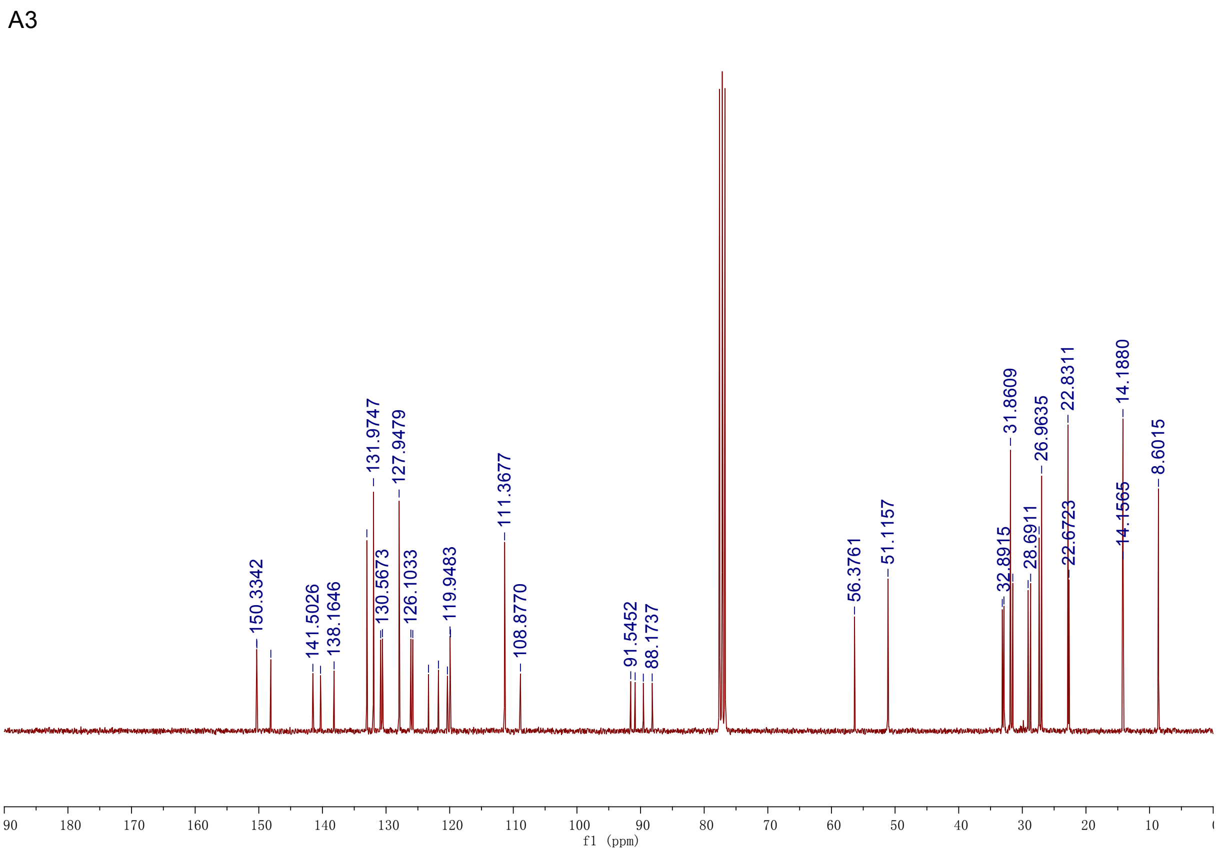

Compound **A3**: HR-MS

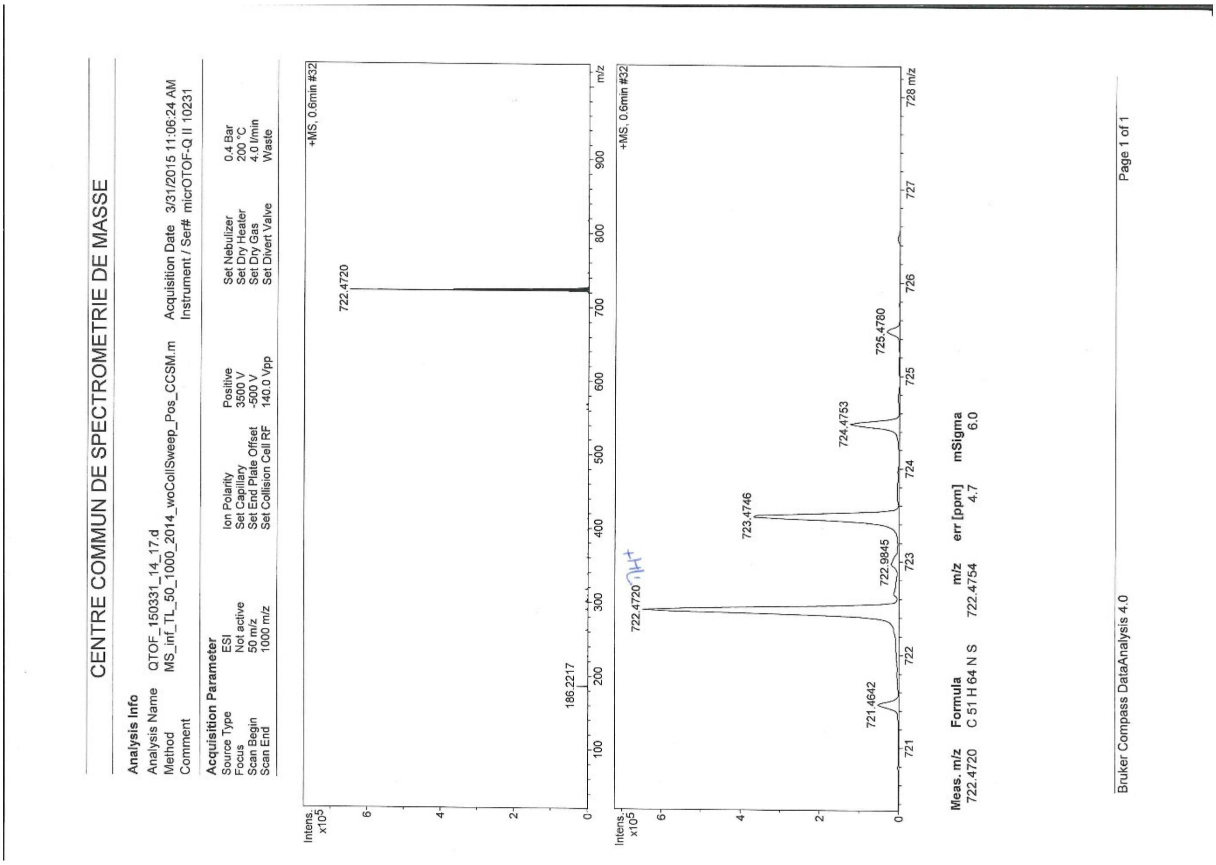

Compound **A4**: ^{1}H NMR (300 MHz, $CDCl_3$) full spectrum

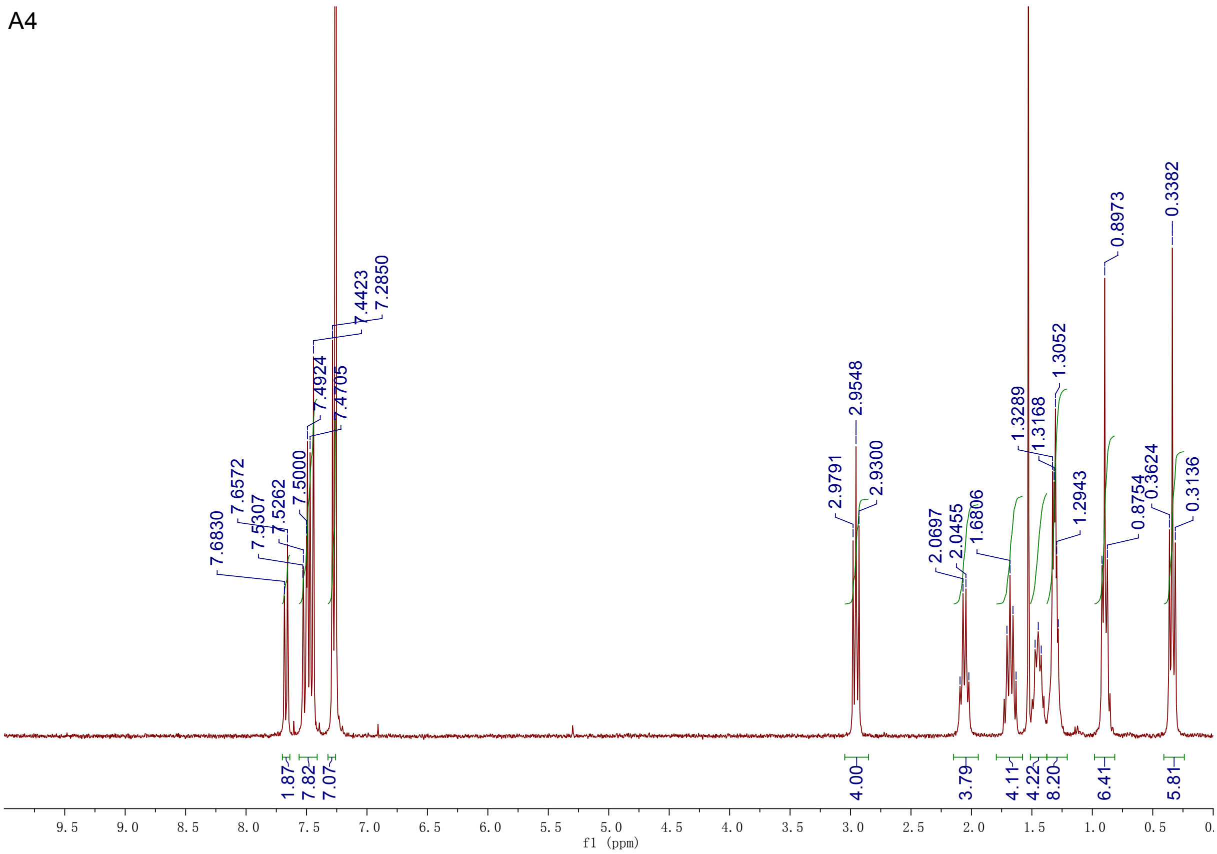

Compound **A4**: ^{1}H NMR (300 MHz, $CDCl_3$) expansion aromatic protons

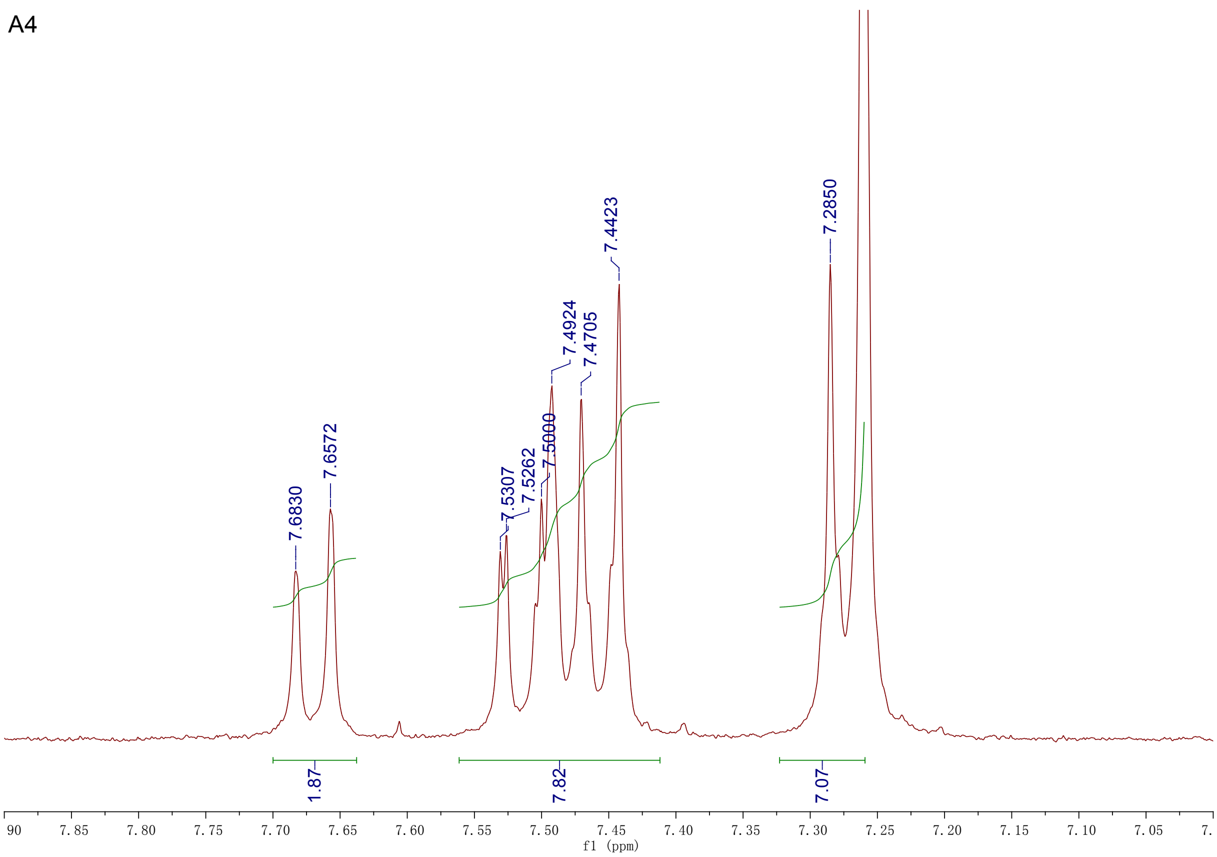

Compound **A4**: ^{13}C NMR (75 MHz, $CDCl_3$)

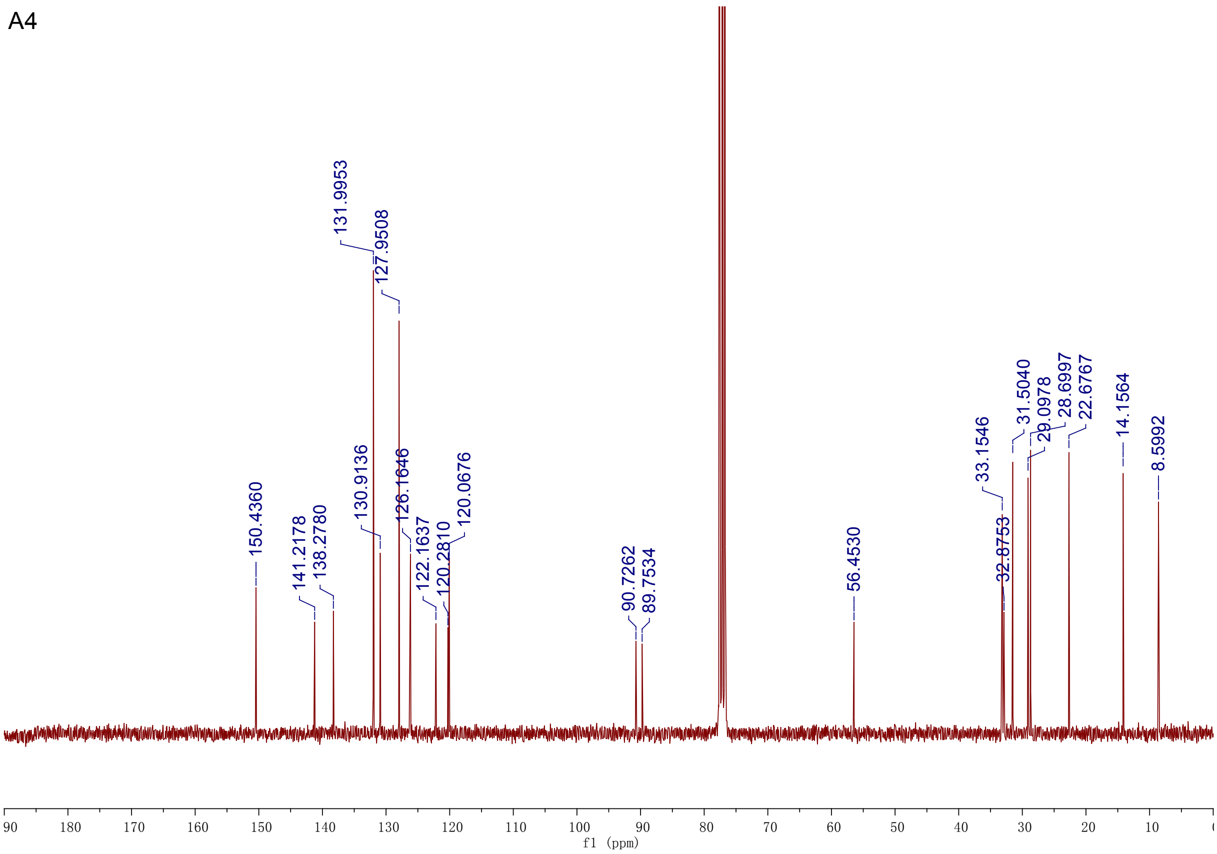

Compound **A4**: HR-MS

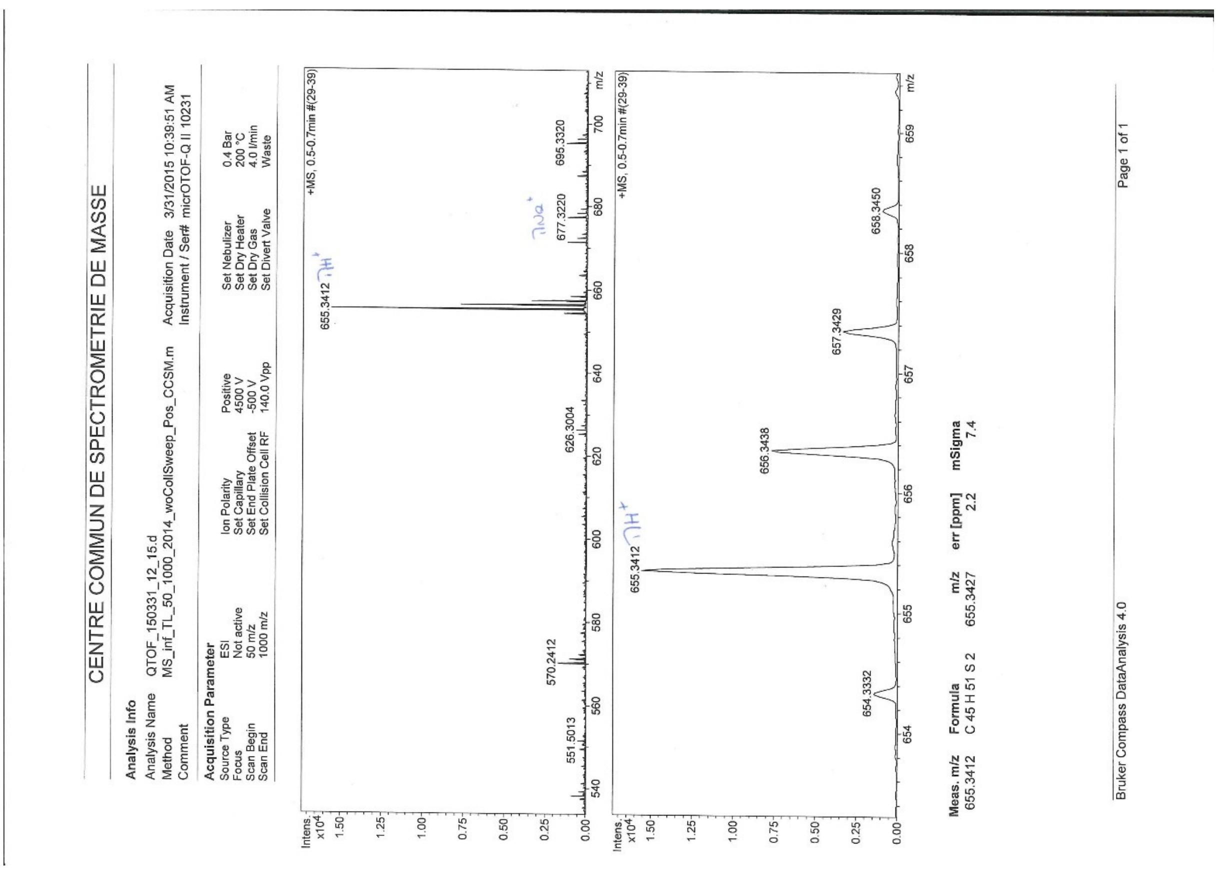

Compound **13**: ^{1}H NMR (300 MHz, Acetone-d_6)

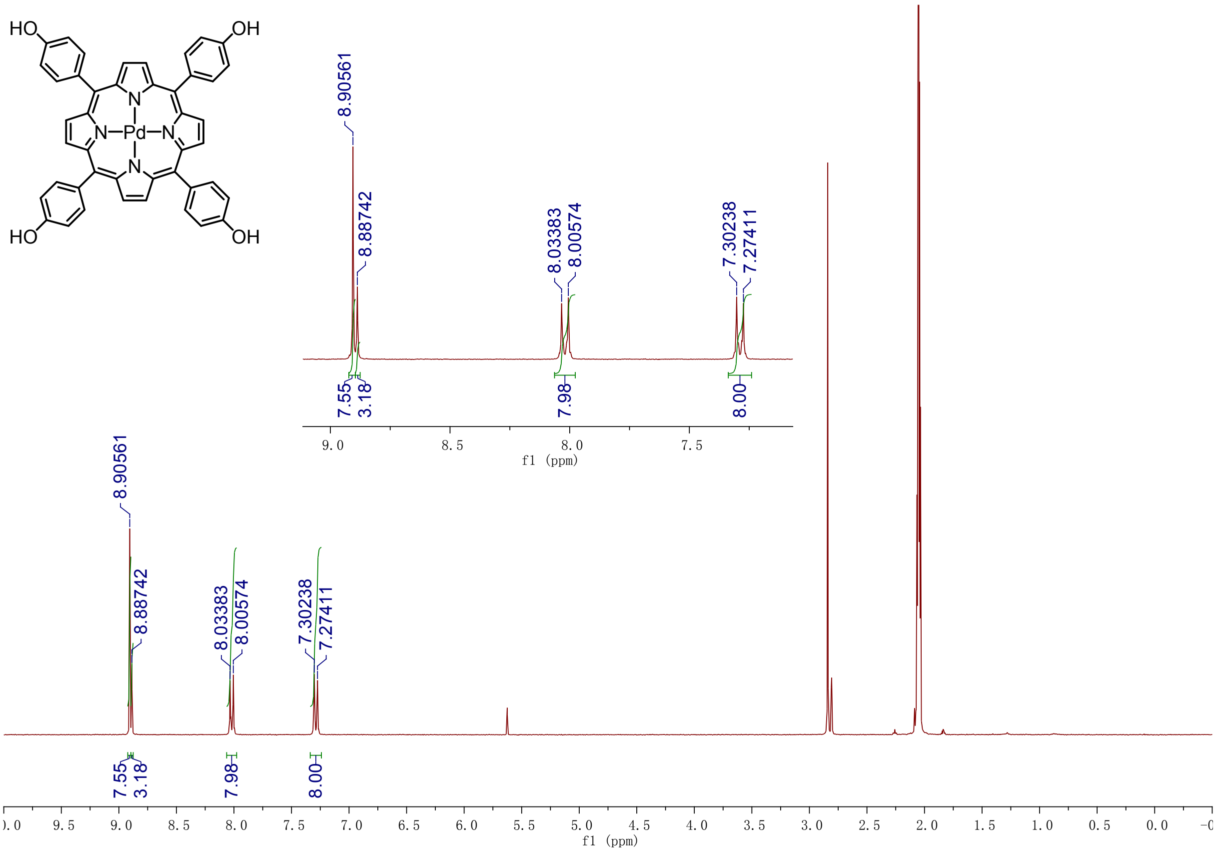

Compound **13**: ^{13}C NMR (75 MHz, Acetone-d_6)

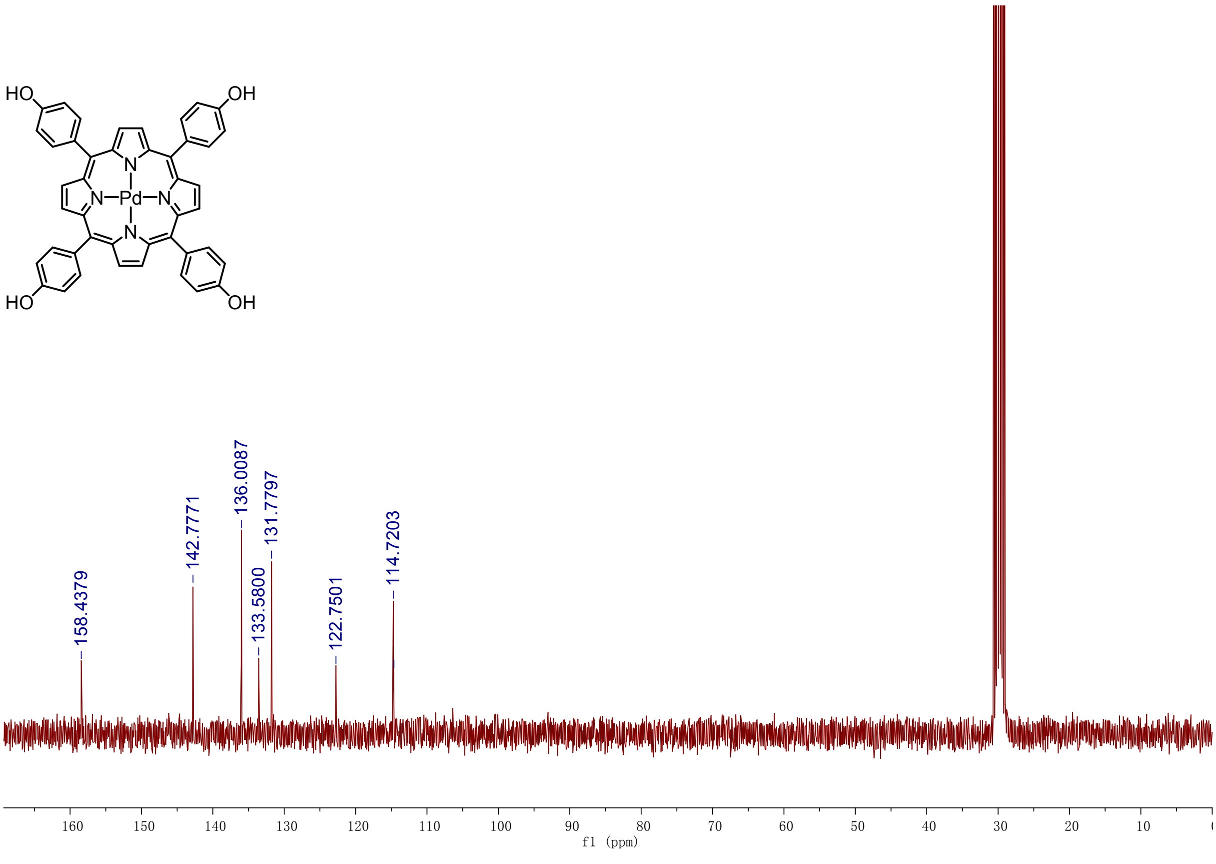

Compound **13**: HR-MS

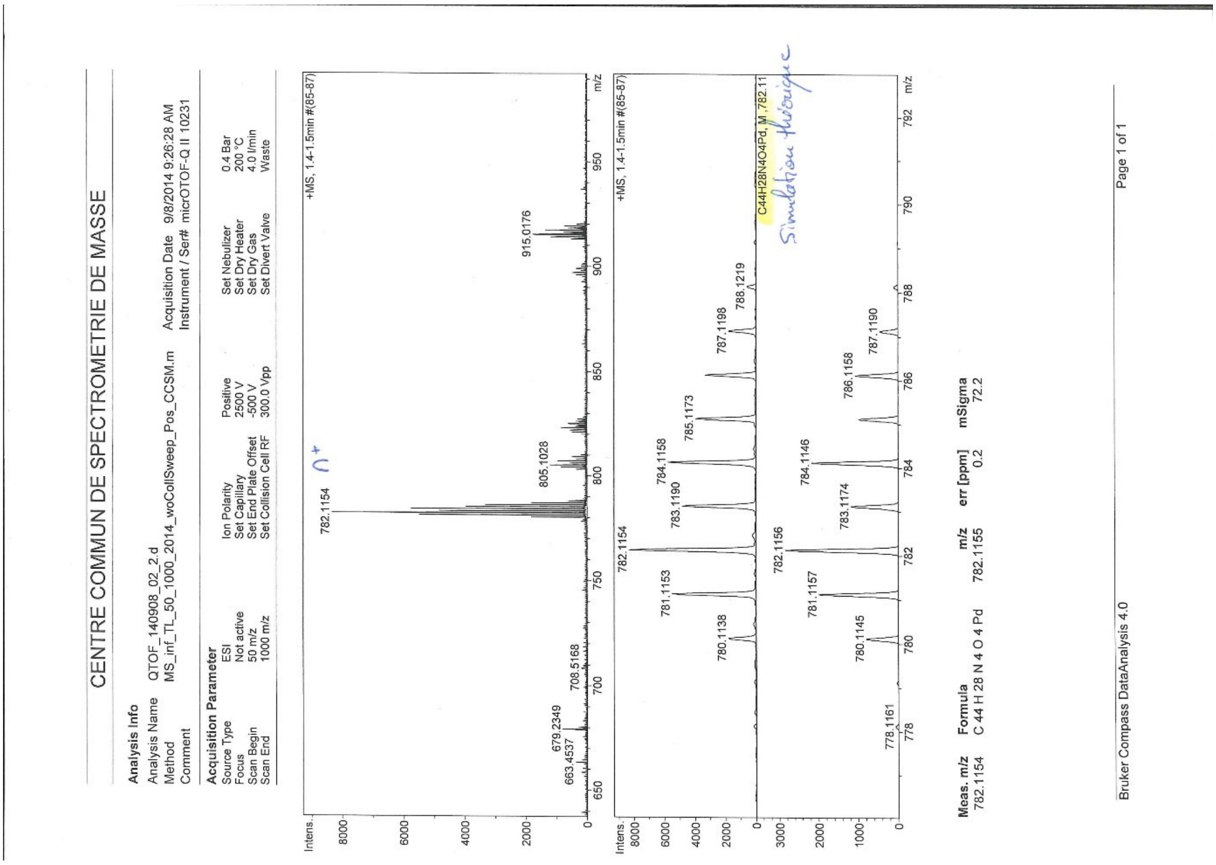

Compound **14**: ^{1}H NMR (300 MHz, $CDCl_3$)

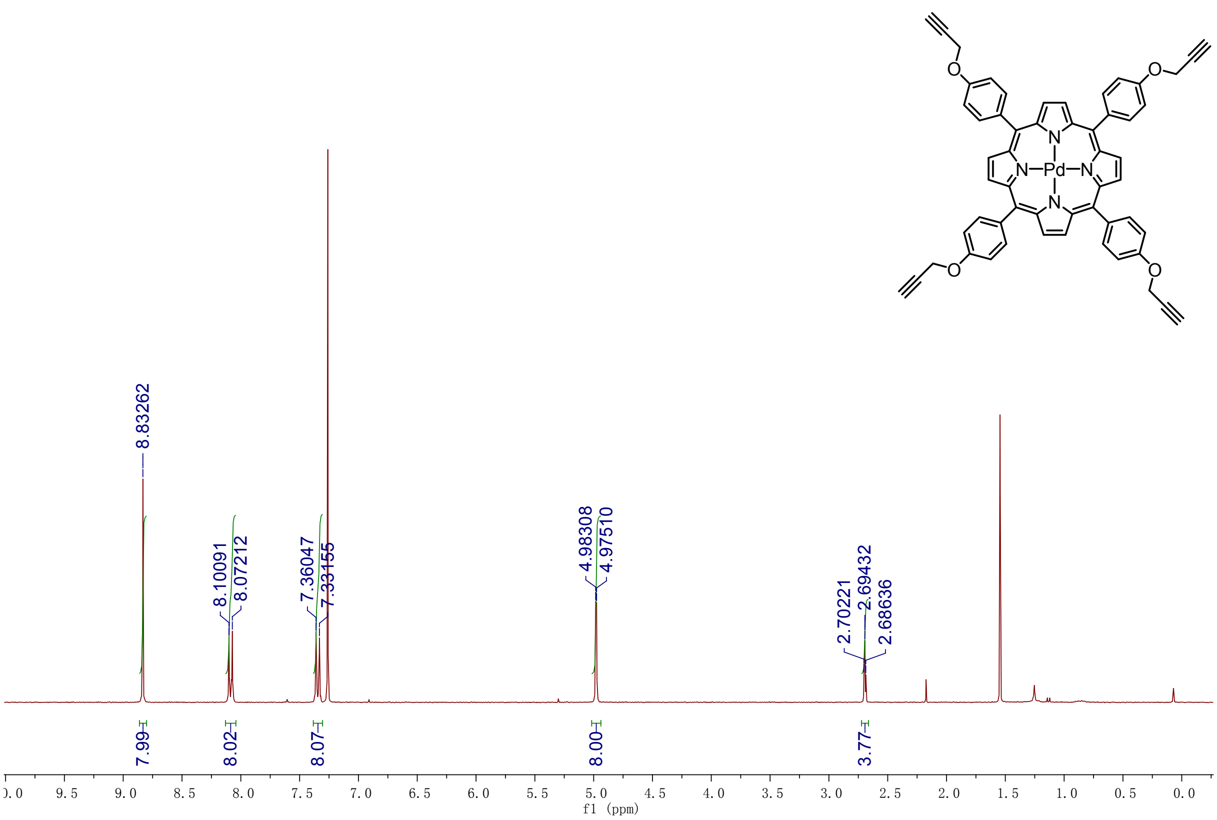

Compound **14**: ^{13}C NMR (75 MHz, $CDCl_3$)

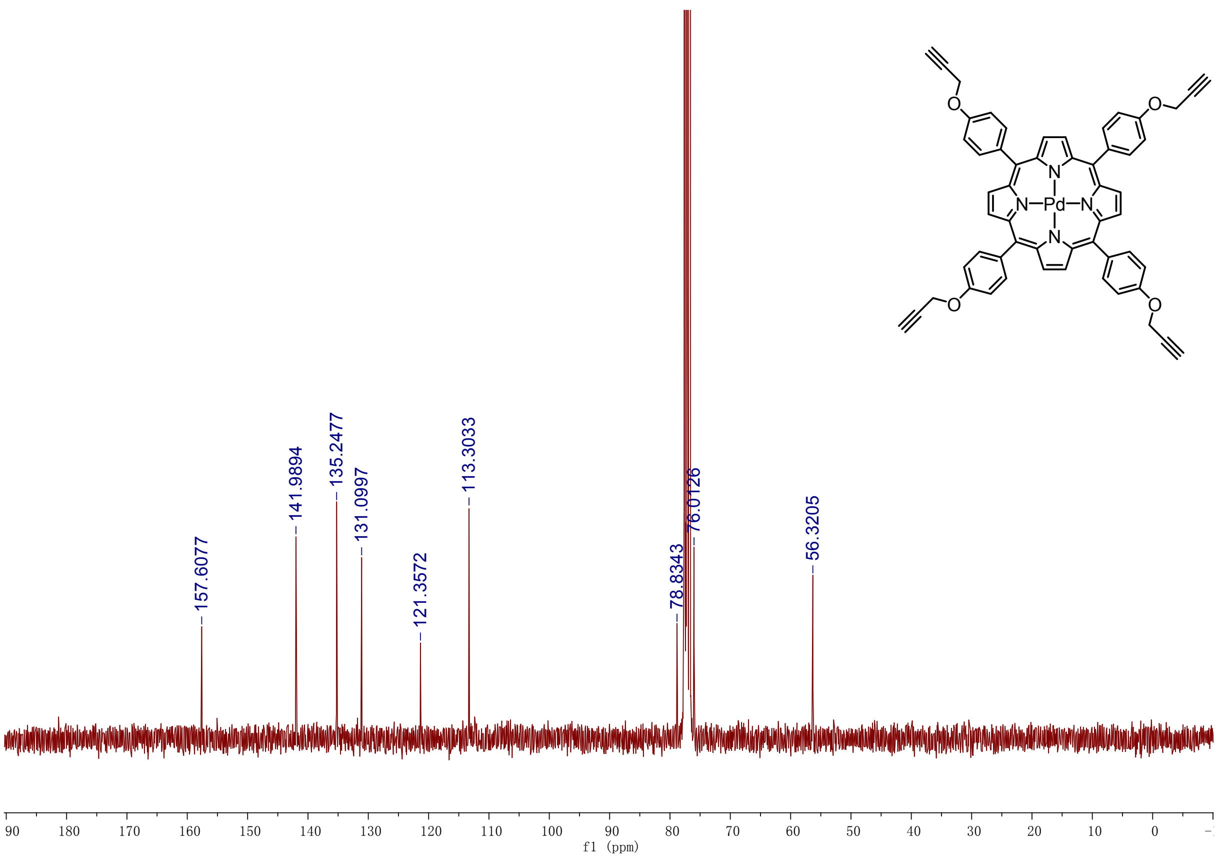

Compound **14**: HR-MS

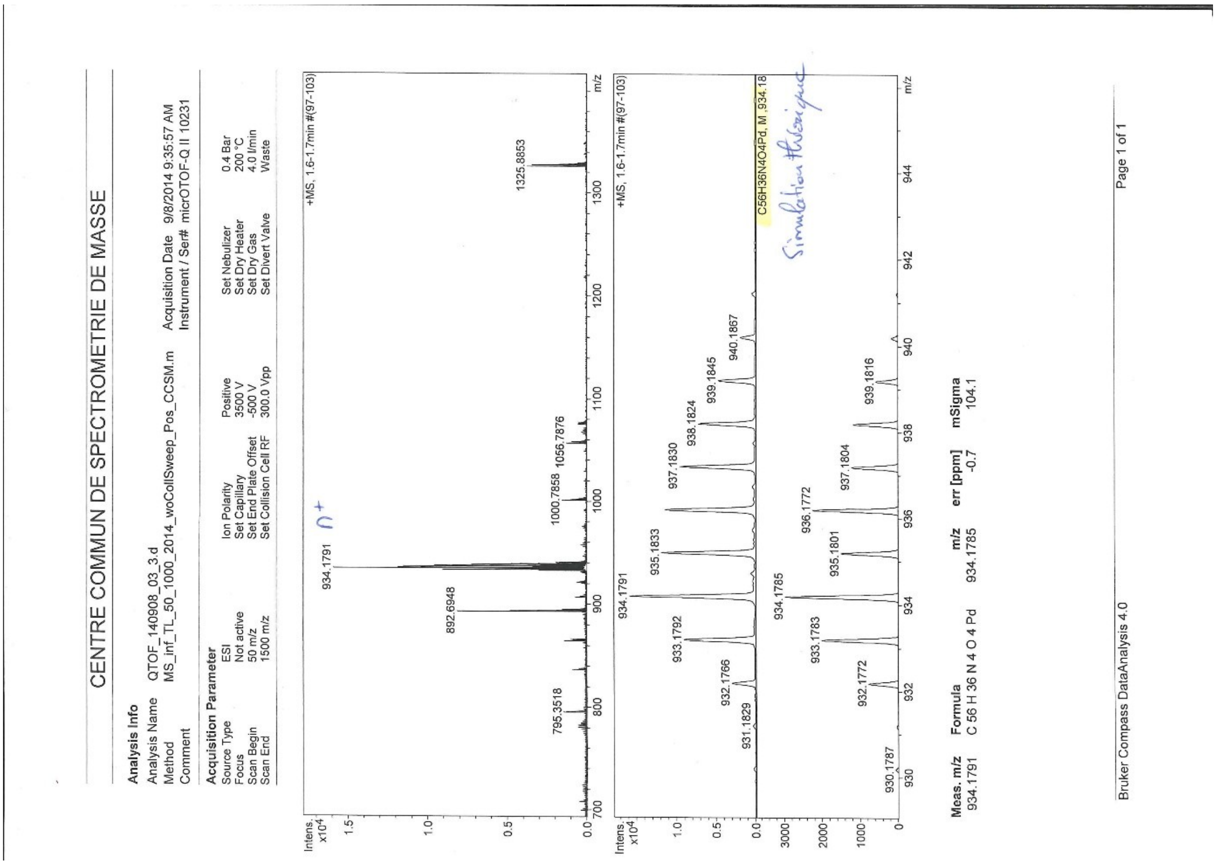

Compound **15**: ^{1}H NMR (300 MHz, Acetone-d_6)

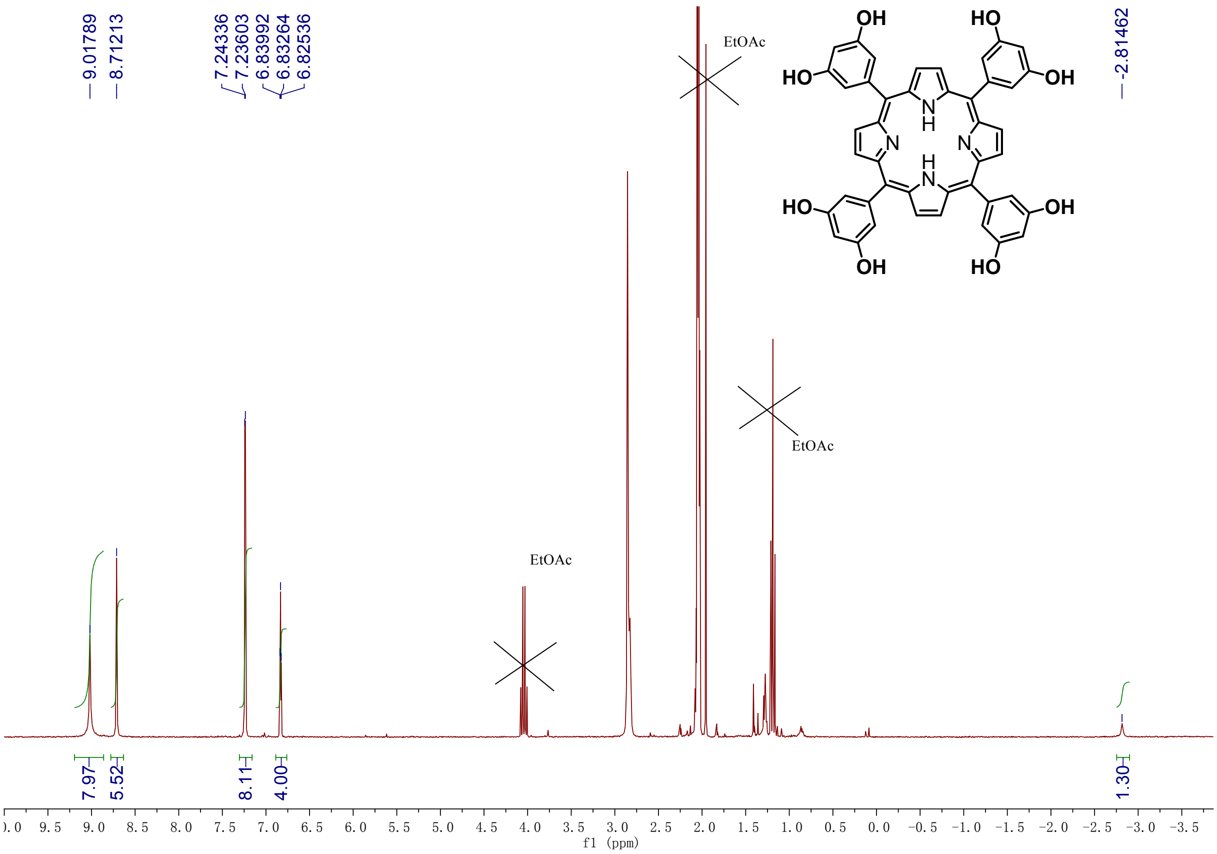

Compound **15**: ^{13}C NMR (75 MHz, Acetone-d_6)

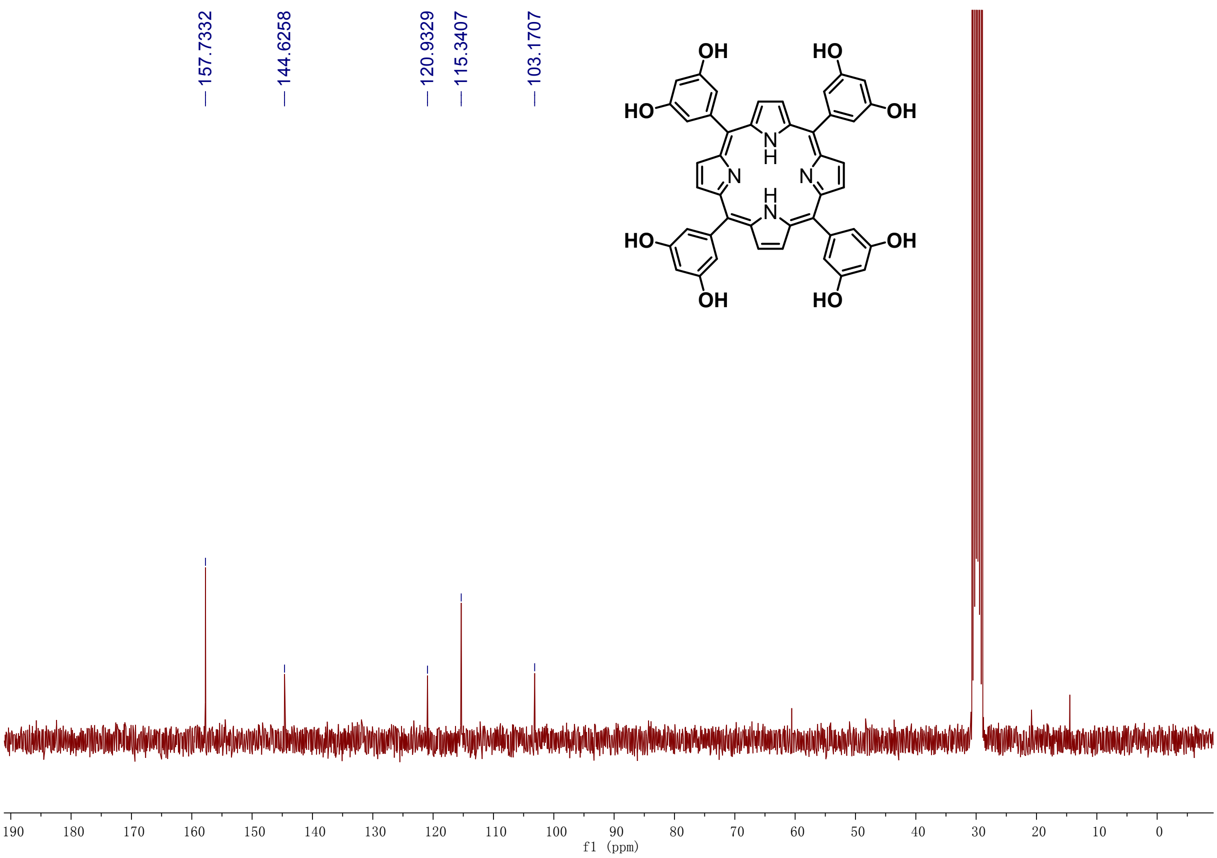

Compound **15**: HR-MS

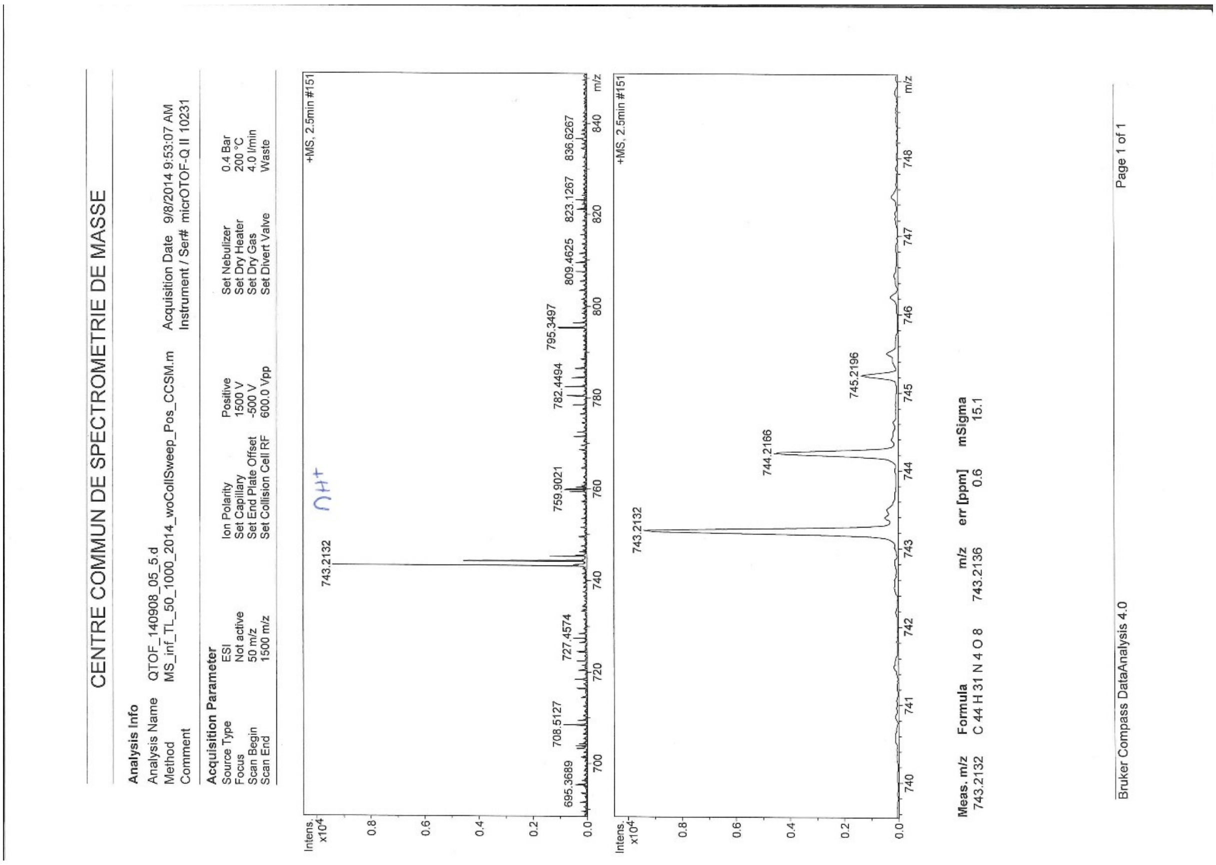

Compound **16**: ^{1}H NMR (300 MHz, Acetone-d_6)

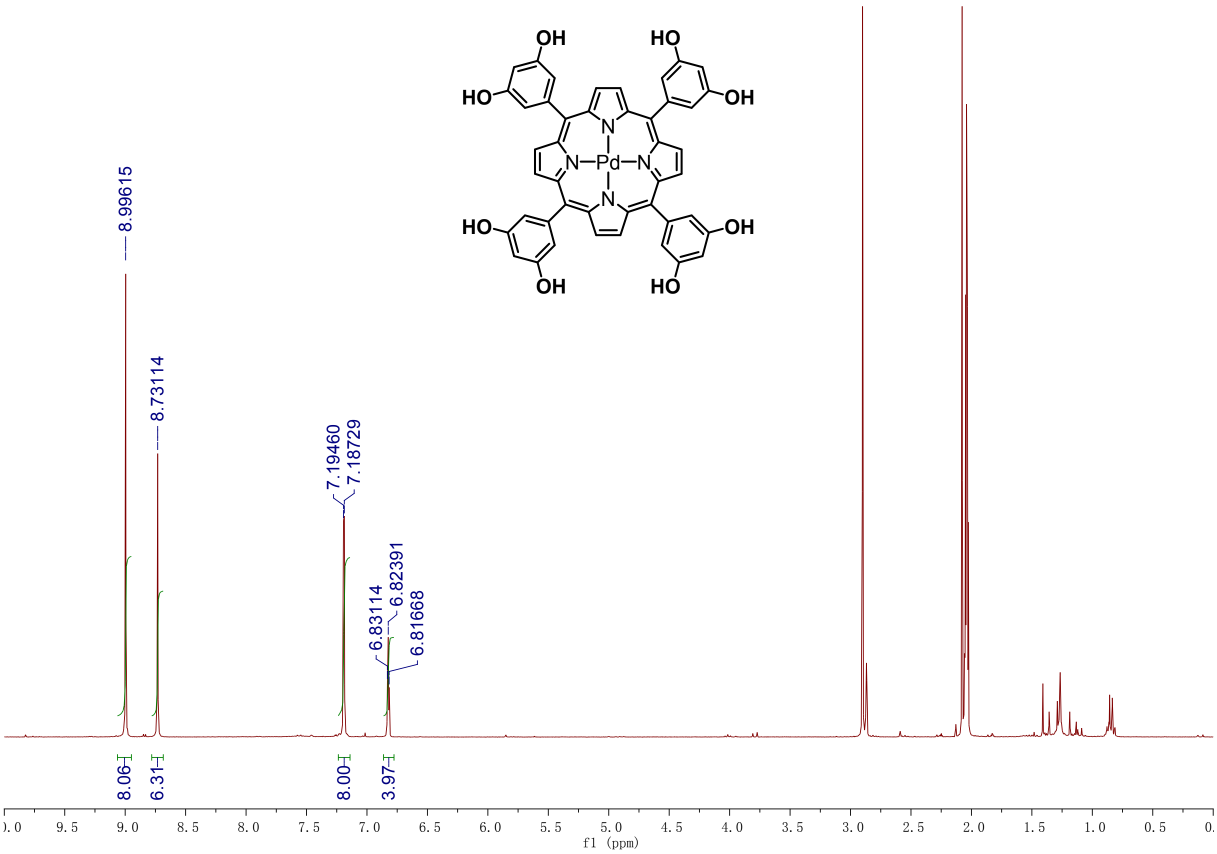

Compound **16**: ^{13}C NMR (75 MHz, Acetone-d_6)

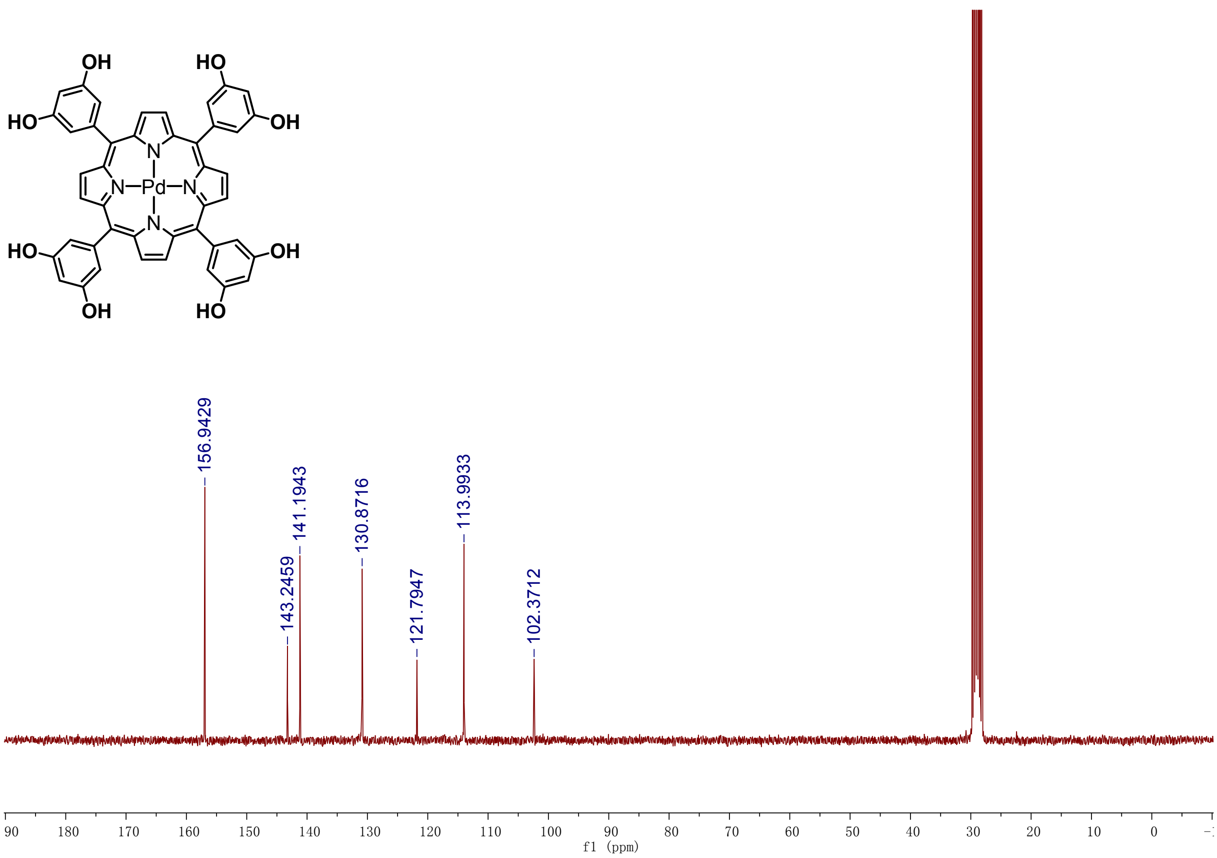

Compound **16**: HR-MS

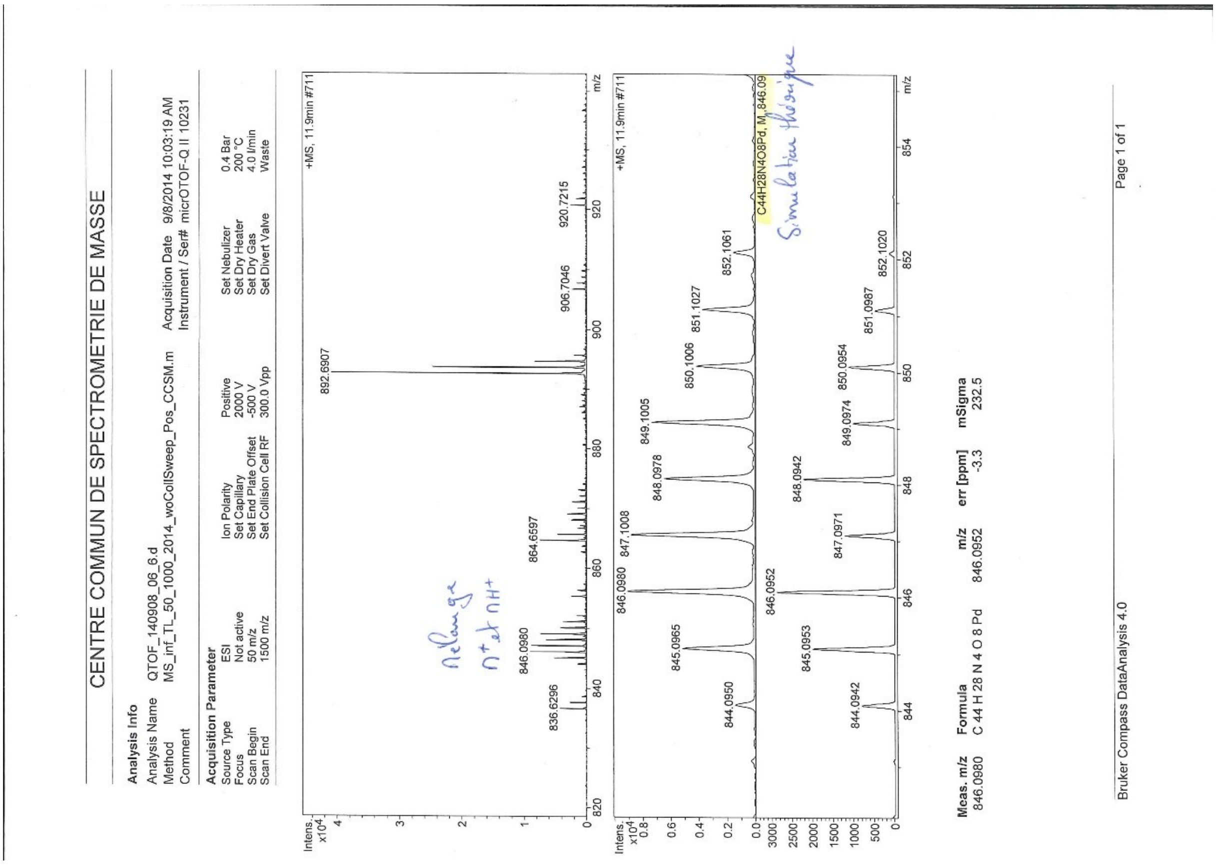

Compound **17**: ^{1}H NMR (300 MHz, $CDCl_3$)

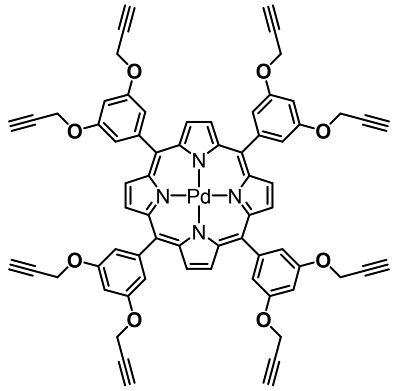

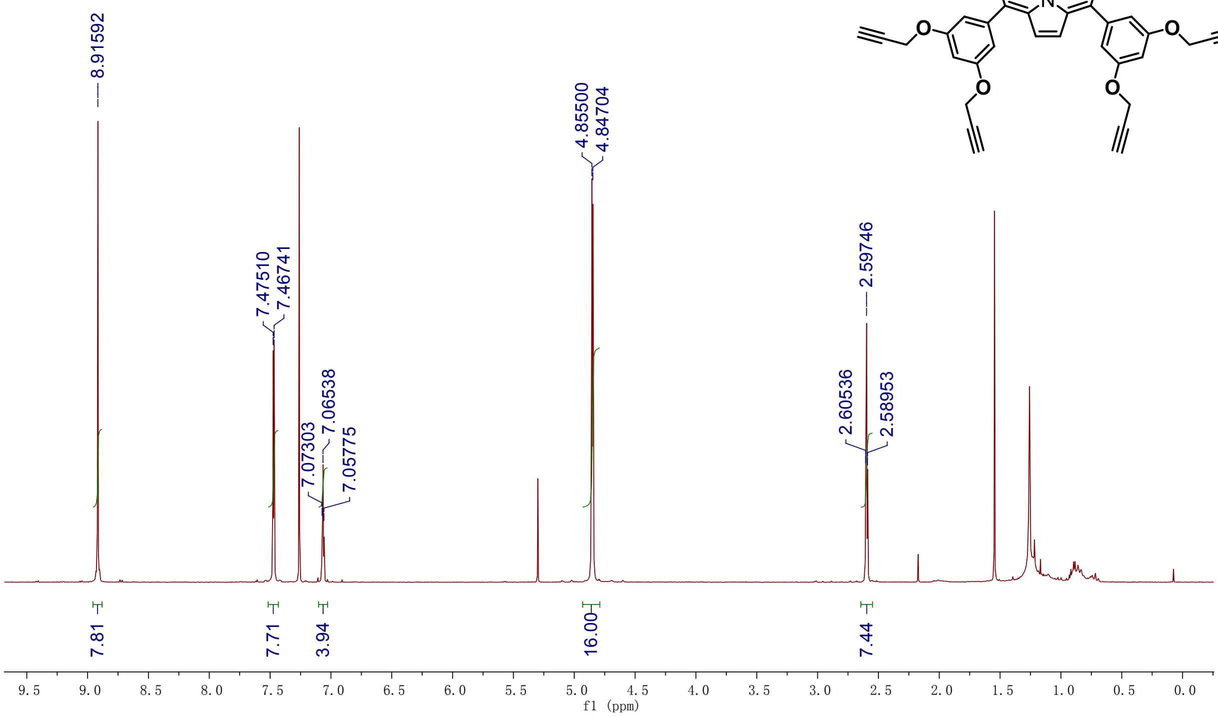

Compound **17**: ^{13}C NMR (75 MHz, $CDCl_3$)

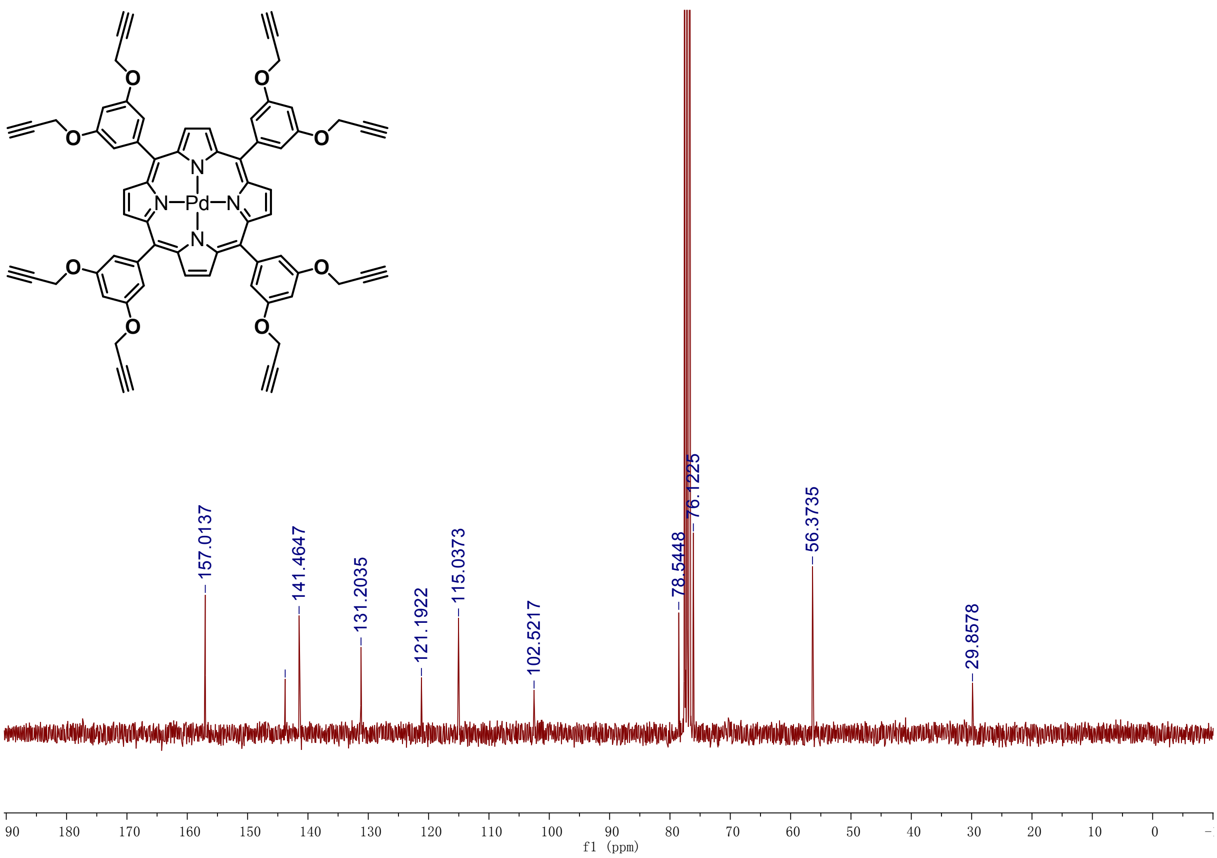

Compound **17**: HR-MS

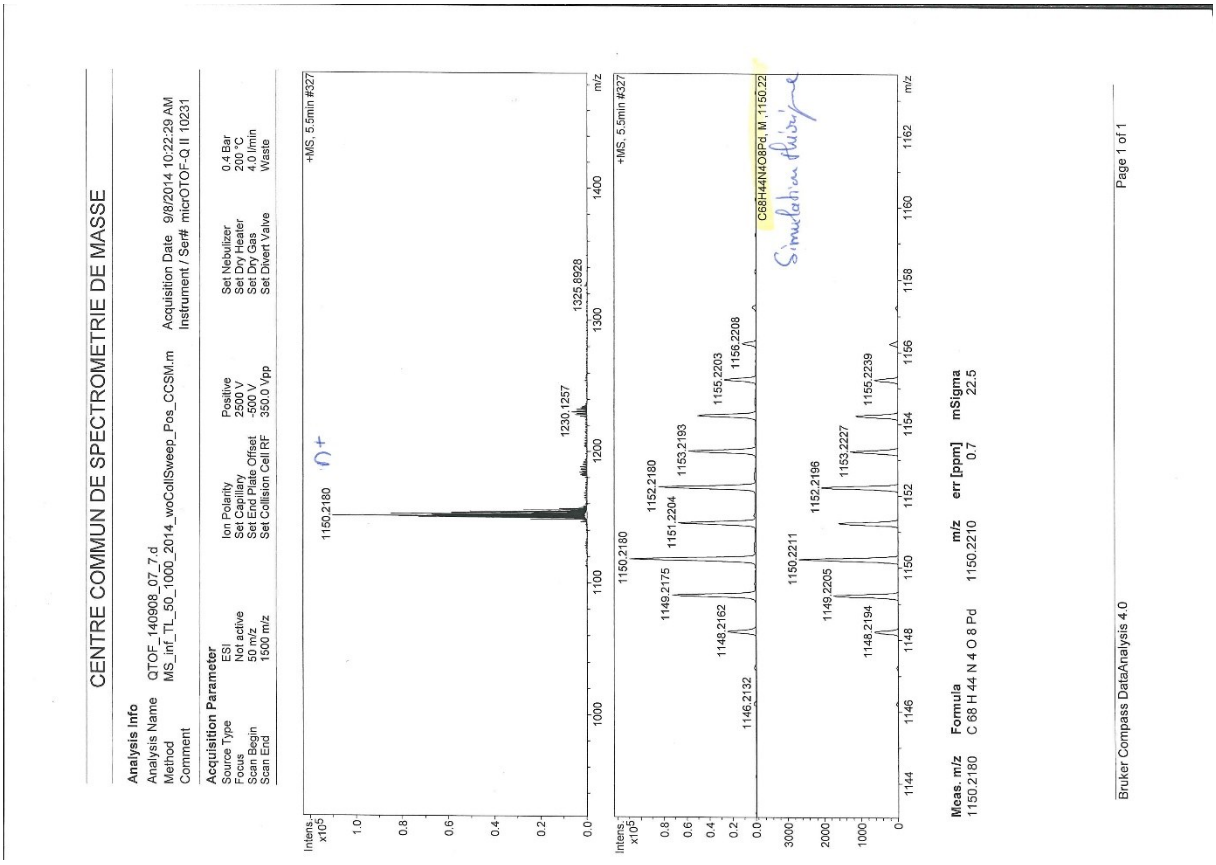

Compound **18**: ^{1}H NMR (300 MHz, $CDCl_3$)

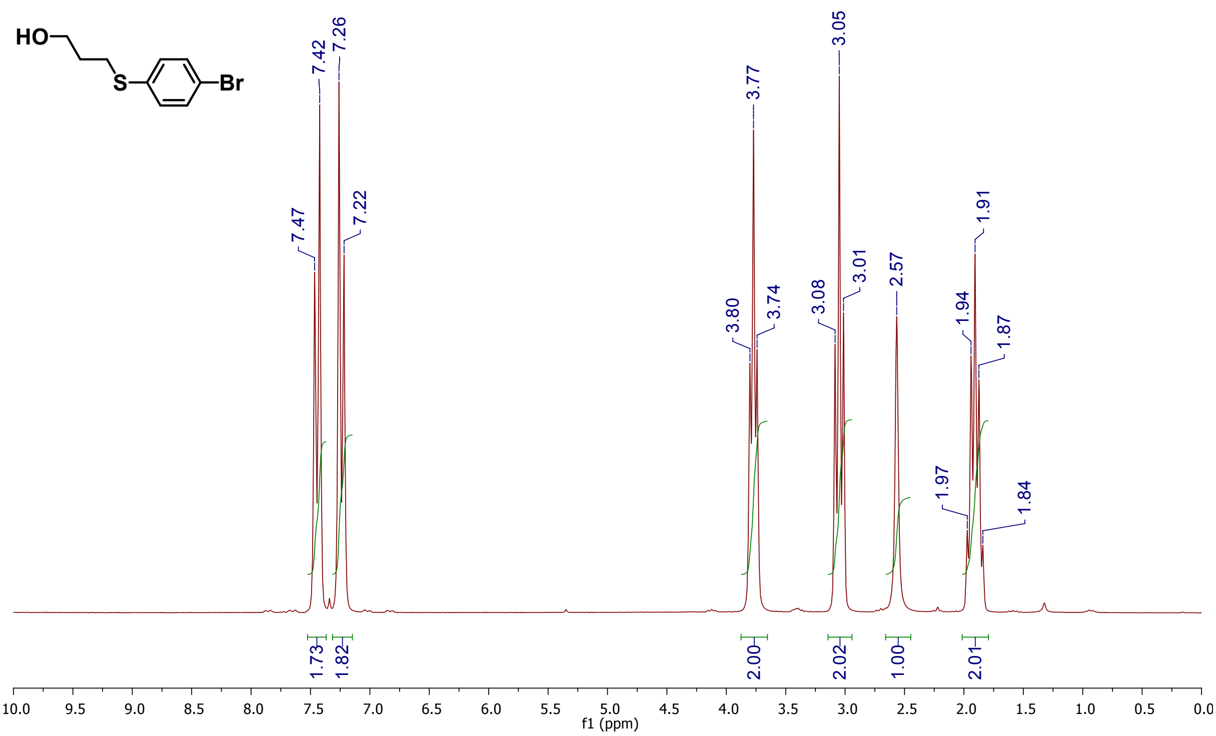

Compound **18**: ^{13}C NMR (75 MHz, $CDCl_3$)

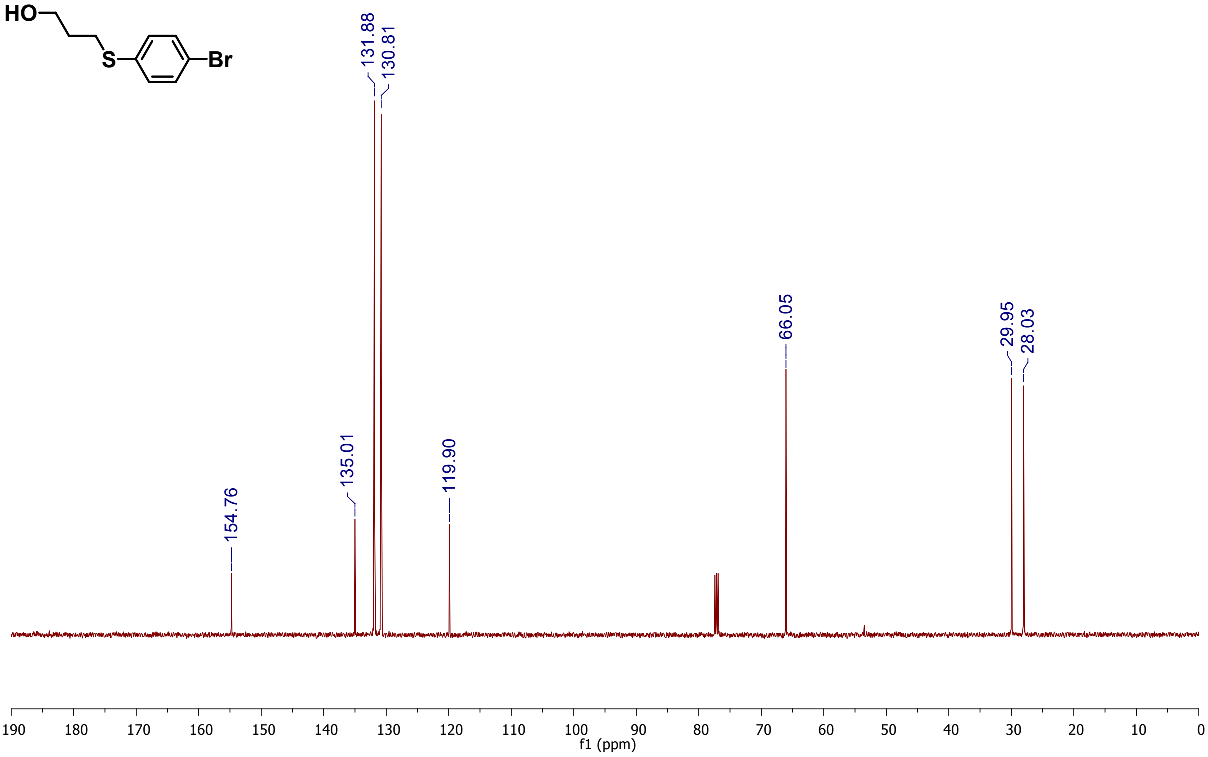
HO
S
Br
131.88
130.81
154.76
135.01
119.90
66.05
29.95
28.03
190 180 170 160 150 140 130 120 110 100 90 80 70 60 50 40 30 20 10 0
f1 (ppm)

3-((4-((trimethylsilyl)ethynyl)phenyl)thio)propan-1-ol: ^{1}H NMR (300 MHz, $CDCl_3$)

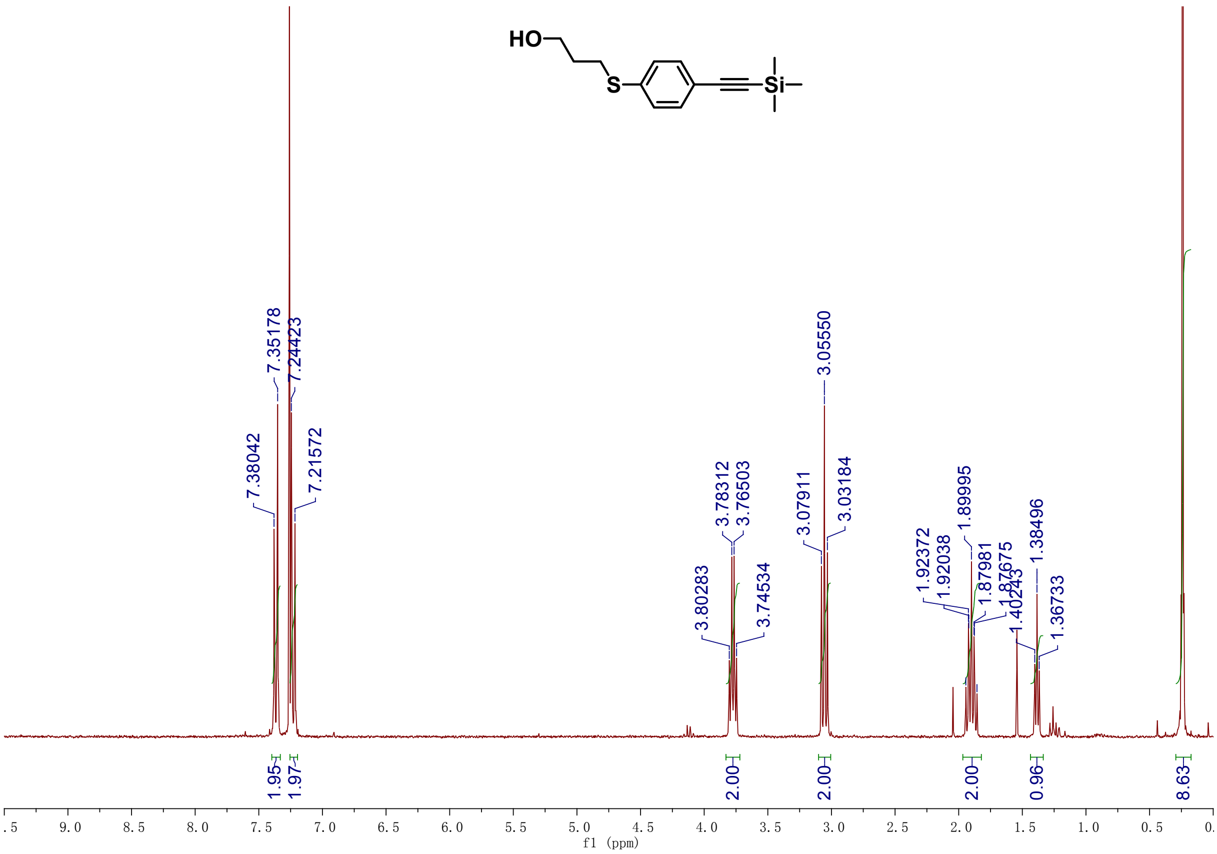

3-((4-((trimethylsilyl)ethynyl)phenyl)thio)propan-1-ol: ^{13}C NMR (75 MHz, $CDCl_3$)

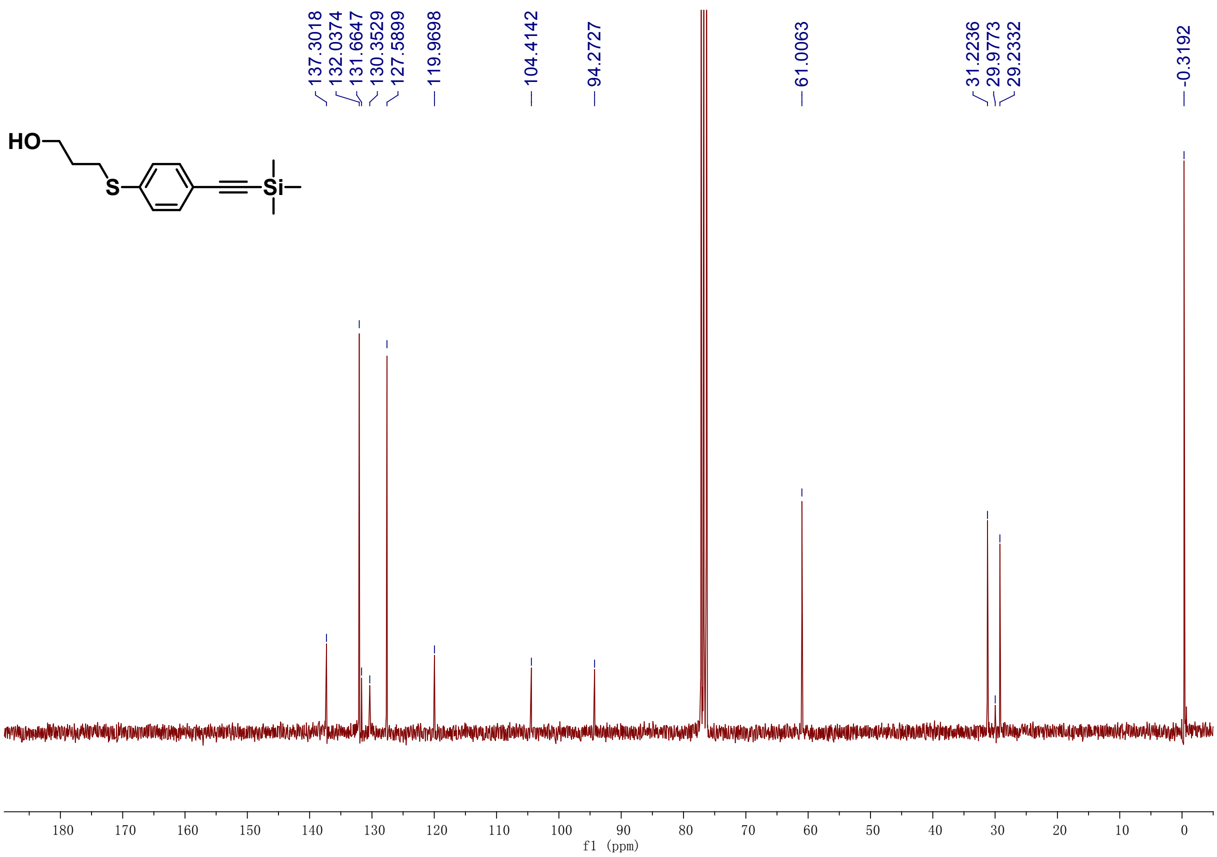

3-((4-((trimethylsilyl)ethynyl)phenyl)thio)propan-1-ol: HR-MS

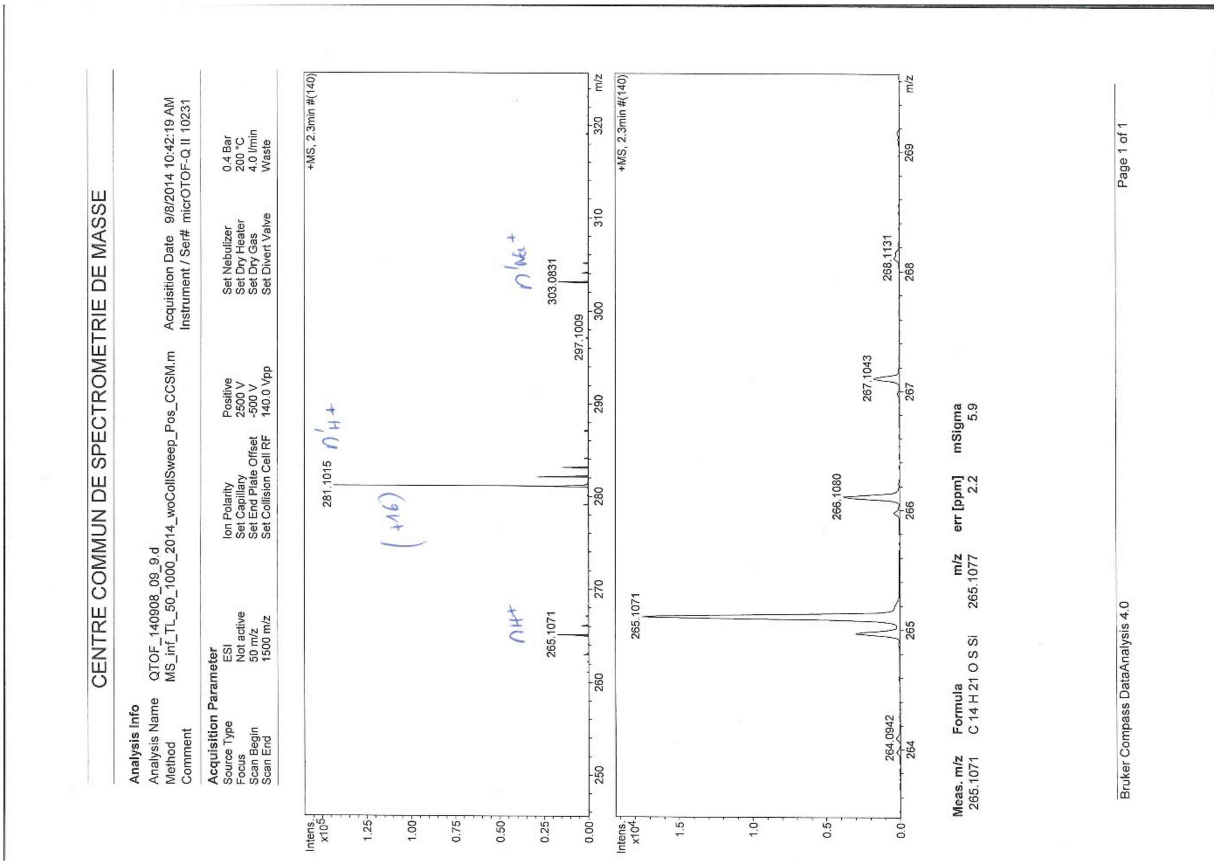

Compound **19**: ^{1}H NMR (300 MHz, $CDCl_3$)

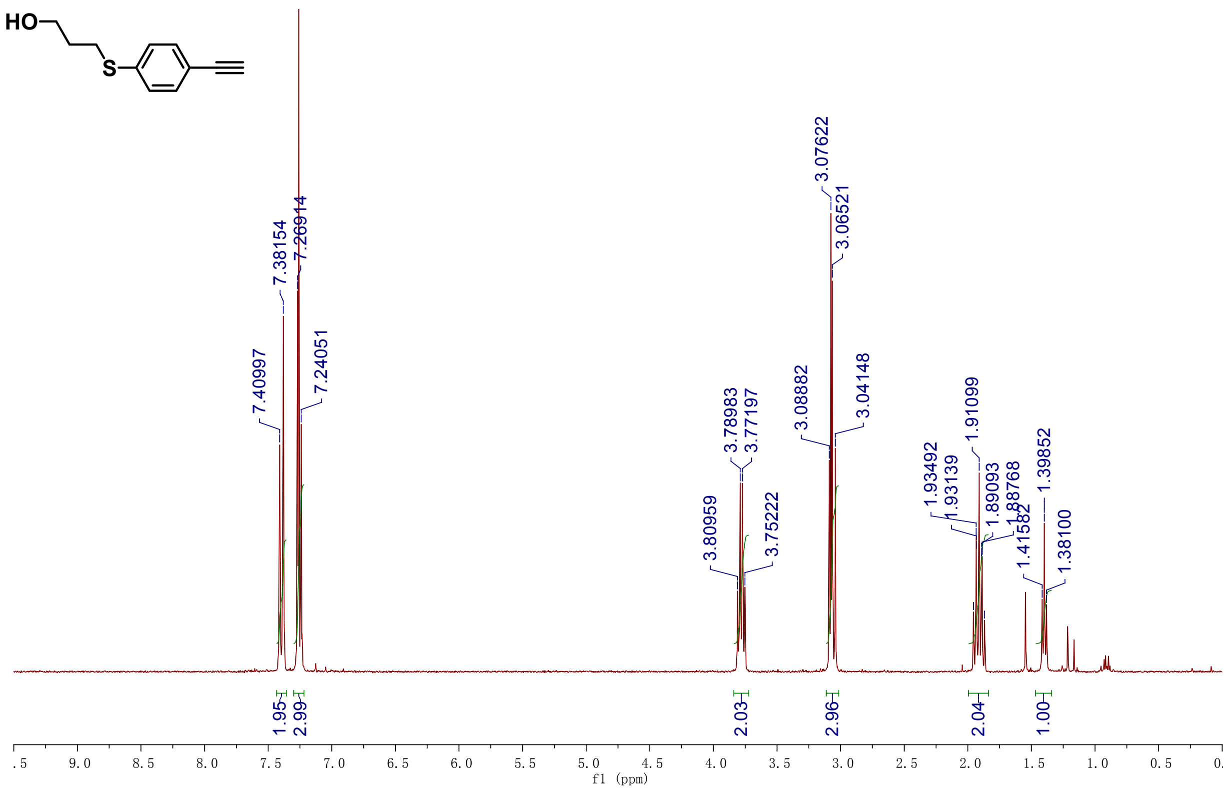

Compound **19**: ^{13}C NMR (75 MHz, $CDCl_3$)

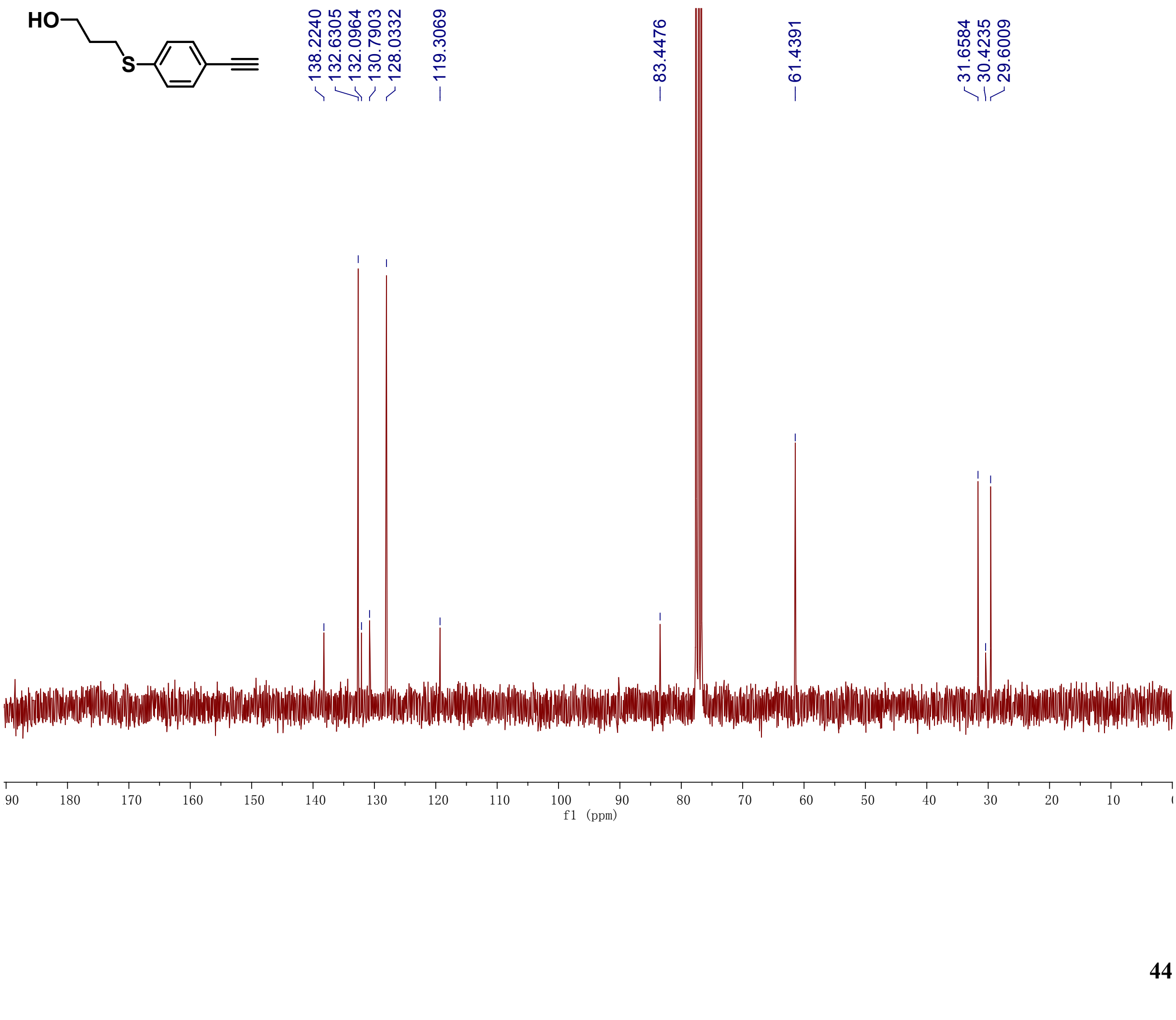

Compound **19**: HR-MS

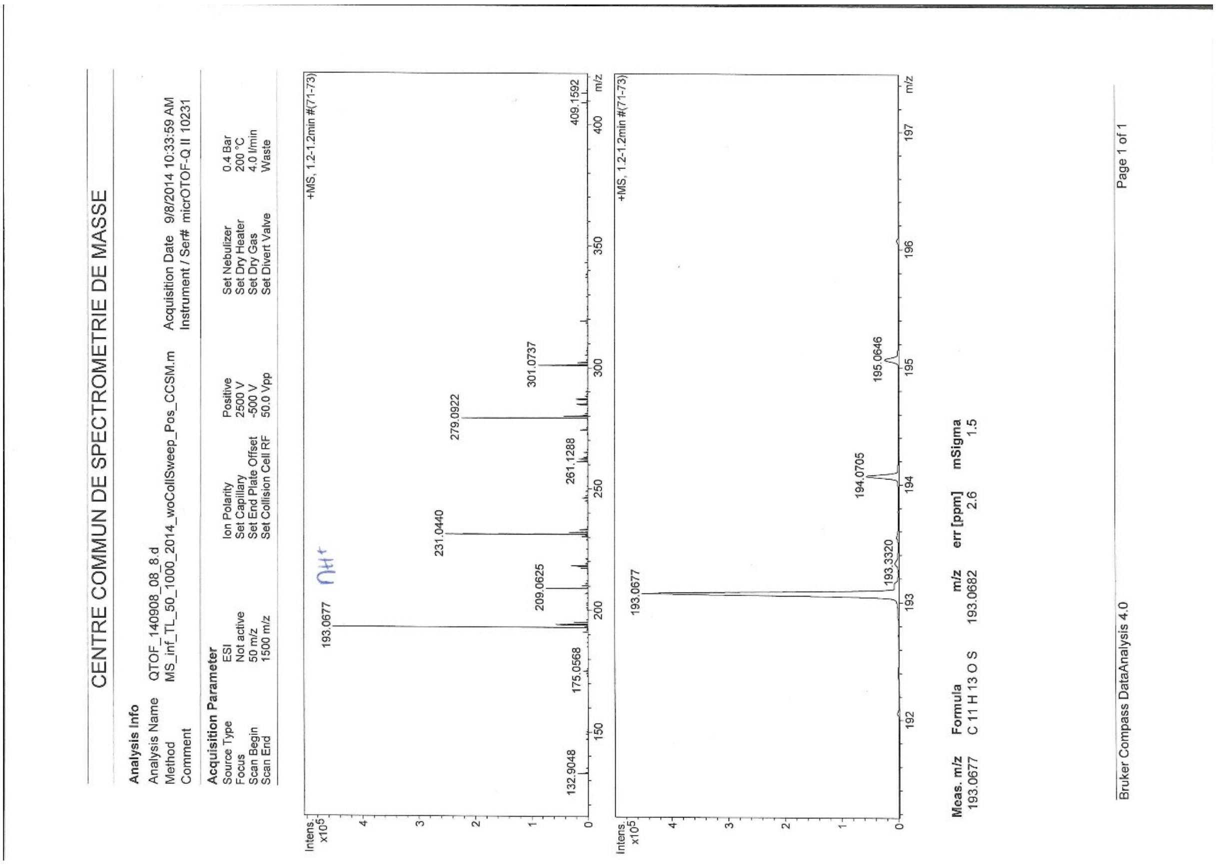

Compound **20**: ^{1}H NMR (300 MHz, $CDCl_3$) full spectrum

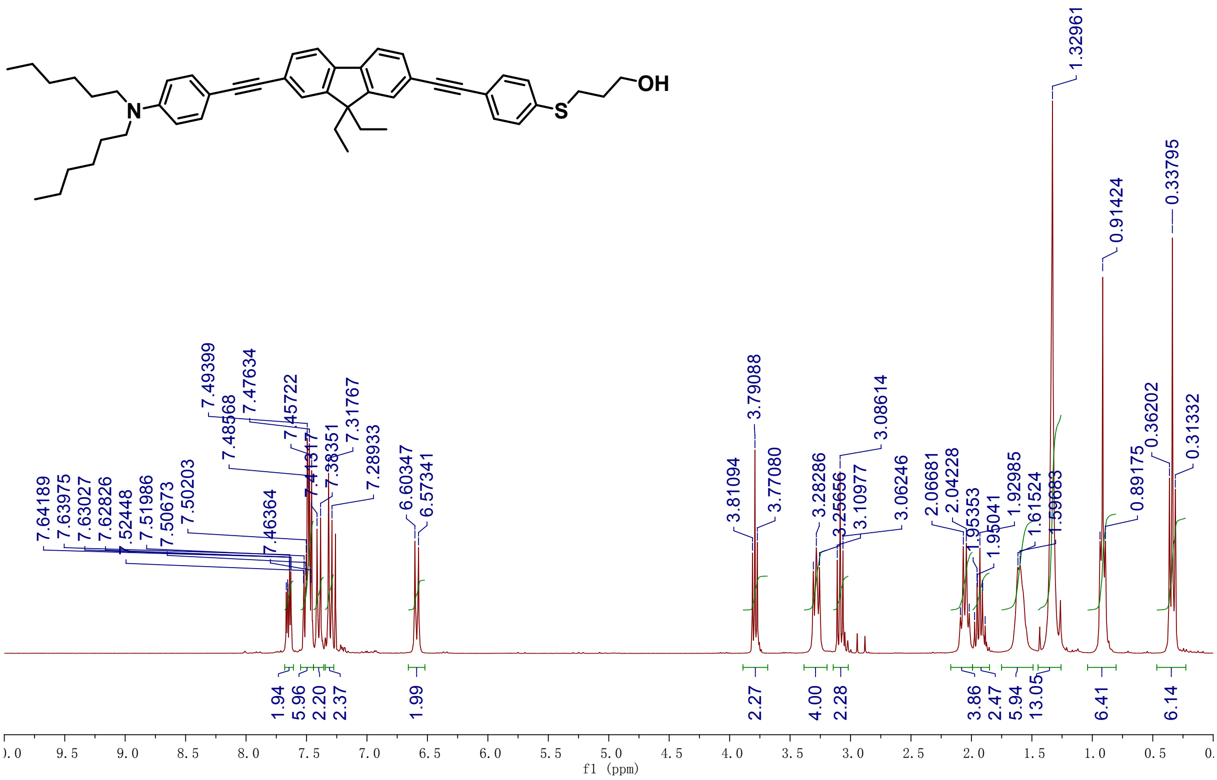

Compound **20**: ^{1}H NMR (300 MHz, $CDCl_3$) expansion aliphatic protons

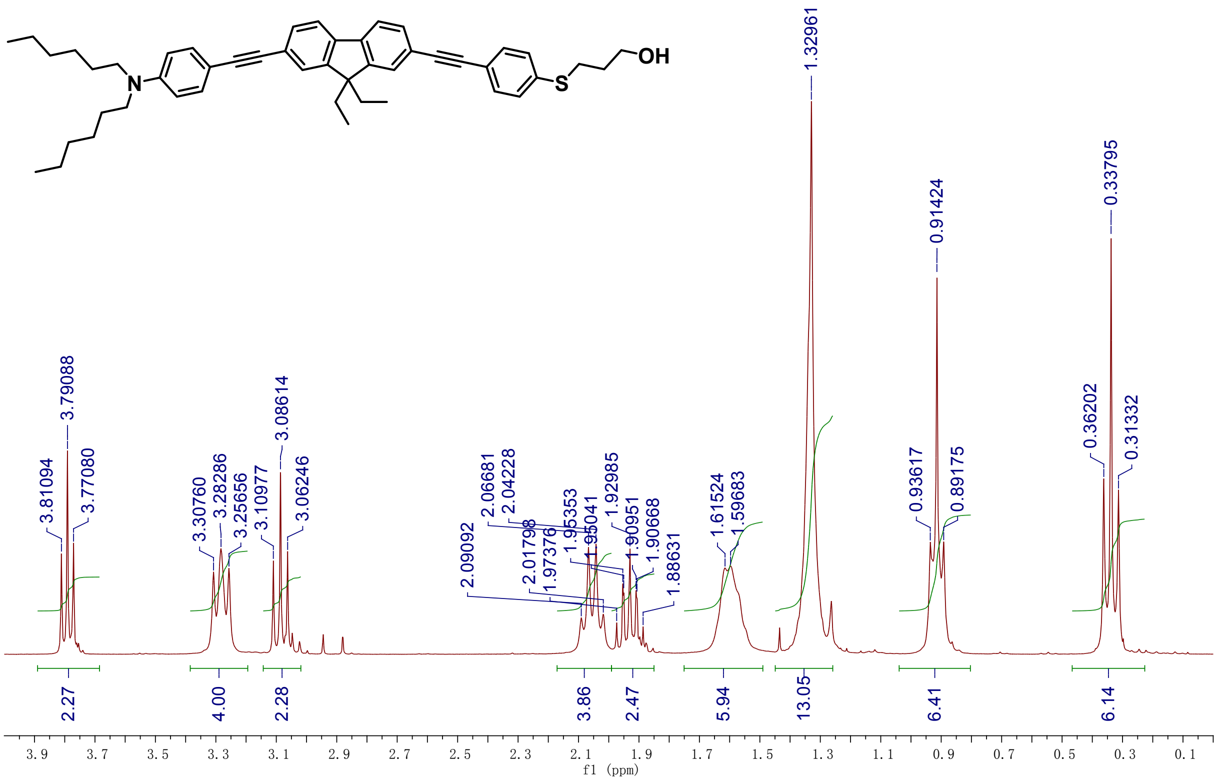

Compound **20**: [1]H NMR (300 MHz, $CDCl_3$) expansion aromatic protons

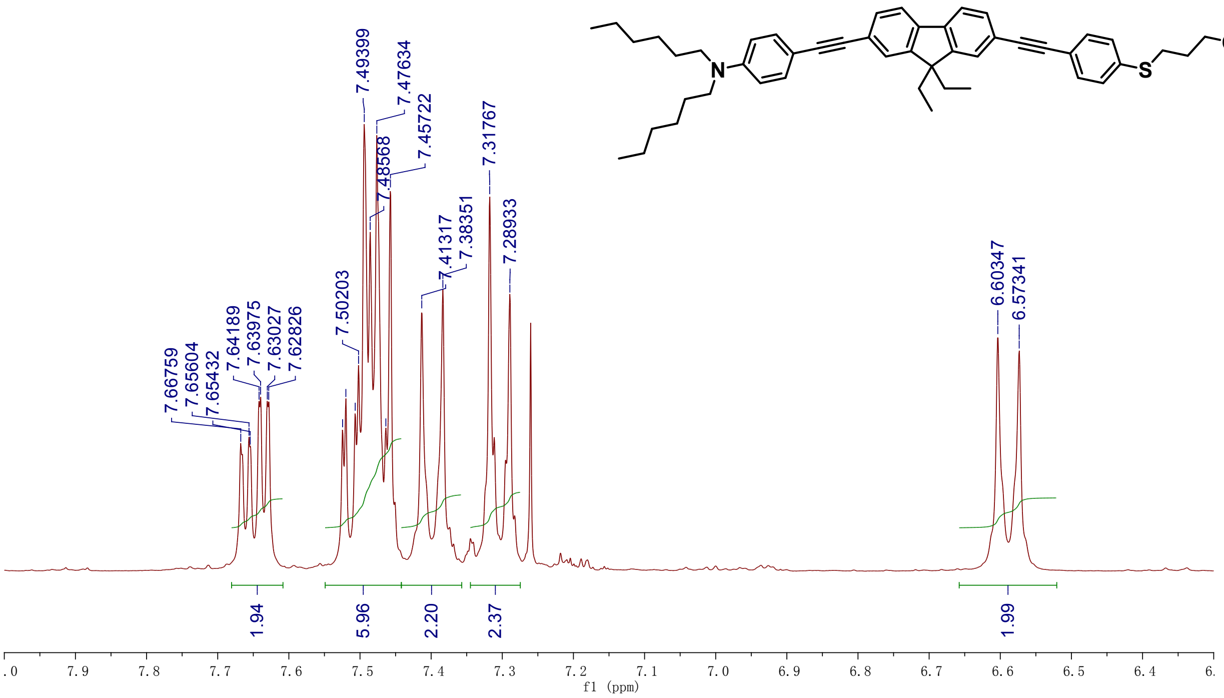

Compound **20**: [13]C NMR (75 MHz, $CDCl_3$)

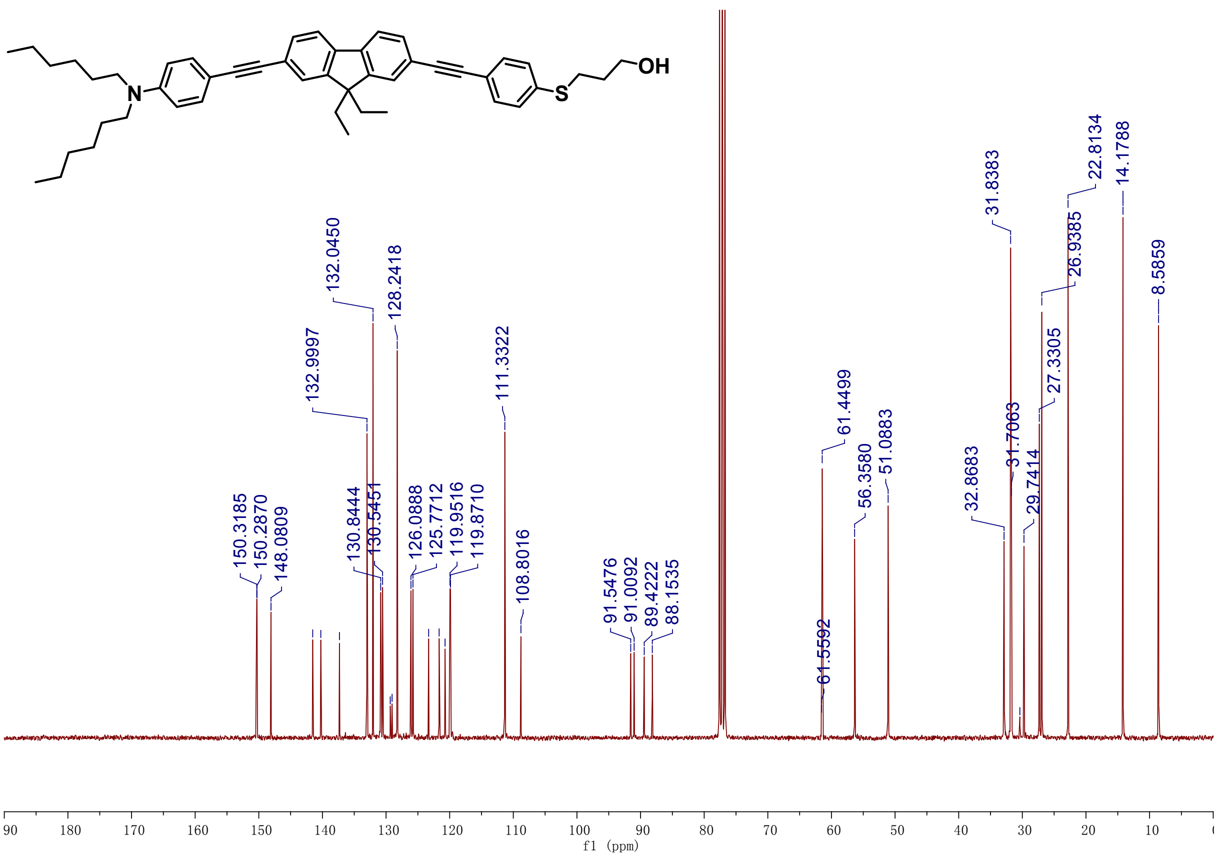

Compound **20**: HR-MS

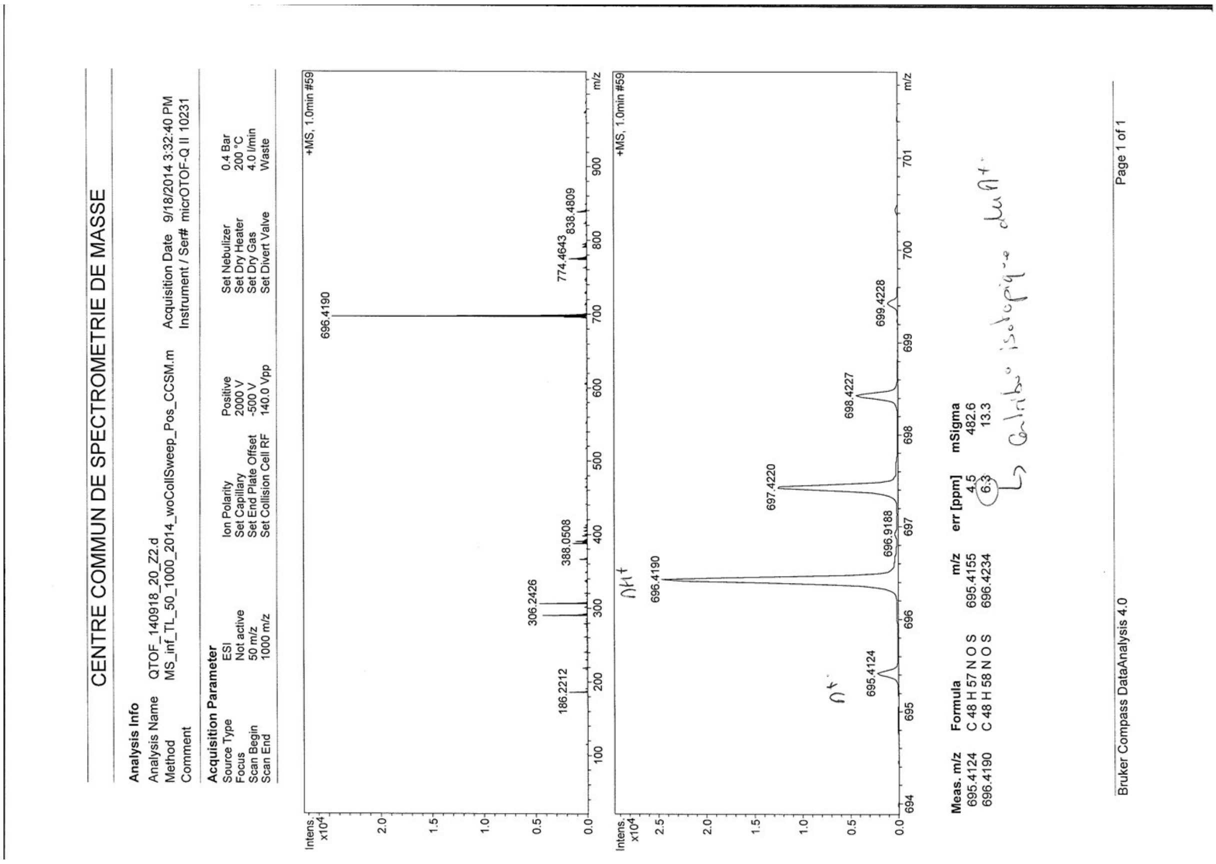

Compound **21**: ^{1}H NMR (300 MHz, $CDCl_3$) full spectrum

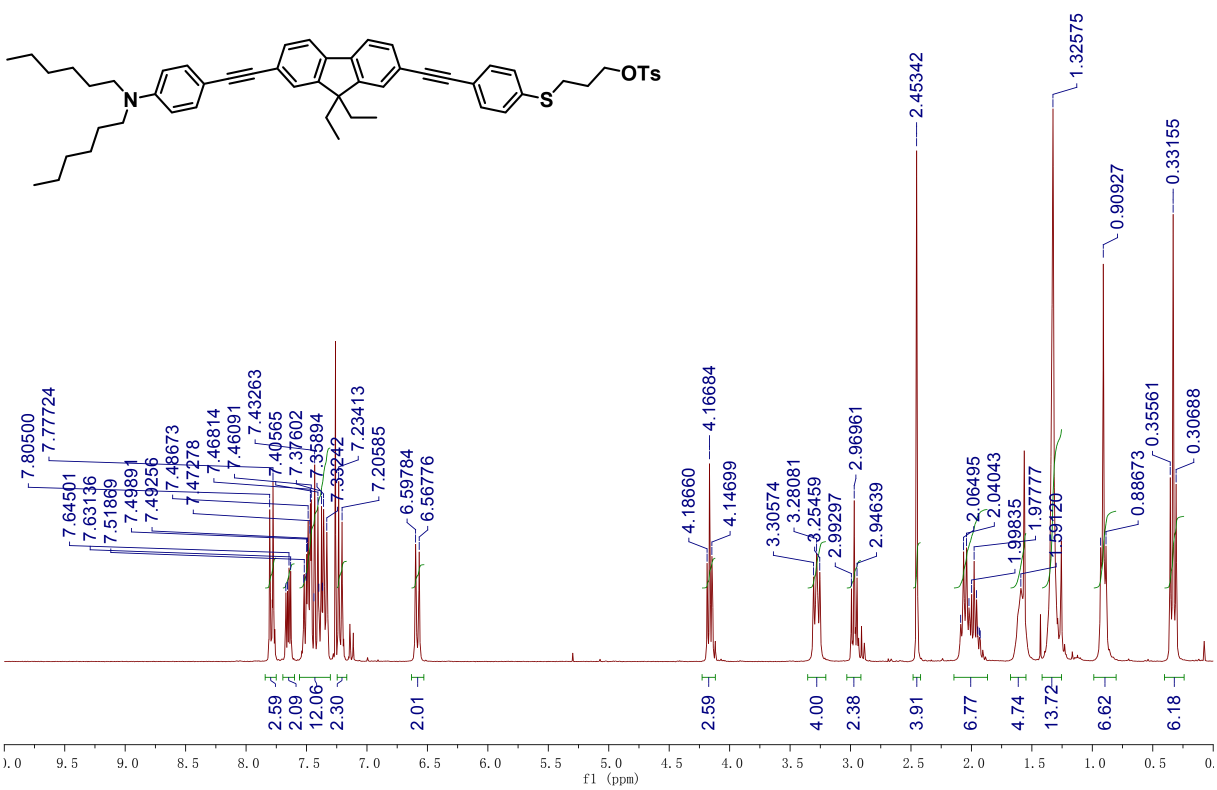

Compound **21**: ^{1}H NMR (300 MHz, $CDCl_3$) expansion aliphatic protons

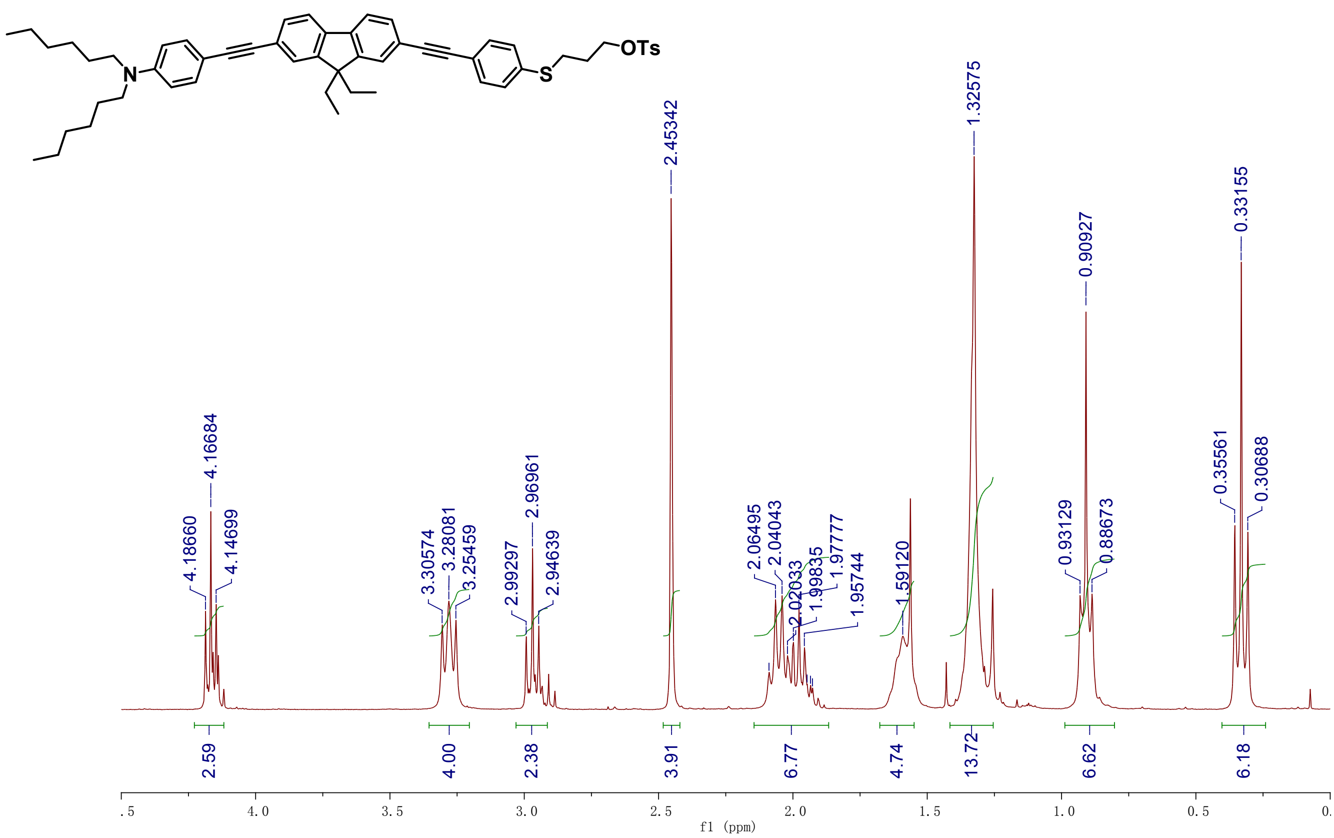

Compound **21**: ^{1}H NMR (300 MHz, $CDCl_3$) expansion aromatic protons

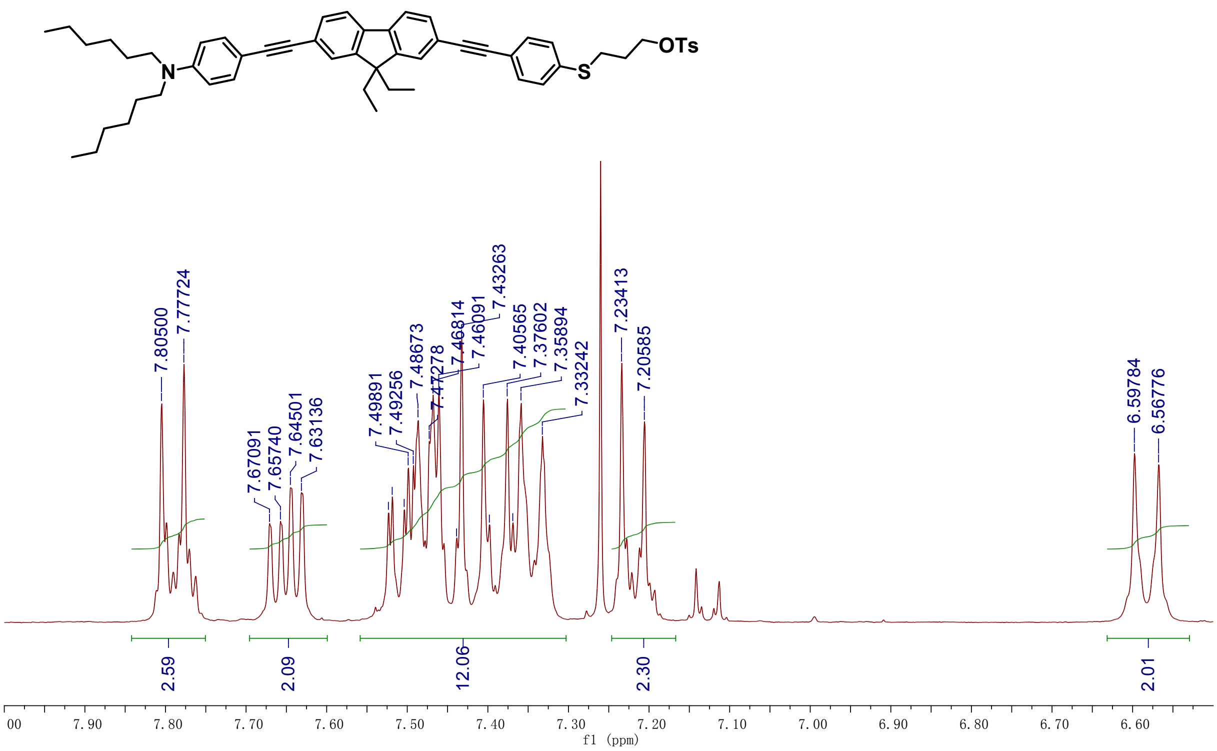

Compound **21**: ^{13}C NMR (75 MHz, $CDCl_3$)

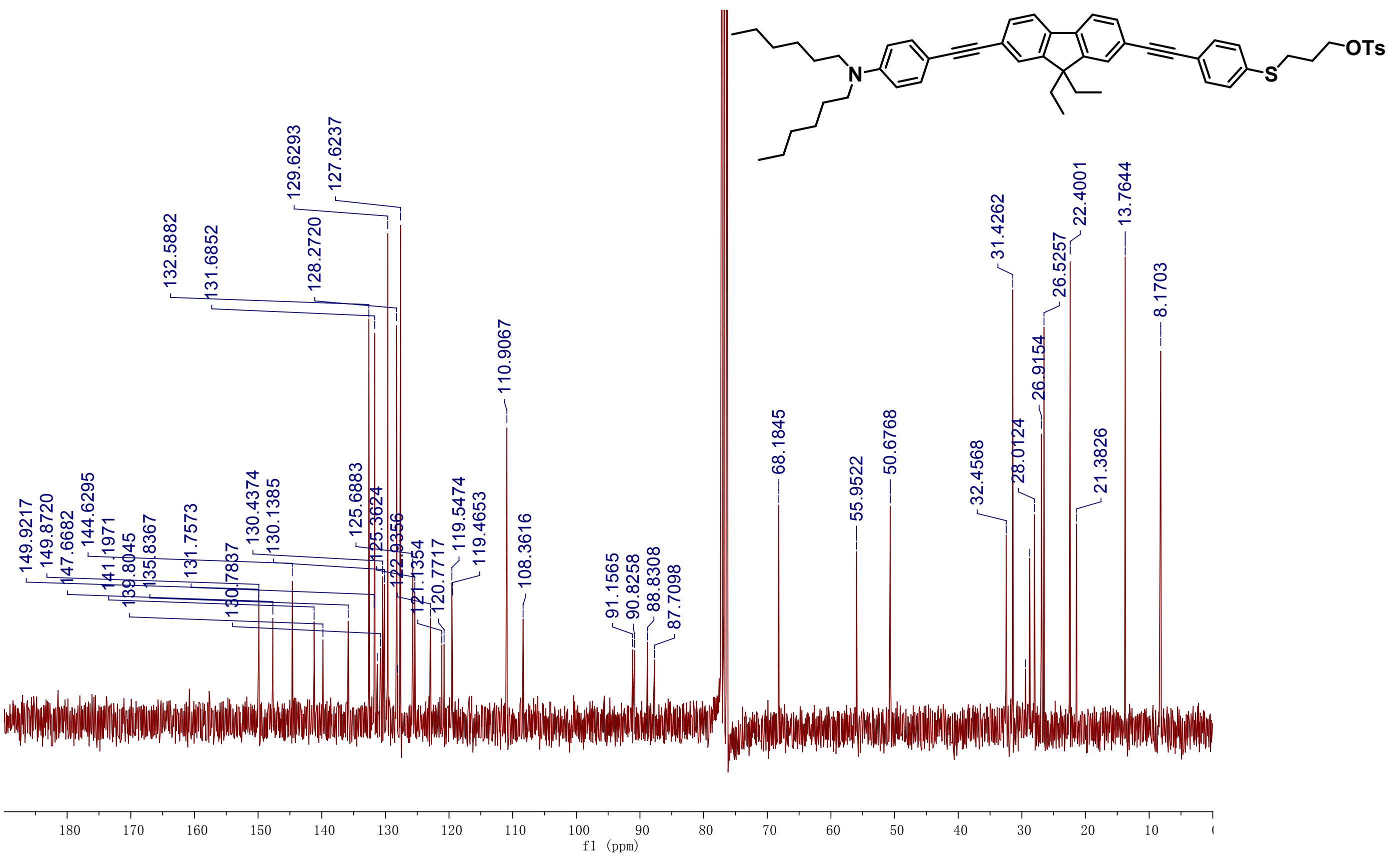

Compound **22**: [1]H NMR (300 MHz, $CDCl_3$) full spectrum

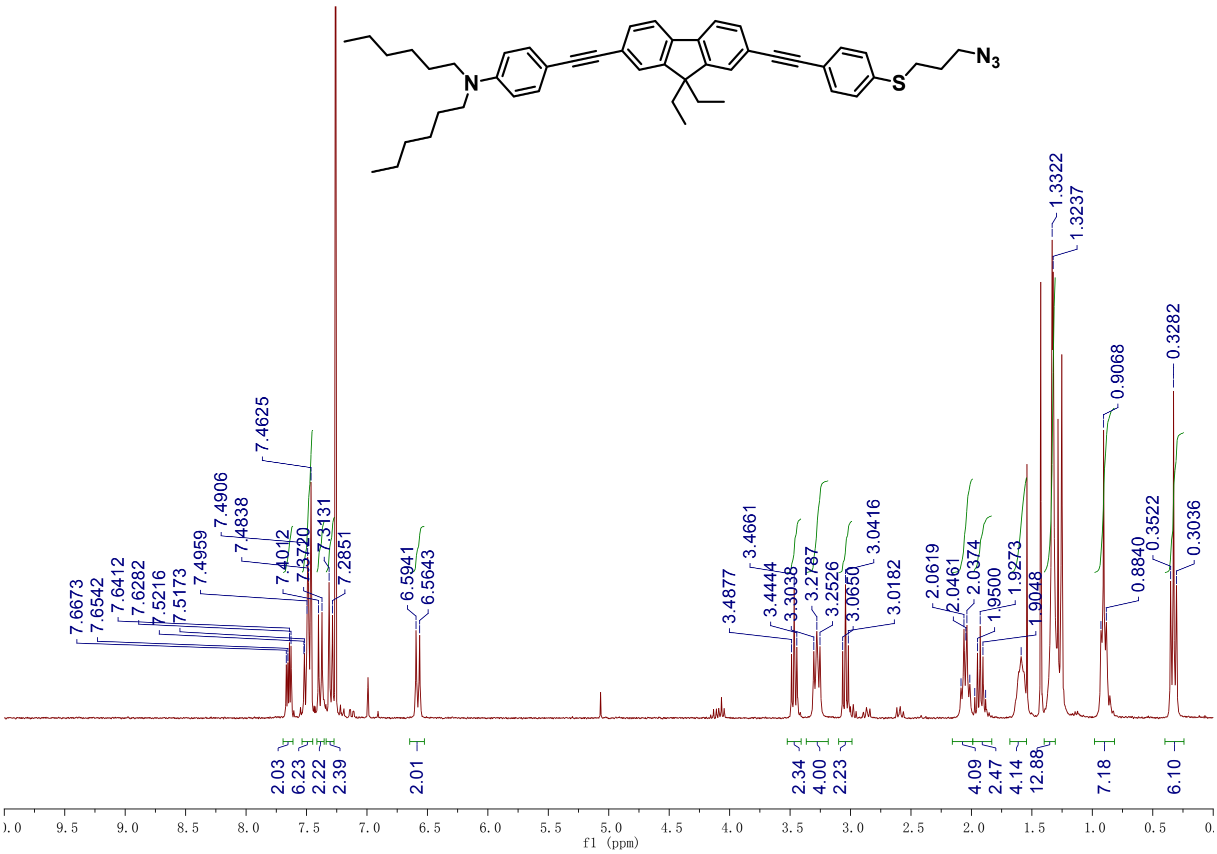

Compound **22**: [1]H NMR (300 MHz, $CDCl_3$) expansion aliphatic protons

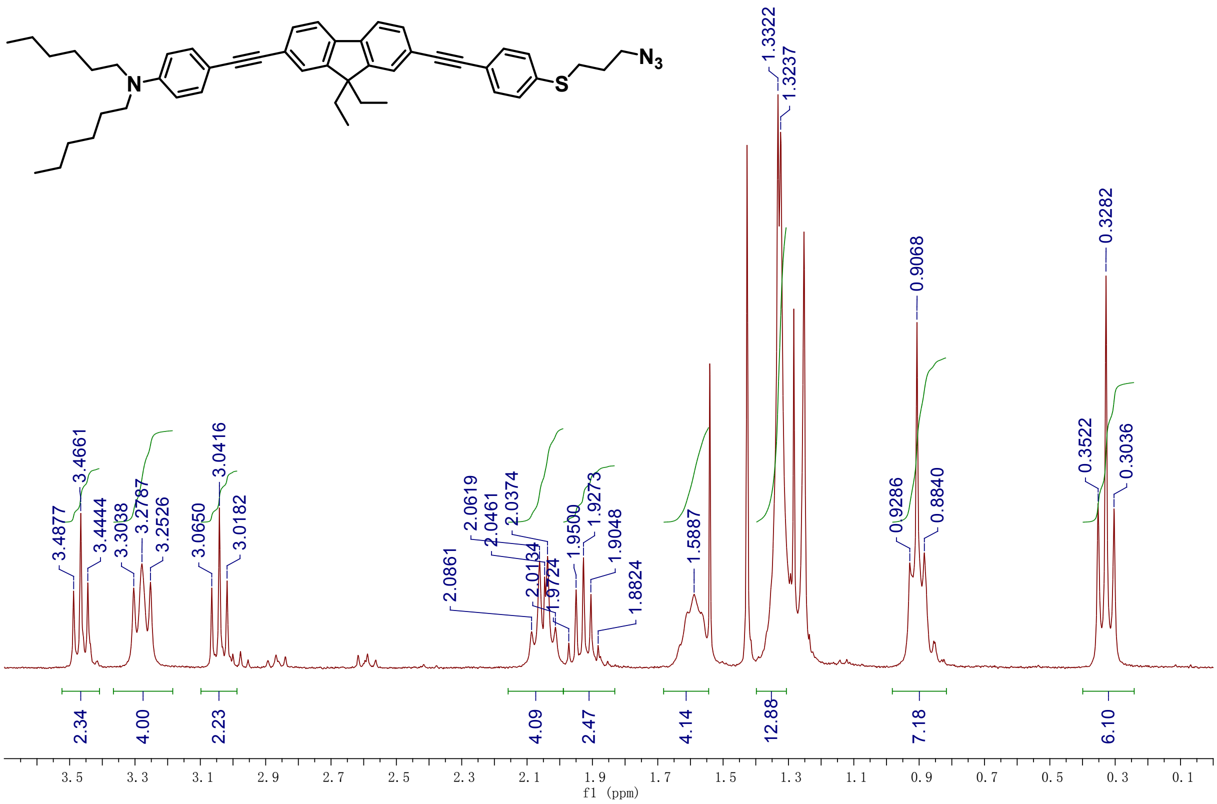

Compound **22**: ^{1}H NMR (300 MHz, $CDCl_3$) expansion aromatic protons

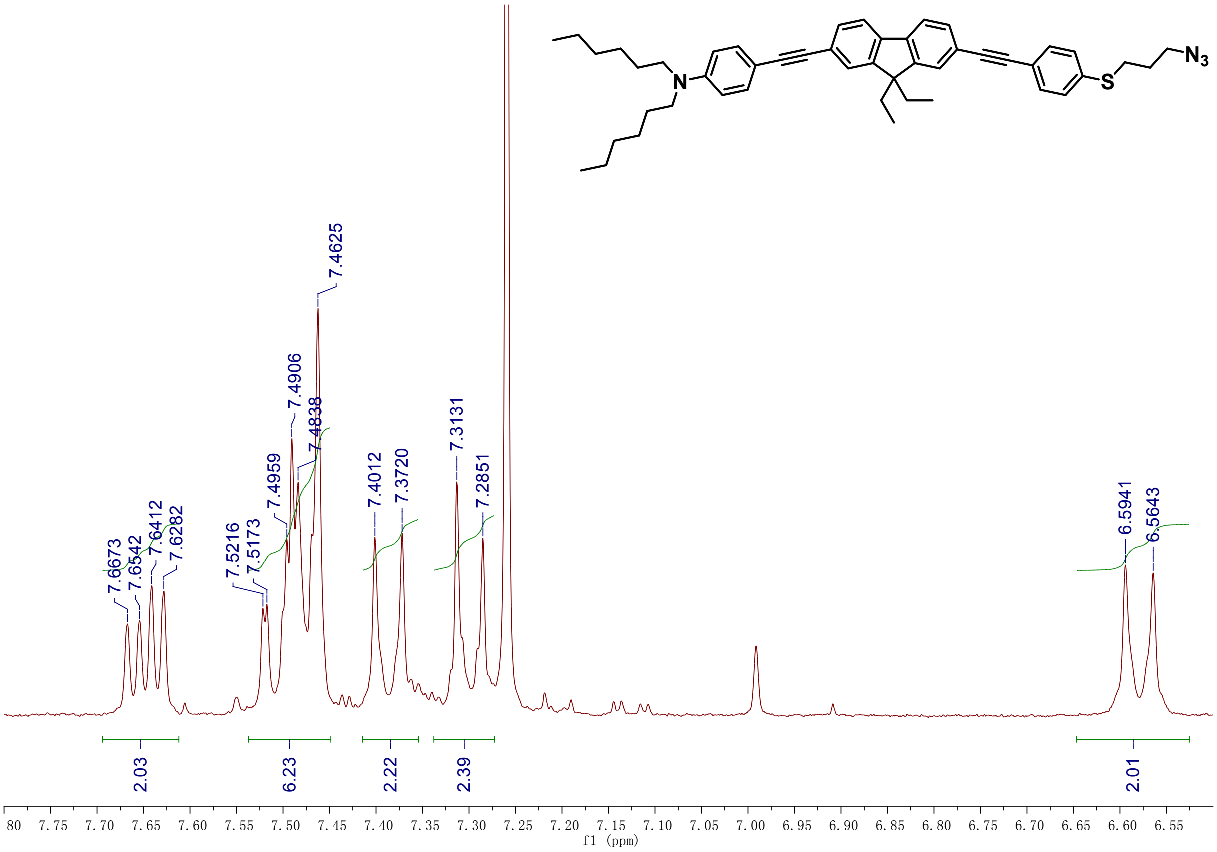

Compound **22**: ^{13}C NMR (75 MHz, $CDCl_3$)

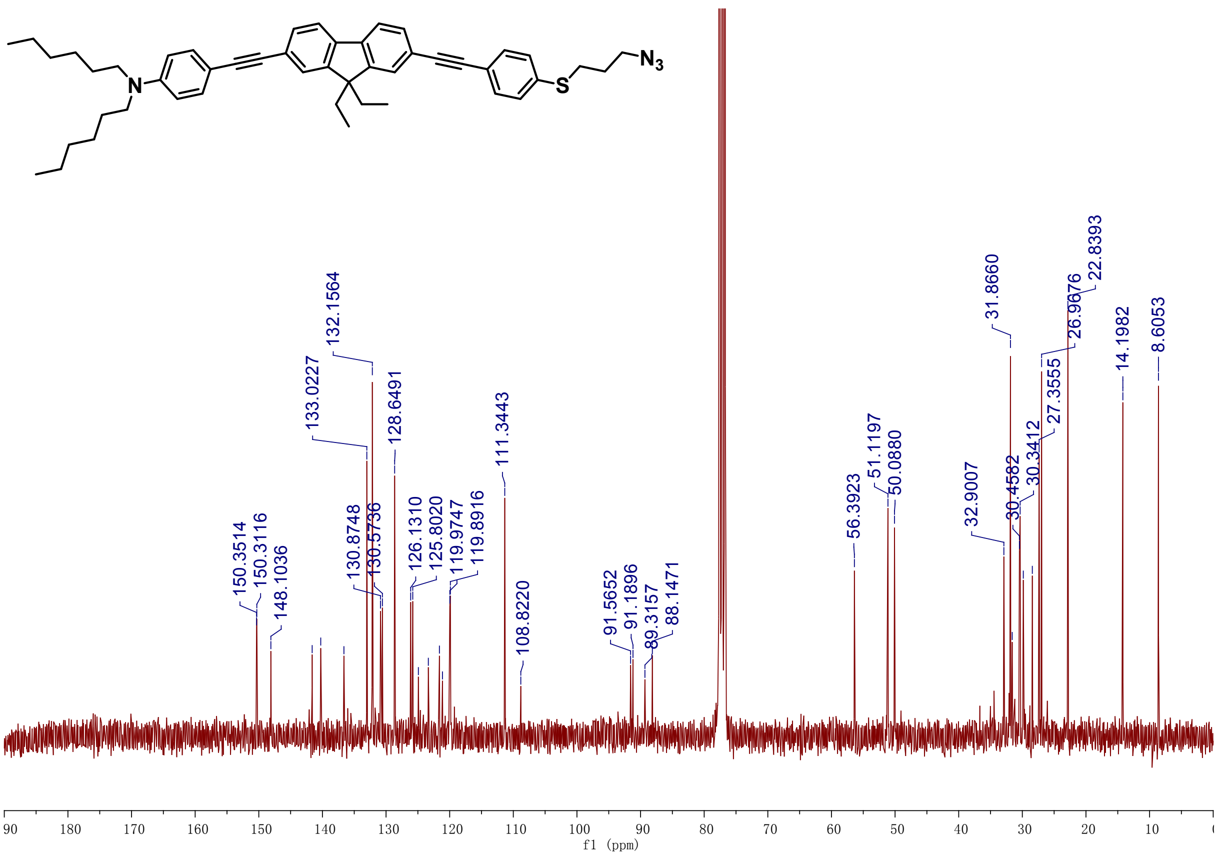

Compound **22**: HR-MS

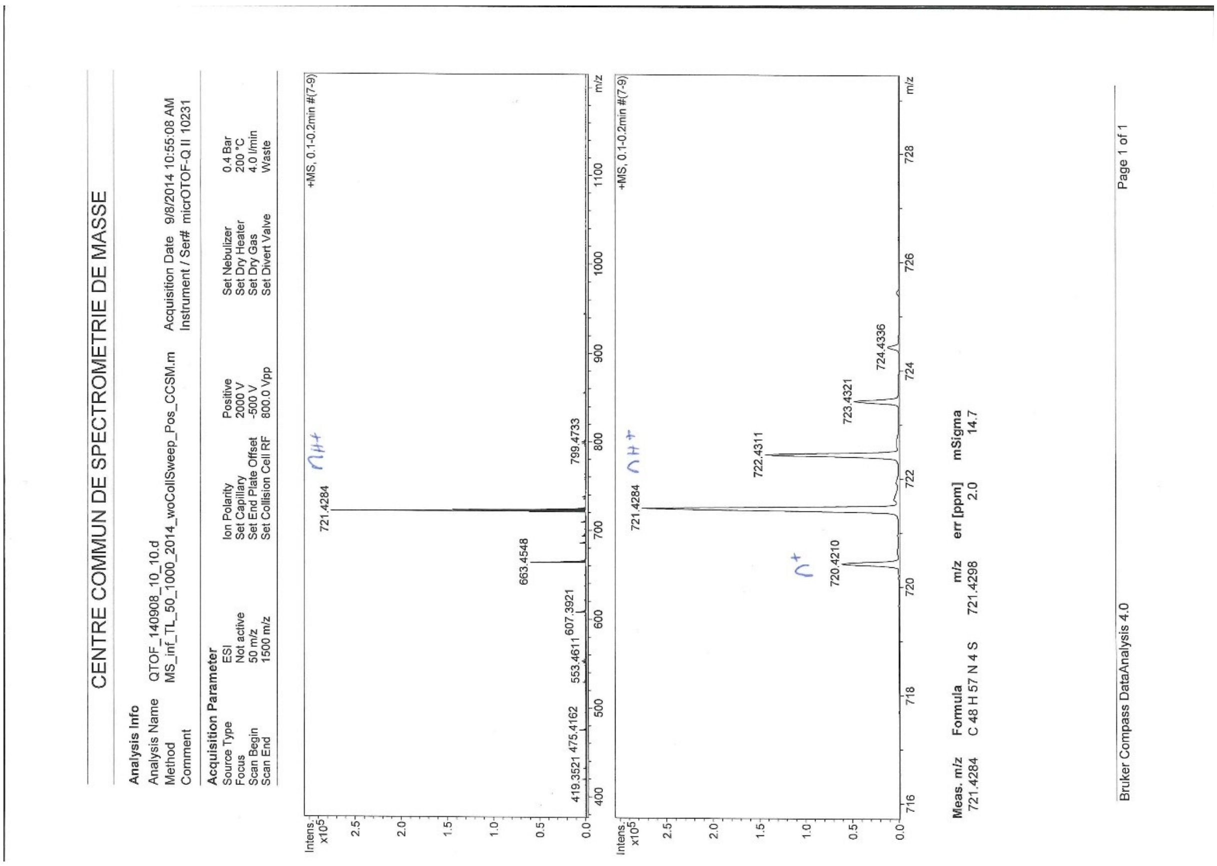

Compound **P1**: ^{1}H NMR (300 MHz, $CDCl_3$) full spectrum

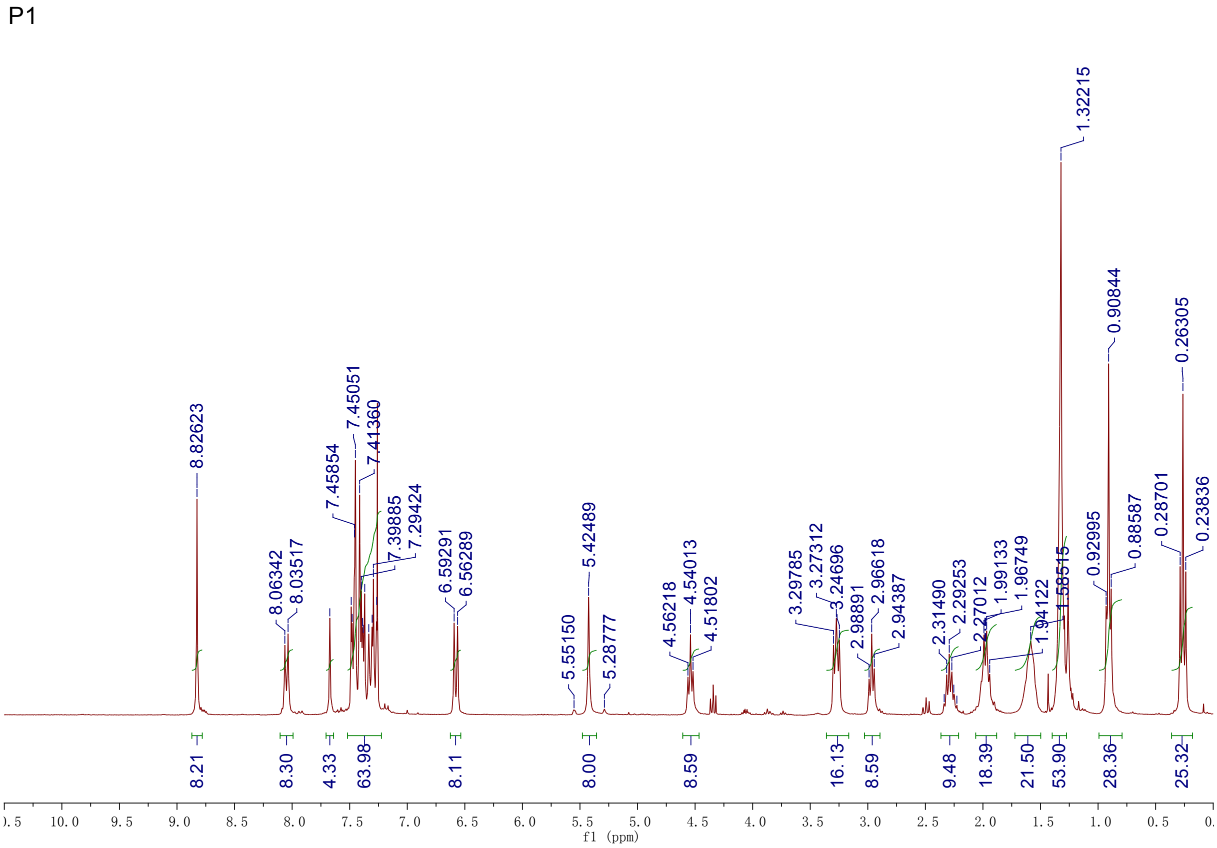

Compound **P1**: ^{1}H NMR (300 MHz, $CDCl_3$) exapnsion aliphatic protons

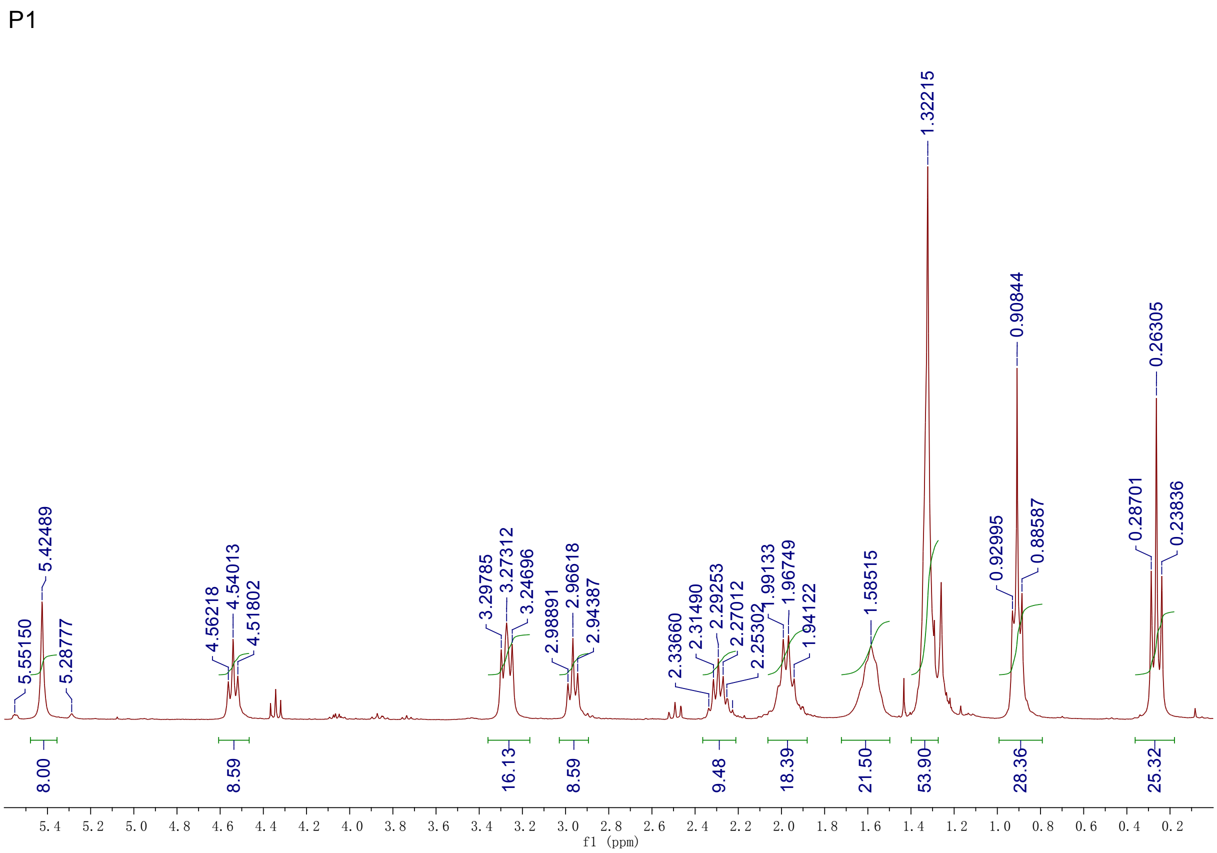

Compound **P1**: ^{1}H NMR (300 MHz, $CDCl_3$) expansion aromatic protons

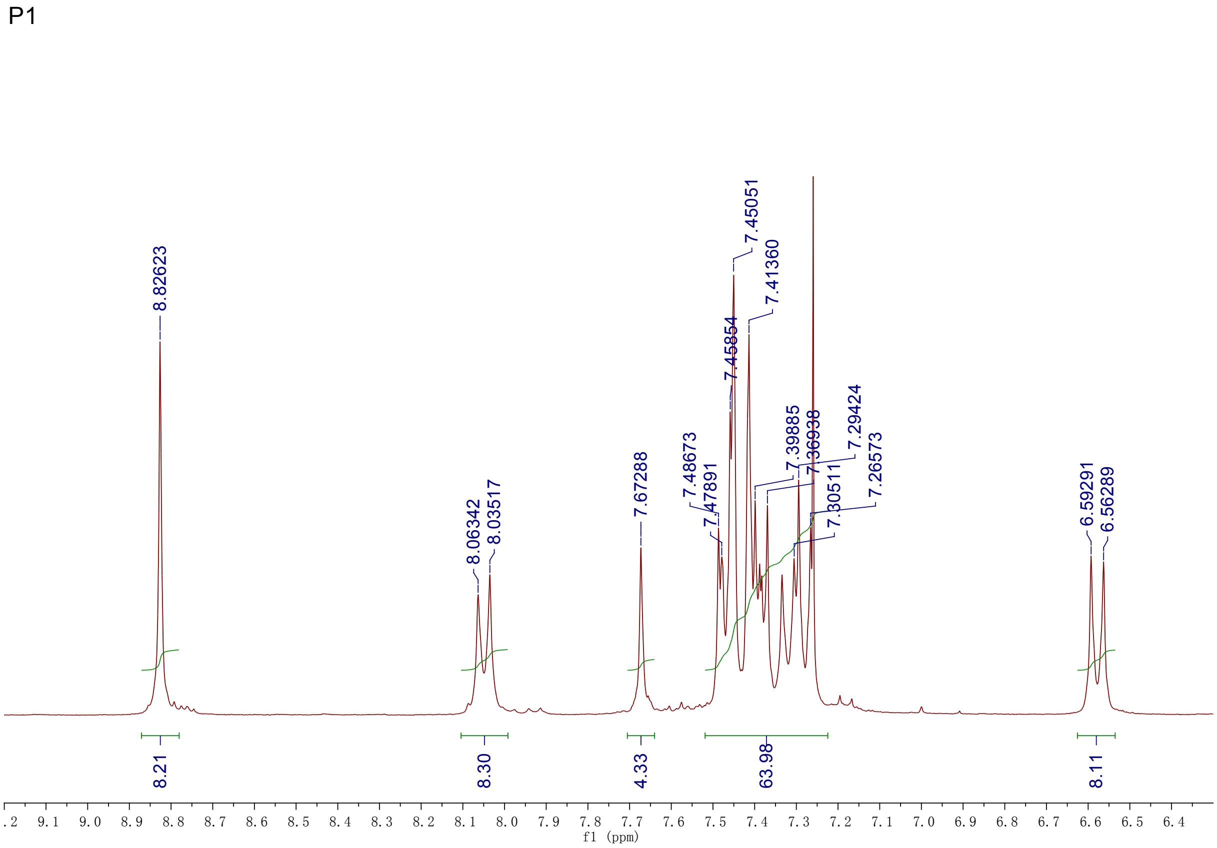

Compound **P1**: ^{13}C NMR (75 MHz, $CDCl_3$)

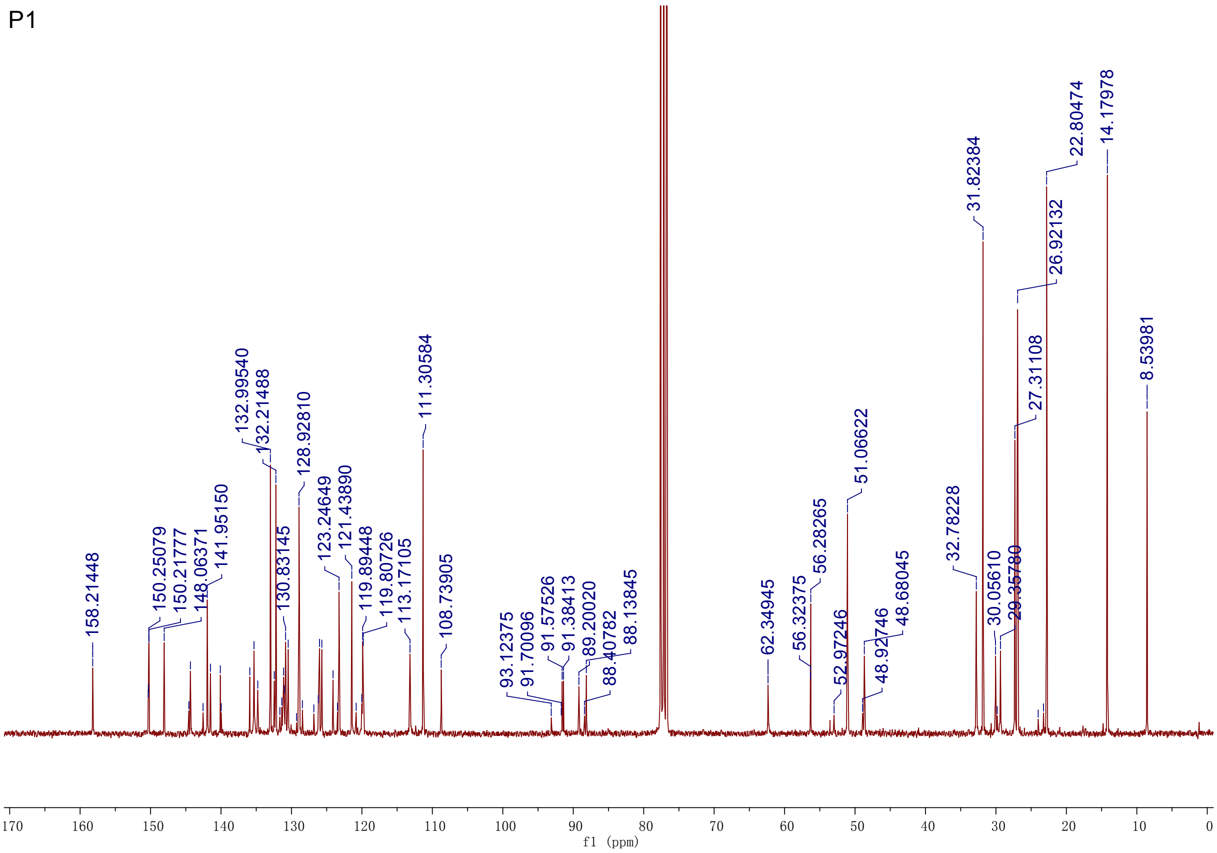

Compound **P1**: MS

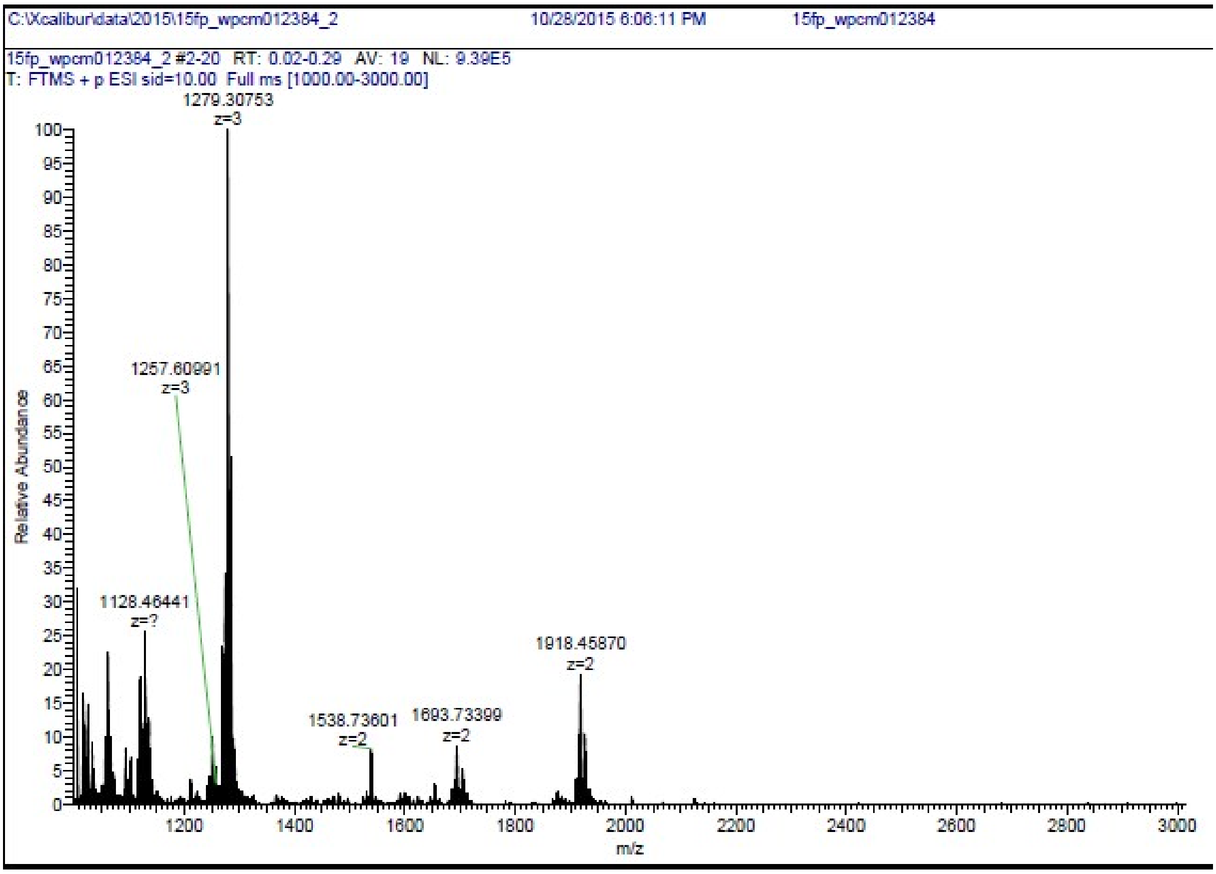

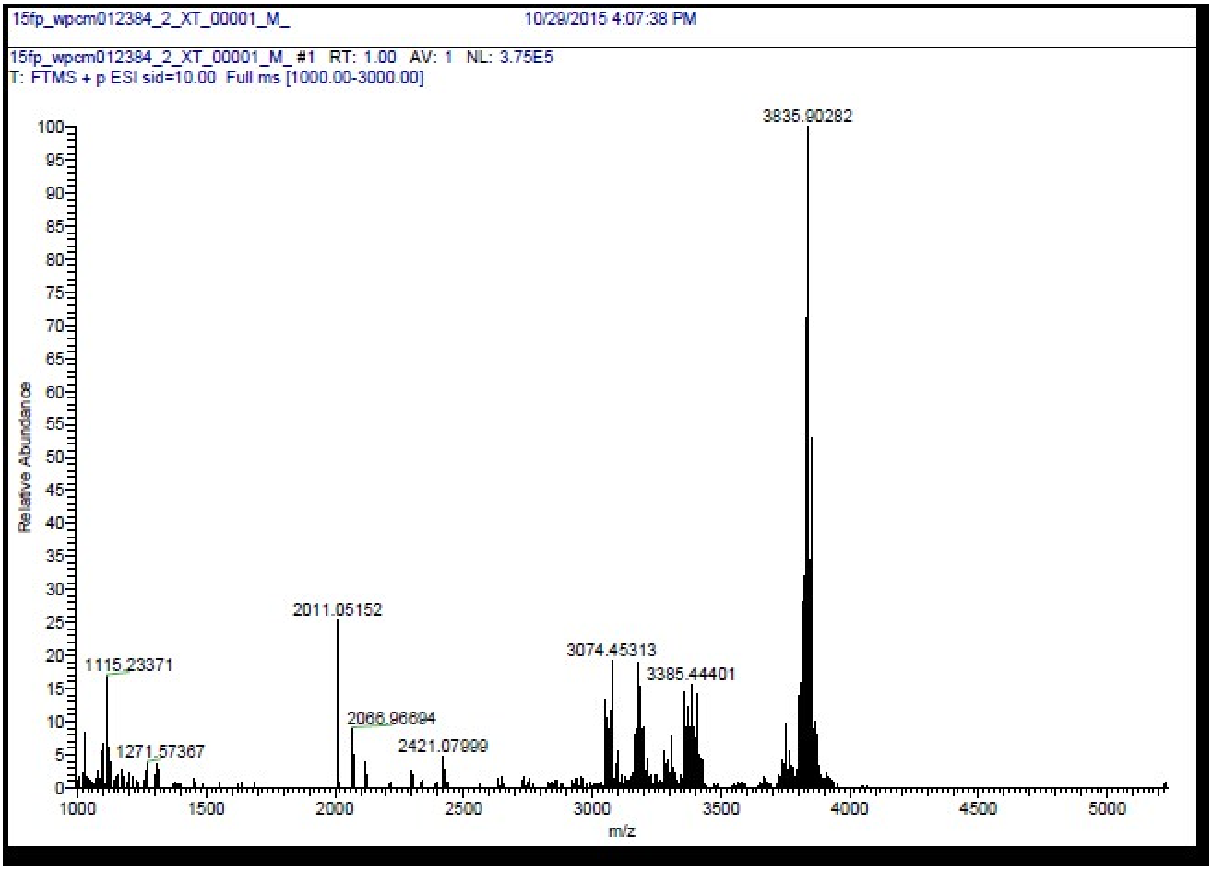

Compound **P2**: ^{1}H NMR (300 MHz, $CDCl_3$) full spectrum

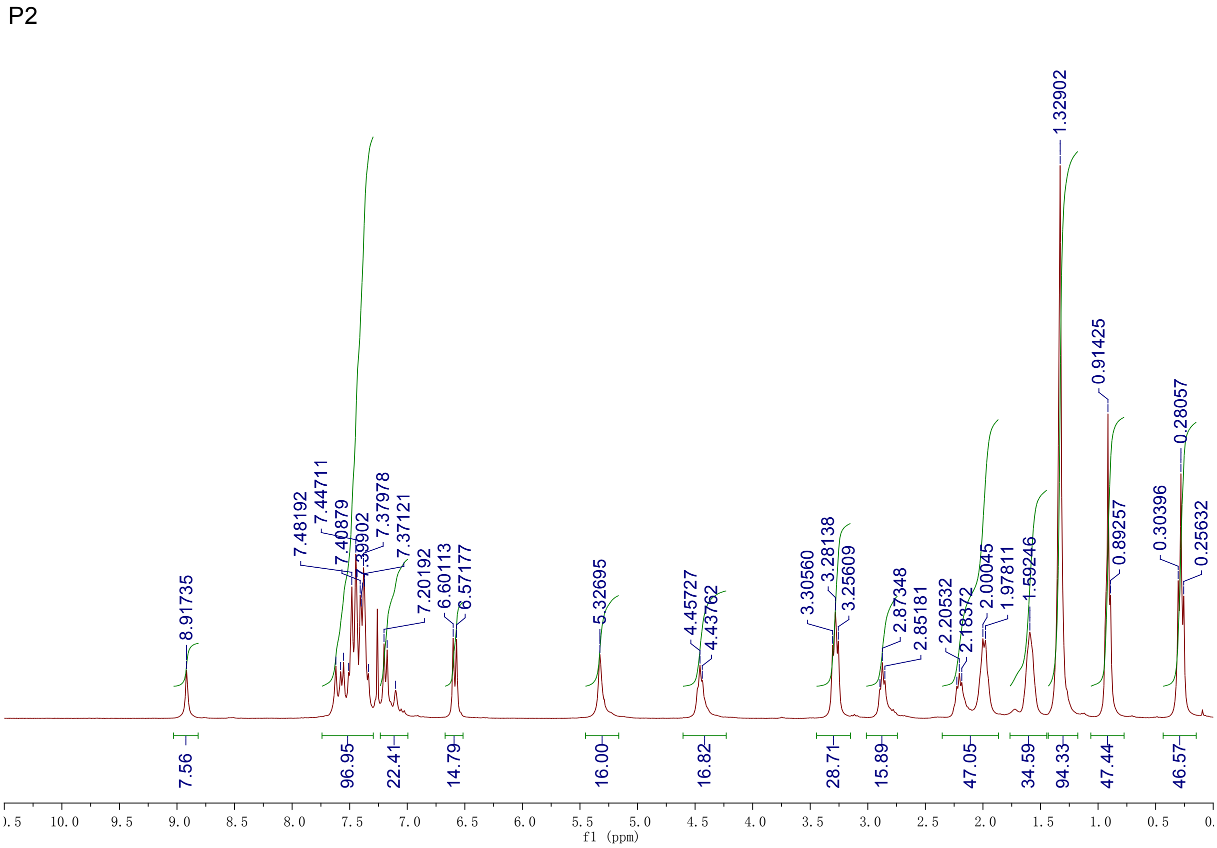

Compound **P2**: ^{1}H NMR (300 MHz, $CDCl_3$) expansion aliphatic protons

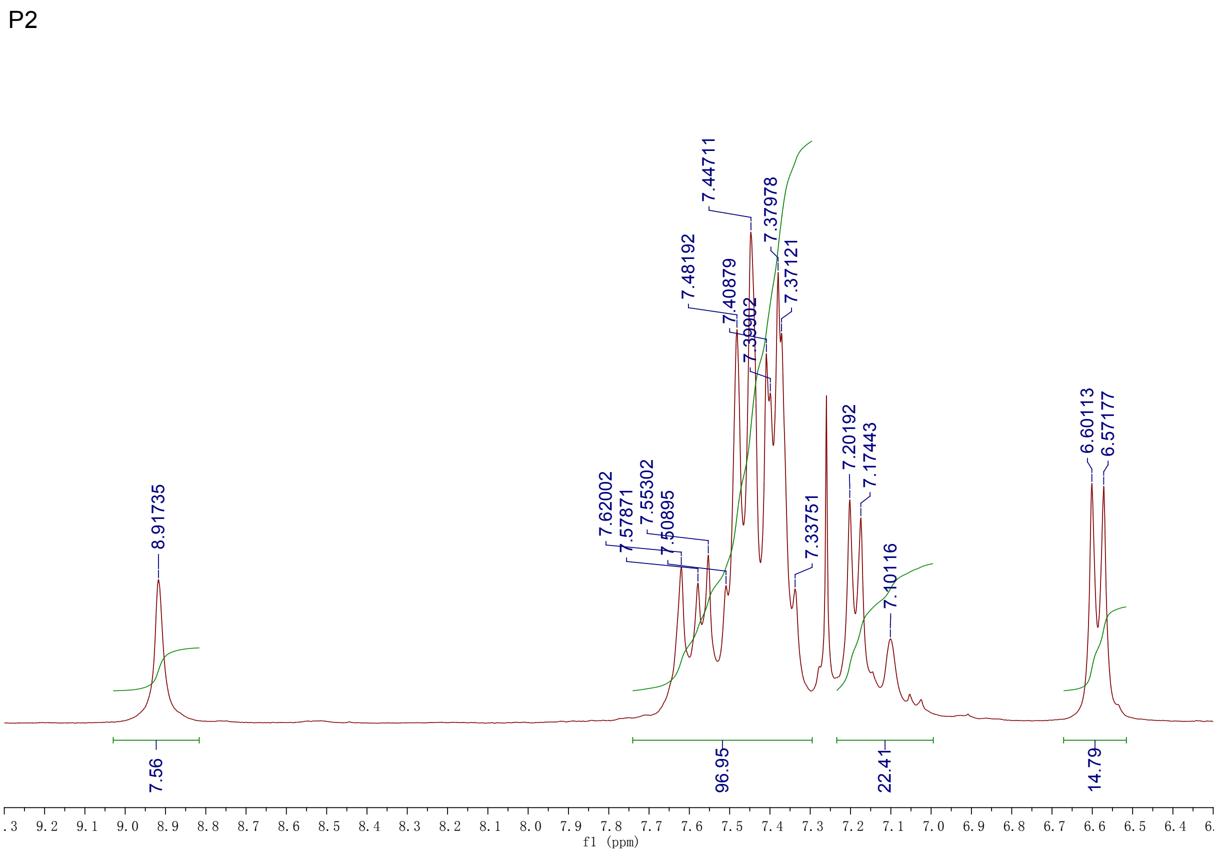

Compound **P2**: ^{1}H NMR (300 MHz, $CDCl_3$) expansion aromatic protons

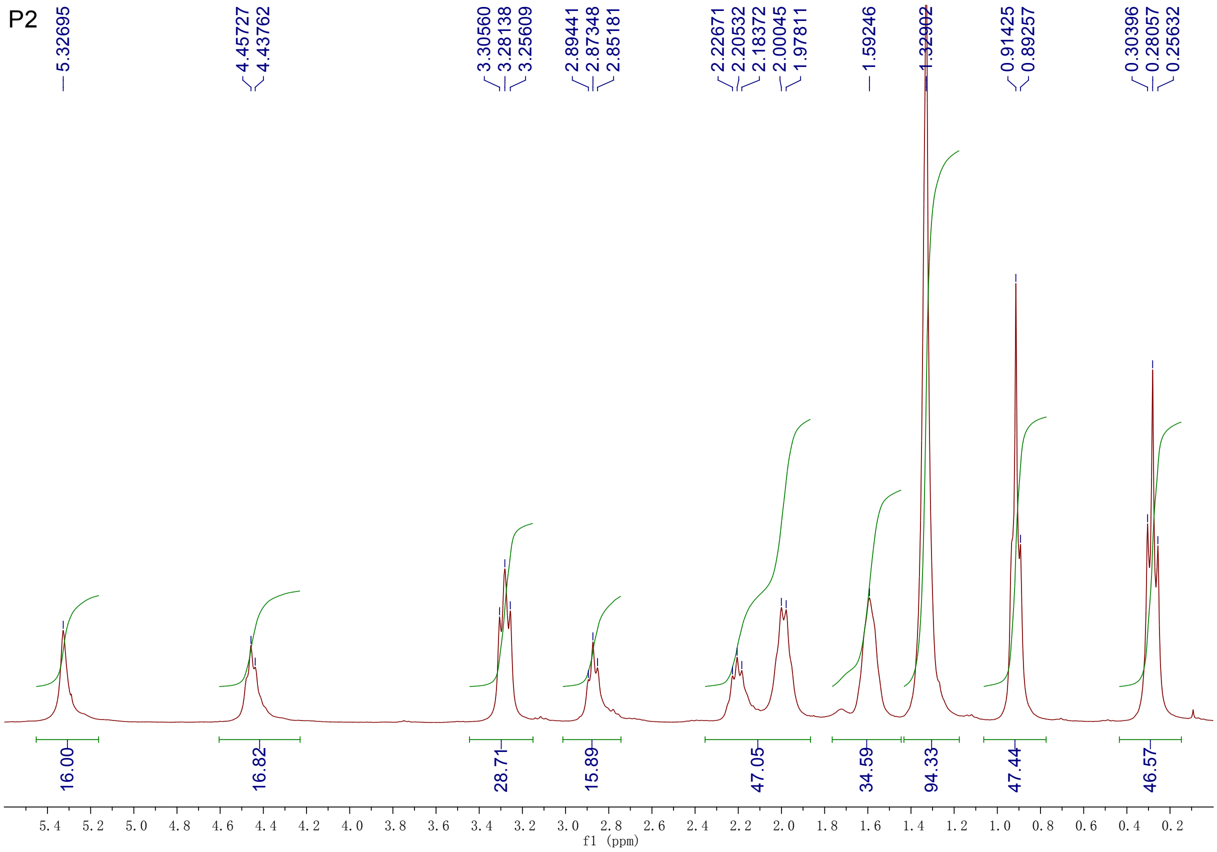

Compound **P2**: ^{13}C NMR (75 MHz, $CDCl_3$)

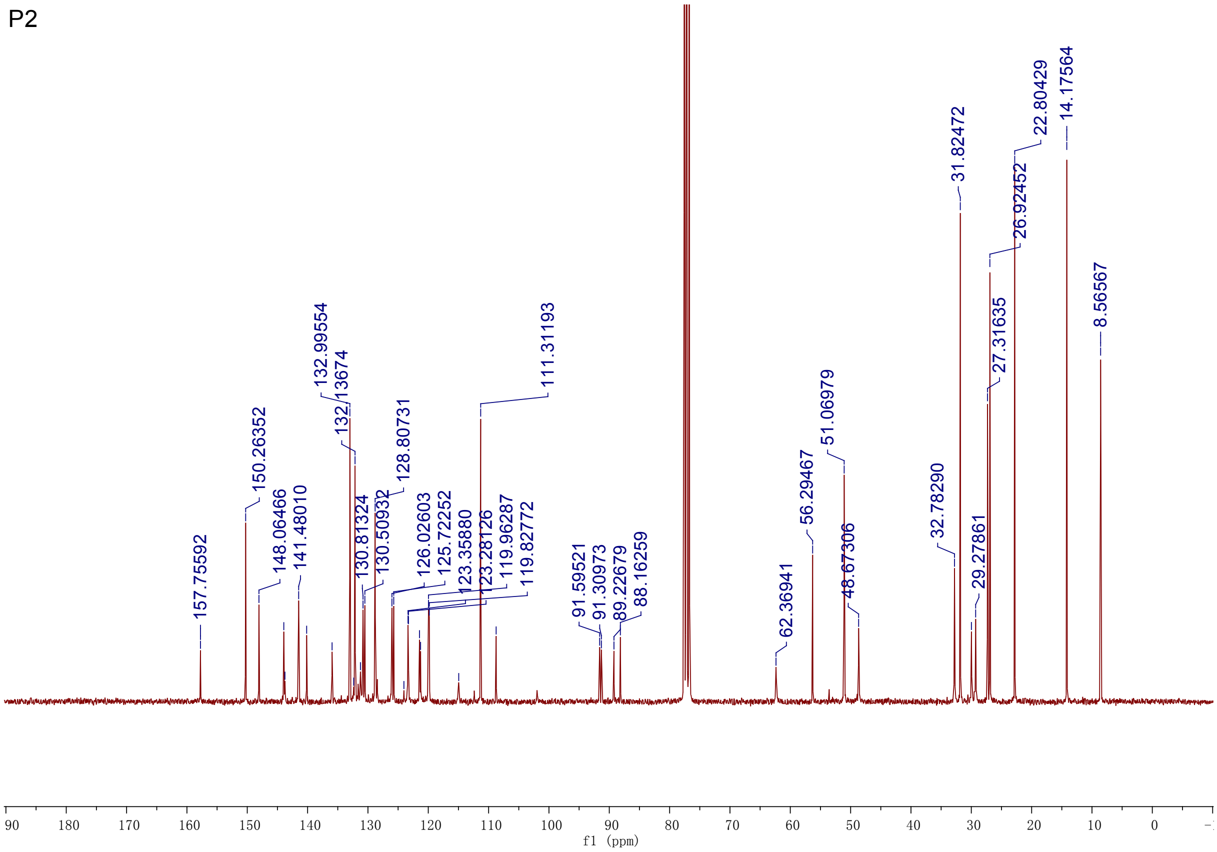

Compound **P2**: MS